2009

ANALYSIS AND BEHAVIOUR OF GUYED TRANSMISSION LINE STRUCTURES UNDER TORNADO WIND LOADING

Ahmed Hamada

ANALYSIS AND BEHAVIOUR OF GUYED TRANSMISSION LINE STRUCTURES UNDER TORNADO WIND LOADING

(Spine Title: Behaviour of Guyed Transmission Line Structures under Tornado)

(Thesis Format: Integrated-Article)

By

Ahmed Hamada

Graduate Program in Engineering Science
Department of Civil and Environmental Engineering

A thesis submitted in partial fulfillment
of the requirements for the degree of
Master of Engineering Science

School of Graduate and Postdoctoral Studies
The University of Western Ontario
London, Ontario, Canada
December, 2009

ABSTRACT

The majority of transmission line failures that have occurred in the past have been attributed to High Intensity Wind (HIW) events in the form of tornadoes and downbursts. A numerical model is developed in the current study to assess the performance of transmission lines under tornado wind loads. The tornado wind field used in the study is based on a Computational Fluid Dynamics (CFD) analysis that was developed and validated in a previous study. Using field measurements, the CFD data is used to estimate the wind fields for F4 and F2 tornadoes. A three-dimensional nonlinear finite element model is developed, and includes a simulation for the towers and the lines. The wind forces associated with the tornado fields are calculated and later incorporated into the numerical model. A comparison is carried out between the forces in the members resulting from both the F4 and F2 tornado wind fields, and those obtained using conventional design wind loads. The study is further extended to represent the first comprehensive investigation that assesses the effect of varying the relative location of the tornado to the tower on the structural performance of the transmission line system. The structural behaviour of the tower under the critical loading cases is described. The nonlinear numerical model is also modified to assess the dynamic behaviour of the transmission line system resulting from the translation motion of the tornado. Dynamic analysis is performed using two different tornado paths. The study reveals the importance of considering tornadoes when designing transmission line systems.

KEYWORDS: tornado, finite element, transmission line, transmission tower, wind load, dynamic analysis, free vibration.

CO-AUTHORSHIP

This thesis has been prepared in accordance with the regulations for an Integrated-Article format thesis stipulated by the School of Graduate and Postdoctoral Studies at the University of Western Ontario and has been co-authored as:

Chapter 2: FINITE ELEMENT MODELLING OF TRANSMISSION LINE STRUCTURES UNDER TORNADO WIND LOADING

All the analytical work was conducted by A. Hamada under close supervision of Dr. A. A. El Damatty. The wind tunnel data was provided by Dr. H. Hangan. Drafts of Chapter 2 were written by A. Hamada and modifications were done under supervision of Dr. A. A. El Damatty. A paper co-authored by A. Hamada, A. A. El Damatty, H. Hangan and A. Y. Shehata was submitted to the *Journal of Wind and Structures.*

Chapter 3: BEHAVIOUR OF TRANSMISSION LINE STRUCTURES UNDER TORNADO WIND LOADING

All the analytical work was conducted by A. Hamada under close supervision of Dr. A. A. El Damatty. Drafts of Chapter 3 were written by A. Hamada and modifications were done under supervision of Dr. A. A. El Damatty. A paper co-authored by A. Hamada and A. A. El Damatty will be submitted to the *Journal of Wind and Structures.*

Chapter 4: DYNAMIC BEHAVIOUR OF TRANSMISSION LINE STRUCTURES UNDER TORNADO WIND LOADING

All the analytical work was conducted by A. Hamada under close supervision of Dr. A. A. El Damatty. Drafts of Chapter 4 were written by A. Hamada and modifications were done under supervision of Dr. A. A. El Damatty. A paper co-authored by A. Hamada and A. A. El Damatty will be submitted to the *Journal of Wind and Structures.*

To my beloved parents *Shadia* and *El Sayed El Mahdy*

To my brother *Mohamed*

For patiently enduring, support, encouragement, patience, and sharing these years of hard work

To my supervisor, *Dr. A. El Damatty*

For his support as well as his sharing knowledge and expertise during these years

ACKNOWLEDGMENTS

I would like to express my appreciation and gratitude to the people who have helped me. Without them, this thesis would have not been completed.

First, Dr. El Damatty, A. A., for his valuable guidance, advice, and encouragement throughout the course of this research work. It has been a privilege to work under his supervision.

Second, I would like to thank my best friend Lisa (Katie) Reipas for her support, patience, and continuous encouragement throughout the research period. Thank you for believing in me.

The author would like to acknowledge Manitoba Hydro Company, Canada, the Natural Sciences and Engineering Research Council of Canada (NSERC), and Centre for Energy Advancement through Technological Innovation (CEATI) for the financial and in-kind support provided to this research work.

The author would like also to express his appreciation to Dr. Hangan, H., Dr. Ho,E., Dr. Miller, C., Dr. Savory, E. and Dr. Surry, D. for their constructive criticism and valuable comments throughout the course of this work. For all the graduate students who supported me and shared their valuable experience with me, thank you.

TABLE OF CONTENTS

LIST OF TABLES

LIST OF FIGURES

LIST OF SYMBOLS

Symbol	Units	Description
A_i	m^2	Projected area perpendicular to " i " direction at the loaded Node
A_x	m^2	Projected area perpendicular to X - direction at the loaded Node
A_y	m^2	Projected area perpendicular to Y - direction at the loaded Node
A_z	m^2	Projected area perpendicular to Z - direction at the loaded Node
C_f	--	force coefficient
C_{fx}	--	average of force coefficients in X - direction
C_{fy}	--	average of force coefficients in Y - direction
C_{fz}	--	average of force coefficients in Z - direction
F_c	kN	Reaction force of the conductors on the tower
F_g	kN	Reaction force of the ground wire on the tower
F_{wi}	N	Nodal point wind force in " i " direction
F_x	N	Total tornado wind force component in global X - direction
F_y	N	Total tornado wind force component in global Y - direction
F_z	N	Total tornado wind force component in global Z - direction
G	--	Gust response factor
h_o	m	Height of the fluid computational domain
K	--	Shielding factor
L_s	--	Length scale ratio
P	kN/m	Distributed tornado force on the tower

R	m	Radial distance between the tower center and the tornado center
r	m	Radial distance relative to the tornado center in the CFD
r_o	m	Radius of the fluid computational domain
R_{fa}	m	Radial full scale distance between point "a" and the tornado centre
R_{ma}	m	Radial distance in the CFD model between point "a" and The tornado centre
S	--	Swirl ratio – $S = 0.5\ (V_t / V_r)$
T	sec	Fundamental natural period
V	m/sec	Wind velocity
V_o	m/sec	Reference velocity for CFD model
V_{ama}	m/sec	CFD axial velocity components of point "a"
V_{AX}	m/sec	Full scale axial velocity component of point "a"
V_i	m/sec	Tornado velocity component in " i " direction
V_m	m/sec	Velocity resulting from the CFD model
V_{ma}	m/sec	Axial velocity resulting from the CFD model
V_{mr}	m/sec	Radial velocity resulting from the CFD model
V_{mt}	m/sec	Tangential velocity resulting from the CFD model
V_r	m/sec	Radial velocity at the boundary layer profile inlet
V_{RD}	m/sec	Full scale radial velocity of point "a"
V_{rma}	m/sec	CFD radial velocity components of point "a"
V_s	--	Velocity scale ratio
V_t	m/sec	Tangential velocity at the boundary layer profile inlet
V_{tma}	m/sec	Tangential CFD velocity components of point "a"

V_{TN}	m/sec	Full scale tangential velocity of point "a"
V_x	m/sec	Nodal tornado velocity component in global X-direction
V_y	m/sec	Nodal tornado velocity component in global Y-direction
V_x'	m/sec	Average tornado velocity component in global X-direction
V_y'	m/sec	Average tornado velocity component in global Y-direction
z	m	Cartesian coordinate of the point in global Z-direction in the CFD model
Z	m	Cartesian coordinate of the point of interest in global Z – direction
Z_o	m	Reference height of the reference velocity in CFD model
Z_{fa}	m	Cartesian full scale coordinate of point "a" in global Z – direction
Z_{ma}	m	Cartesian coordinate of point "a" in global Z-direction in the CFD model
Z_v	--	Terrain factor
ρ_a	kg/m^3	air density
θ	degree	angle between a vertical plane that contains the centre of the tower and the tornado and a vertical plane perpendicular to the transmission line
θ_{fa}	degree	angle between a vertical plane that contains the centre of the tornado and point "a" and a vertical plane perpendicular to the transmission line
θ_{ma}	degree	angle between a vertical plane that contains the centre of the tornado and point "a" and a vertical plane perpendicular to the transmission line

CHAPTER 1

INTRODUCTION

1.1 General

Electricity plays a vital and essential role in our daily life. Almost all business and activities depend on having a reliable source of electricity. Transmission lines are responsible of carrying electricity from the source of production to the end users. Failure of transmission lines can have devastating social and economical consequences, so it is imperative to understand how failure occurs, and how to prevent it. The structural components of a transmission line system are the towers, the conductors, the ground wires, and the insulator strings. The main characteristic of the towers is that they are always slender and flexible, which makes them vulnerable to strong wind loads.

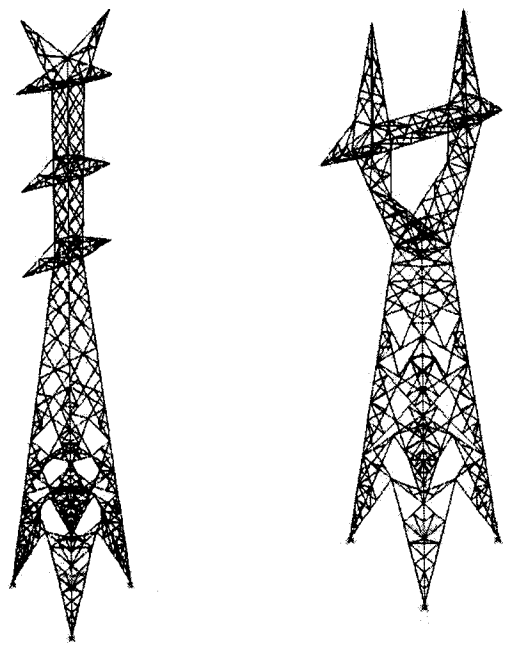

Fig. 1-1 Self-supported Transmission Tower Structures

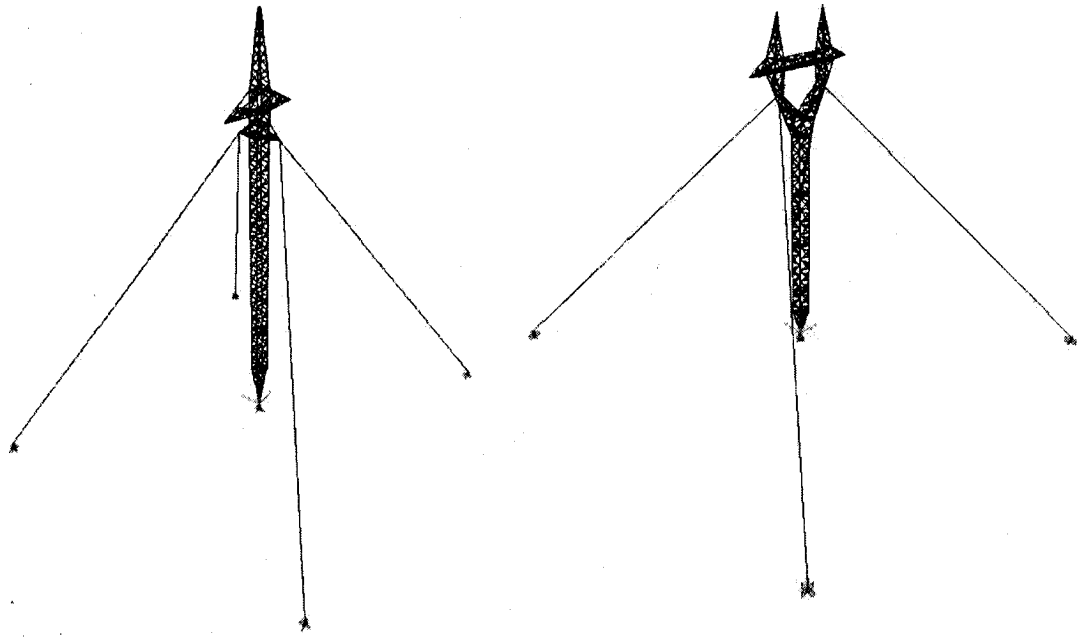

Fig. 1-2 Guyed Transmission Tower Structures

With respect to structural behaviour, transmission towers can be classified as either self-supported or guyed towers, which depends on how they are attached to the ground. Fig. 1-1 and Fig. 1-2 show skeletons of self-supported and guyed towers, respectively. Self-supported towers are most commonly used, however, guyed towers are more economical. Both types are typically made of steel. Conductors are attached to the towers via insulators strings. For lightning protection, the ground wires are attached directly to the top of the towers. The current study focuses on the guyed transmission towers.

1.2 Background

More than 80% of all weather-related failures of transmission line systems are believed to be related to High Intensity Wind (HIW) events like tornadoes and downbursts (Dempsey and White 1996). Li (2000) reported that 90% of transmission line failures in Australia are caused by HIW events. Ishac and White (1994) reported that of all the populated

areas in Canada, southwestern Ontario experiences the highest rate of tornado incidences, about two tornadoes per 10,000 (km^2) every year, and most of transmission line failures in this area are caused by tornadoes. 92% of these tornadoes were F2 or less on the Fujita scale. Despite these facts, the codes of practice, design guidelines, and utilities design methodologies are based on the loads resulting from large-scale synoptic events with conventional boundary layer wind profiles. Conventional wind profiles are characterized by a monotonic increase in velocity with height, which is different than wind profiles attributed to tornadoes where the maximum wind speed occurs near the ground. In addition, a significant vertical wind component exists in the tornado wind profile. The complexity in analyzing transmission line structures under HIW arises from the fact that tornadoes are very localized events with relatively narrow path width. Due to the localized nature of tornadoes, the forces acting on the tower and the conductors vary based on the location of the event relative to the tower. The behaviour of the lines is quite complicated. As a result, the ASCE No.74 guideline (1991) recommends that the tornado loads on the lines should be neglected because of such complexity. However, the probability of transmission lines being crossed by a tornado is high as reported by Ishac and White (1994).

Tornadoes are rotating wind vortices with high wind speeds affecting relatively narrow paths as defined by Fujita (1981). They originate from convective clouds that generate rotating columns of air (Twisdale 1982). Fujita scale (Fujita and Pearson 1973) is the most widely tornado scale used now. The scale categorizes the tornadoes between F0 to F5 based on maximum wind speed, path length, path width, and damage. The size and intensity of tornadoes cannot be measured in the field by traditional recording stations

due to the severity and the localized nature of these events. Photographic analysis using videos of moving objects in tornadoes, Doppler radar, and damage investigations are the only available methods to estimate the tornado wind speeds (McCarthy and Melsness 1996). This explains the lack of full scale data for tornadoes in the literature. Recently, field measurements were recorded by Wurman (1998) and were introduced by Sarkar, *et al.* (2005) for the 1998 Spencer South Dakota F4 tornado and by Lee and Wurman (2005) for the 1999 Mulhall F4 tornado. Doppler radars are used to obtain the tornado field measurements but the recorded data is not very accurate for the near ground region. Laboratory simulations of tornadoes are used to obtain the behaviour in the near ground region and to provide characteristics about the tornado-like-vortices phenomena. The first laboratory attempts were made by Ward (1972) by developing the Ward-type simulator. Tornado simulators were developed over time and led to the creation of Tornado Vortex Chambers (TVC), which provide a good simulation of the characteristics inside a tornado. However, the results from the laboratory simulation are sensitive to the applied boundary conditions. Numerical simulations can be done using fluid dynamic software which provides a good assessment of the flow field near the ground.

The tornado wind field used in this study is obtained from a three-dimensional Computational Fluid Dynamic (CFD) simulation conducted by Hangan and Kim (2008). Hangan and Kim (2008) studied the swirl ratio effect on tornado vortices in the relation of Fujita scale, where, the swirl ratio is the ratio between the tangential and radial velocity at the computational domain boundaries. The CFD simulation was conducted using the commercial program FLUENT (FLUENT Inc. 2005). The simulations of tornado-like vortices included the formation of a laminar vortex at low swirl ratio,

followed by turbulent vortex breakdowns and vortex touch downs at higher swirl ratio values. The simulation was initially conducted using a swirl ratio S = 0.28. This is the same swirl ratio applied in the experimental program conducted by Baker (1981) using a Ward-type vortex chamber. The results of the CFD analysis with S = 0.28 were validated by Hangan and Kim (2008) through a comparison with Baker's experimental results. The numerical analysis was then extended by Hangan and Kim (2008) by considering values of S = 0.10, 0.4, 0.7, 0.8, 1.0 and 2.0, respectively. An extensive study was conducted by Hangan and Kim (2008) to estimate the proper swirl ratio that should be applied to the numerical model in order to obtain good matching between the numerical results and the F4 tornado field measurements. Hangan and Kim (2008) introduced a geometry scale and a velocity scale which can be applied to CFD results to develop velocity fields simulating F4 tornadoes. No field data measurements are available in literature for F2 tornadoes. This is despite the fact that 86% of categorized tornadoes are associated with F2 tornadoes or less as stated by the ASCE No. 74 guidelines (1991). In the current study procedures are employed to estimate a velocity field for F2 tornadoes from the CFD data. Many research studies and hydro companies conducted valuable research in the area of the transmission line behaviour under wind loads. The majority of the research was focused on assessing the response of transmission line components separately to large scale boundary layer wind events. Very few attempts have been made in the literature to investigate the behaviour of transmission line systems under HIW events. The modelling and assessment of the behaviour of transmission lines under downburst loading was conducted by Shehata, *et al.* (2005) and Shehata and El Damatty (2007). In this study, a three-dimensional finite element model simulating the towers and a two-dimensional

model simulating the conductors were developed to assess the structural performance of transmission towers under downburst loading. An extensive parametric study was conducted in the same investigation to evaluate the critical downburst loading cases and downburst parameters. The study was extended later to investigate the structural performance of the tower under these critical downburst loading cases. The failure of a transmission tower during a downburst event, which occurred in Manitoba, Canada in 1996, was assessed by Shehata and El Damatty (2008). In this study, a numerical scheme, which included a failure model, was developed to study the progressive collapse of the guyed tower. Shehata, *et al.* (2008) extended the numerical model by including an optimization routine. This model is capable of predicting the critical downburst parameters and the corresponding forces. The failure of a self supported lattice tower under modelled tornado and microburst wind profiles was investigated by Savory, *et al.* (2001). The mathematical dynamic tornado wind model used in this study is based on the model developed by Wen (1975) where the tornado force can be obtained per unit height of the obstacle at any given time. Only the horizontal wind profile corresponding to F3 tornado on the Fujita scale was used in the analysis without considering the vertical component of the tornado wind. The turbulence component associated with the tornado and the downburst wind loading was neglected. The tower members were modelled as three-dimensional truss elements. The dynamic analysis was done for the tower alone including the self weight of the towers and the conductors, without modelling the transmission lines. The structure's response showed initial quasi-static response before failure under excessive tornado wind loads. The failure observed in this study under tornado loads was a shear failure, which is similar to field observations. Very little

research is available in the area of the dynamic response of transmission structures under tornado winds. Loredo-Souza and Davenport (1998) investigated experimentally in wind tunnels the transmission line failures in strong wind events. The experimental work compared successfully with the theoretical predictions obtained from the statistical method using influence lines. The study shows how the dynamic behaviour of the lines is affected mainly by the value of the aerodynamic damping which can be as high as 60% of the critical damping. The aerodynamic damping is directly proportional to the wind velocity and inversely proportional to the line mass. The study concluded that the background response is indeed the main contributor for the total fluctuating response, however, the resonant component can be also important depending on the line characteristics and wind velocities which may lead to smaller value of the aerodynamic damping. Therefore, the study proves the importance of turbulence in the dynamic response of the lines and shows the important role of the aerodynamic damping. Darwish, *et al.* (2009) modified the two-dimensional nonlinear finite element model of the transmission lines developed by Shehata, *et al.* (2005) to study the dynamic characteristics of the conductors under turbulent downburst loading. The modified model accounted for the large deformations and the pretension loading, and was used to predict the natural frequencies and mode shapes. In this study, the turbulence component was extracted from full scale data and added to the mean component of the downburst wind field developed by Kim and Hangan (2007). The study concluded that the resonant component due to the turbulence is negligible due to the large aerodynamic damping. In addition, the study discussed the effect of the pretension force on the natural period and mode shapes of the conductors. Loredo-Souza and Davenport (2003) reviewed the

influence of the design procedure for the establishment of wind loading on transmission tower response. Davenport's gust response and statistical method, using the influence lines procedure for estimating wind loading on transmission structures, were compared. The second approach accounts for the effect of the higher mode. Based on the tower response conducted in this research, Loredo-Souza and Davenport (2003) concluded that the dynamic response of transmission towers is strongly dependent on the turbulence intensity and both the structural and aerodynamic damping of the towers.

1.3 Objective of the Study

The main objectives of the current study are summarized below:

1- Develop a numerical model to analyze the structural behaviour of transmission line system under F4 and F2 tornado wind fields.

2- Assess the effect of varying the tornado characteristics such as size and location relative to the tower of interest on the structural performance of the transmission structures.

3- Develop a numerical model to conduct the dynamic response of transmission line system under tornado loading.

1.4 Scope of the Thesis

This thesis has been prepared in 'Integrated-Article' format. In the present chapter, a review of the studies related to transmission lines and tornadoes are provided. The objective of the study is provided. The following three chapters address the thesis objectives. Chapter five presents the conclusion of the study together with suggestions for further research work.

1.4.1 Finite Element Modelling of Transmission Line Structures under Tornado Wind Loading

The objective of chapter 2 is to develop a numerical model that can be used to analyze transmission line systems under F4 and F2 tornado wind loads. The chapter starts with a summary about the CFD model developed by Hangan and Kim (2008) to simulate F4 and F2 tornadoes. A procedure to scale the CFD results to match full scale F4 and F2 tornadoes is illustrated. The tornado wind fields are converted into forces acting on the transmission line components. A three-dimensional nonlinear finite element model is developed to simulate the towers, the conductors, the guys, the insulator strings, and the ground wire. The tornado forces are incorporated into the finite element model. To assess the importance of considering tornado loading in the design of the transmission lines, the developed model is used to calculate the internal forces in the tower under different tornado configurations. These forces are compared to those used in the initial design of the tower under normal wind loads.

1.4.2 Behaviour of Transmission Line Structures under Tornado Wind Loading

In chapter 3, a comprehensive parametric study is conducted to assess the effect of varying the tornado location relative to the tower of interest on the structural performance of the transmission line system. The same model developed in chapter 2 is used. A comparison is carried out between the results of F4 tornadoes, F2 tornadoes, downbursts and the design capacity of the tower members. The results are used to evaluate the critical loading cases for the tower of interest. The behaviour of the tower under the critical loading cases is described.

1.4.3 Dynamic Behaviour of Transmission Line Structures under Tornado Wind Loading

Chapter 3 assesses the dynamic response of the transmission line system under moving tornadoes. The F4 tornado wind field discussed in chapter 2 is used in this study. A three-dimensional nonlinear finite element model is developed to simulate the transmission line system. A set of free vibration analyses are conducted to evaluate the natural periods and mode shapes of the line components. A numerical model is developed to conduct the nodal loading functions for two main dynamic loading cases. Finally, the dynamic response of the towers and the lines under translation F4 tornadoes is described.

1.5 References

American Society of Civil Engineers (ASCE) (1991), "Guidelines for electrical transmission line structural loading", *ASCE Manuals and Reports on Engineering Practice,* No. 74, NY.

Baker, D. E. (1981). "Boundary layers in laminar vortex flows." Ph.D. thesis, Purdue University.

Darwish, M. M., El Damatty, A. A., and Hangan, H. (2009), " Dynamic characteristics of transmission line conductors and behaviour under turbulent downburst loading", *Wind and Structures, an International Journal.*

Dempsey, D., and White, H., (1996) "Winds wreak havoc on lines.", *Transmission and Distribution World*, vol. **48**(6), pp. 32–37.

Fluent 6.2 User's Guide (2005), Fluent Inc.,Lebanon

Fujita, T. T. (1981), "Tornadoes and downbursts in the context of generalized planetary scales", *J. Atmos. Sci.*, **38**, 1511-1534.

Fujita, T.T., and Pearson, A.D. (1973). " Results of FPP Classification of 1971 and 1972 Tornadoes," *Preprints, Eighth Conference on Severe Local Storm, American Meteorological Societ,* Boston, Mass., USA, pp. 142-145.

Hangan, H., and Kim, J. (2008). "Swirl ratio effects on tornado vortices in relation to the Fujita scale." *Wind and Structures,* **11**(4), 291-302.

Ishac, M. F., and White, H. B. (1994). "Effect of tornado loads on transmission lines" *Proceedings of the 1994 IEEE Power Engineering Society Transmission and Distribution Conference*, Chicago, IL, USA, April

Kim, J., and Hangan, H. (2007). "Numerical simulations of impinging jets with application to downbursts." *J.Wind Eng.Ind.Aerodyn.,* **95**(4), 279-298.

Lee, Wen-Chau., and Wurman, J. (2005). "Diagnosed three-dimensional axisymmetric structure of the Mulhall tornado on 3 May 1999." *J.Atmos.Sci.,* **62**(7), 2373-93.

Li, C. Q. (2000), "A stochastic model of severe thunderstorms for transmission line design", *Prob. Eng. Mech.*,**15**, 359-364.

Loredo-Souza, A., and Davenport, A. G. (2003). "The influence of the design methodology in the response of transmission towers to wind loading." *J.Wind Eng.Ind.Aerodyn.,* **91**(8), 995-1005.

Loredo-Souza, A., and Davenport, A. G. (1998). "The effects of high winds on transmission lines." *J.Wind Eng.Ind.Aerodyn.,* **74-76**, 987-994.

McCarthy, P.,Melsness, M. (1996) "Severe weather elements associated with September 5, 1996 hydro tower failures near Grosse Isle, Manitoba, Canada." Manitoba Environmental Service Centre, Environment Canada,, 21pp.

National Research Council of Canada (NRCC) (1990), Supplement to the National Building Code of Canada 1990. *Associate Committee on the National Building Code*, Canada.

SAP2000 V.12 (2008), CSI Analysis Reference Manual, Computer and Structures, Inc. Berkeley, California, USA

Sarkar, P., Haan, F., Gallus, Jr., W., Le, K. and Wurman, J. (2005). "Velocity measurements in a laboratory tornado simulator and their comparison with numerical and full-scale data." *37th Joint Meeting Panel on Wind and Seismic Effects.*

Savory, E., Parke, G. A. R., Zeinoddini, M., Toy, N., and Disney, P. (2001). "Modelling of tornado and microburst-induced wind loading and failure of a lattice transmission tower." *Eng.Struct.,* **23**(4), 365-375.

Shehata, A. Y., and El Damatty, A. A. (2008). "Failure analysis of a transmission tower during a microburst." *Wind and Structures,* **11**(3), 193-208.

Shehata, A. Y., and El Damatty, A. A. (2007). "Behaviour of guyed transmission line structures under downburst wind loading." *Wind and Structures, an International Journal,* **10**(3), 249-268.

Shehata, A. Y., El Damatty, A. A., and Savory, E. (2005). "Finite element modelling of transmission line under downburst wind loading." *Finite Elements Anal.Des.,* **42**, 71-89.

Shehata, A. Y., Nassef, A. O., and El Damatty, A. A. (2008). "A coupled finite element-optimization technique to determine critical microburst parameters for transmission towers." *Finite Elements Anal.Des.,* **45**(1), 1-12.

Twisdale, L. A. (1982). "Wind-loading underestimate in transmission line design" *Transmission & Distribution,* **34** (13), 40-46.

Ward, N. B. (1972), " The exploration of certain features of tornado dynamic using a laboratory model', *journal of the Atmospheric Science*, **26** (6), 1194-1204

Wen, Y. (1975). "Dynamic tornadic wind loads on tall buildings", *ASCE Journal of the Structural Division*, **101**(1), 169-185.

Wurman, J. (1998). "Preliminary results from the ROTATE-98 tornado study", *Preprints, 19th Conf. On severe local storms,* Minneapolis, MN, 14-18 September.

CHAPTER 2

FINITE ELEMENT MODELLING OF TRANSMISSION LINE STRUCTURES UNDER TORNADO WIND LOADING[1]

2.1 Introduction

Localized severe wind events in the form of tornadoes, downbursts and microburst are referred to as "High Intensity Wind (HIW) events". Such events are believed to hold responsibility for more than 80% of all weather-related transmission line failures worldwide (Dempsey and White 1996). Despite this fact, the codes of practice and design for transmission line structures are based on the wind characteristics resulting from large-scale synoptic events. The vertical profile of the boundary layer wind of a large-scale event is characterized by a monotonic increase in velocity with height. Such a profile is different than the velocity profiles of tornadoes. In addition, a significant vertical velocity component exists in the case of tornadoes. The current study focuses on assessing the response of transmission line structures to tornado loading.

The complexity in analyzing transmission line structures under HIW arises from the fact that the forces acting on the tower and the conductors vary according to the location of the event relative to the tower. This is due to the localized nature of these events. Also, depending on the location of the event relative to the tower, various spans of conductors can be subjected to different, and in some cases, uneven distribution of wind loads. This can lead to a resultant longitudinal force (parallel to the conductors) acting on the tower cross arms. Tornadoes are one of the HIW events. They are short-lived, localized, surface vortex flows that originate from thunderstorms. They have a severe rotating column of air

[1] A version of this chapter has been submitted to the *Journal Wind and Structures*

that extends from the clouds to the earth. The tornado path width can reach up to 500 (m); therefore, field measurements are difficult to obtain and are poorly defined (Hangan and Kim 2008). Recently, field measurements were introduced by Sarkar, *et al.* (2005) for the 1998 Spencer South Dakota F4 tornado and by Lee and Wurman (2005) for the 1999 Mulhall F4 tornado. Doppler radar was used to obtain the tornado field measurements. However, the recorded data is not very accurate for the near ground region (for height less than 50 (m)) (Hangan and Kim 2008). Due to the complexity and difficulty of obtaining full-scale data, especially for the near ground region, laboratory simulations are used. These include the Tornado Vortex Chambers (TVC), in which tornadoes are represented as vortices. The TVC's provide a good simulation of the characteristics inside a tornado, but the results are sensitive and are affected by the applied boundary conditions (Hangan and Kim 2008). For the near ground region, numerical simulations can be done using fluid dynamic software, such as the commercial program FLUENT (FLUENT Inc. 2005). Numerical simulations can provide a good assessment of the flow field near the ground.

Few studies related to the behaviour of transmission lines under HIW events are available in the literature. The modelling and assessment of the behaviour of transmission lines under downburst loading were conducted by Shehata, *et al.* (2005) and Shehata and El Damatty (2007). The failure of a transmission tower during a downburst event, which occurred in Manitoba, Canada in 1996, was assessed by Shehata and El Damatty (2008). The failure of a self supported lattice tower under tornado and microburst wind profiles was investigated by Savory, *et al.* (2001). The analysis was done for the tower alone,

without modelling the transmission lines, and without considering the vertical velocity component.

In the current study, the numerical model developed by Hangan and Kim (2008) and the field data recorded by Sarkar, *et al.* (2005) are used to estimate the wind velocity profile for both F4 and F2 tornadoes. Both an axisymmetric and a three dimensional profile are considered. The spatial variation of those wind fields are described in this paper. A nonlinear finite element model is developed, simulating the structural behaviour of the towers and the conductors. The nonlinear behaviour of the conductors, including the pretension and sagging effects, is included in the model. The velocity profiles mentioned above, associated with F4 and F2 scale tornadoes are incorporated into the finite element simulation. Details of the numerical model are described, including steps conducted to estimate the wind loads. A case study for a guyed transmission line system is considered. Forces that develop in selected members of the tower due to both the F4 and F2 tornadoes are evaluated. They are compared to the corresponding forces associated with normal wind loads, based on the ASCE No. 74 guideline (1991).

2.2 Tornado CFD Numerical Model

The velocity wind field associated with tornadoes used in this study is obtained from a three-dimensional Computational Fluid Dynamic (CFD) simulation conducted by Hangan and Kim (2008). The CFD simulation was conducted using the commercial program FLUENT (FLUENT Inc. 2005). The simulations of tornado-like vortices included the formation of a laminar vortex at low swirl ratio, followed by turbulent vortex breakdowns and vortex touch downs at higher swirl ratio values. A schematic of the computational

domain is shown in Fig. 2-1. In this figure, r_o and h_o are the radius and height of the computational domain, respectively.

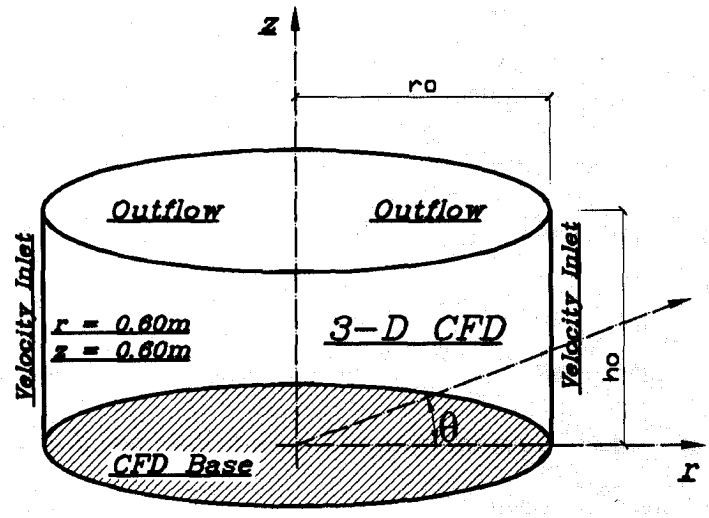

Fig. 2-1 Computational Domain for the 3-D Simulations of Tornadoes

The boundary conditions applied in the CFD analysis are shown in Fig. 2-1. At the inlet, a boundary layer profile is assumed for the radial velocity, V_r, and the tangential velocity, V_t, that are described by Eq. (1) and (2), respectively:

$$V_r(z)=V_o \times (z/z_o)^{\frac{1}{7}} \quad (1)$$

$$V_t(z)=2 \times S \times V_r(z) \quad (2)$$

Where: V_o = reference velocity, z_o = reference height and S (swirl ratio) = $0.5\ V_t/V_r$

In the simulation, values of 0.3 m/sec and 0.025 m were assumed for V_o and z_o, respectively. More details about the CFD simulation including the applied turbulence model can be found at Hangan and Kim (2008).

The simulation was initially conducted using a value of S = 0.28. This is the same swirl ratio applied in the experimental program conducted by Baker (1981) using a Ward-type

vortex chamber. The results of the CFD analysis with S = 0.28 were validated by Hangan and Kim (2008) through a comparison with Baker (1981) experimental results. The numerical analysis was then extended by Hangan and Kim (2008) by considering values of S = 0.10, 0.4, 0.7, 0.8, 1.0 and 2.0, respectively. It should be noted that the CFD analysis is conducted at steady-state manner and, therefore, the resulting velocity field has no variation with time. The velocity field resulting from the CFD analysis $V_m(r, \theta, z)$ has a three dimensional spatial variation and is given as a function of the cylindrical coordinates r, θ and z.

An averaging data is conducted along the circumference, eliminating the variation of the velocity profile with θ, and leading to an axisymmetric set of data $V_m(r, z)$. Both the 3-D and the axisymmetric set of data are used in the analysis conducted in this study. It should be noted that the velocity field $V_m(r, \theta, z)$ has three velocity components: the radial $V_{mr}(r, \theta, z)$, the tangential $V_{mt}(r, \theta, z)$ and the axial $V_{ma}(r, \theta, z)$. Similar components exist for the axisymmetric velocity profile.

2.3 F4 – Tornado Wind Field

Full scale data for the F4 tornado, which occurred in Spencer, South Dakota, USA, in May 30,1998, was recorded by Wurman (1998) using the "Doppler on Wheels" system (DOW). This set of tornado field measurements was also presented by Sarkar, *et al.* (2005). The measurements predicted that the maximum tangential velocity had a magnitude of 142 (m/sec) and occurred at coordinates r = 158 (m) and z = 28 (m), where r is the radial distance relative to the tornado centre and z is the vertical distance relative to ground. An extensive study was conducted by Hangan and Kim (2008) to estimate the proper swirl ratio that should be applied to the numerical model in order to obtain good

matching between the numerical results and the F4 tornado field measurements. Also, the proper length scale ratio (L_s) and velocity scale ratio (V_s), to be applied to the CFD data in order to simulate the F4 tornado, were obtained in this study. Hangan and Kim (2008) found that the values of S = 2, L_s = 4000 and, V_s = 13 provided a very good match between the scaled CFD data and the field measurements, in terms of the radial profile of the tangential velocity. These scaling factors are applied to the 3-D and the axisymmetric data to obtain 3-D and axisymmetric velocity fields simulating F4 tornadoes.

The magnitude and location of the maximum values of the three velocity components of the axisymmetric velocity field are provided in Table 2-1, where, negative values are towards tornado center and downward. The tabulated values indicate that the radial and axial components are significantly less than the tangential component. The ratio between the maximum radial and maximum tangential component is about 1:2. Also, it can be noticed that the maximum values of the three components occur at three different locations.

Table 2-1 Peak Values and Corresponding Location for the Velocity Components for F4 and F2 tornadoes

Tornado	Direction	Velocity (m/sec)	r (m)	z (m)
F4	Peak Tangential	142	158	28
	Peak Radial	-79	273	7
	Peak Axial	62	246	158
F2	Peak Tangential	78	96	19
	Peak Radial	-49	146	6
	Peak Axial	37	171	127

In order to gain an insight into the F4 tornado wind field, various vertical profiles for the tangential velocity component of the axisymmetric data are provided in Fig. 2-2. As shown in the figure, the vertical profiles are provided at various radial distances "r".

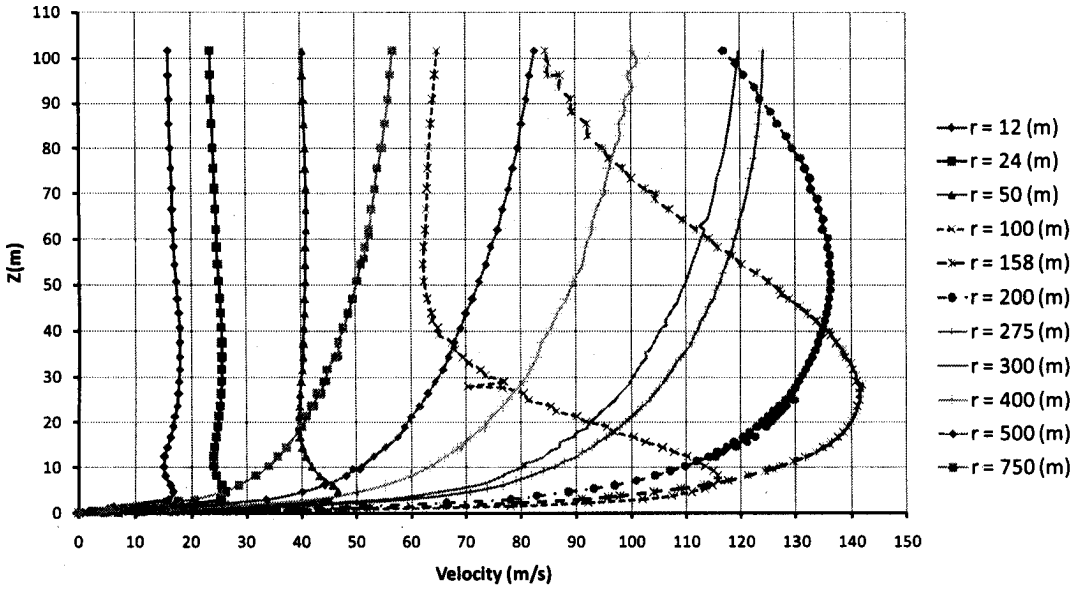

Fig. 2-2 Vertical Profile of Tangential Component for Different Radial Distances from Tornado Centre (F4 Tornado)

The following observations can be drawn from the plot:

- For radial distance $r \leq 300$ (m), the profile is different than the conventional boundary wind profile, which is typically characterized by a monotonic increase of the velocity with height. For values of $r > 300$ (m), the tornado profile becomes similar to the boundary layer profile.
- For very small values of r, the vertical location of the peak values becomes very close to the ground. The vertical location of the peak value increases with the increase of r. At r = 200 (m), the peak value occurs at a height of about 50 (m).

- The absolute maximum tangential velocity of 142 (m/sec) occurs at r = 158 (m) and z = 28 (m), agreeing with the values given in Table 2-1.

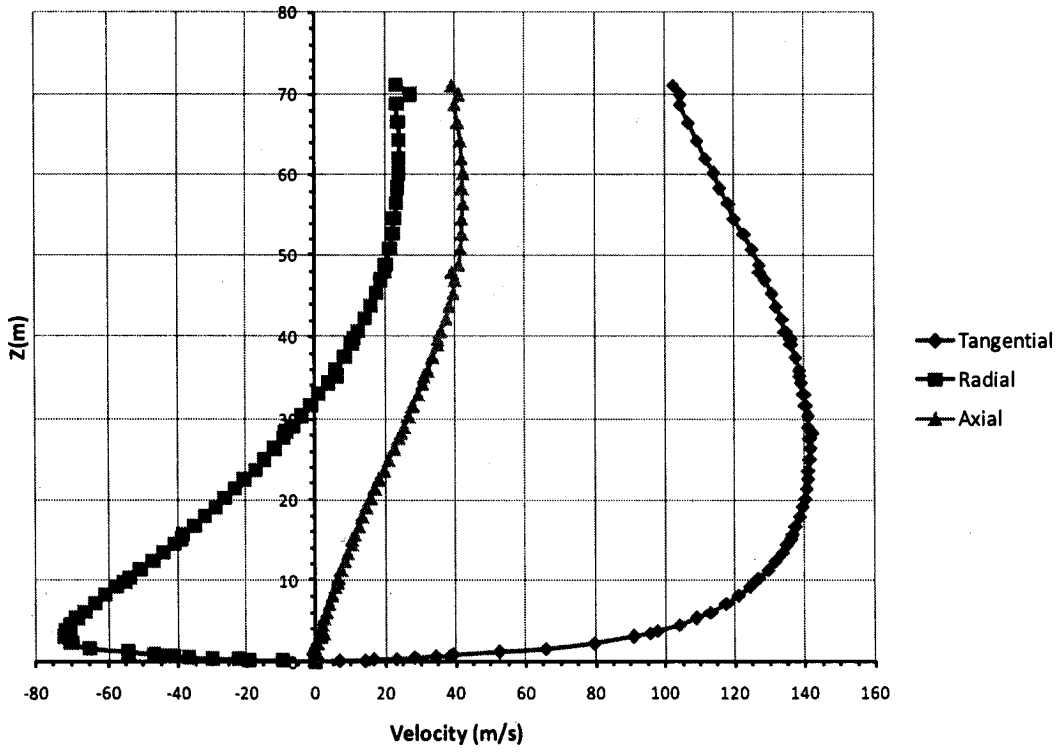

Fig. 2-3 Variation of the Three Velocity Components of F4 Tornado along the Height at r = 158 (m)

The vertical profiles of the radial and the axial components, corresponding to the location of maximum tangential velocity V = 142 (m/sec), are plotted in Fig. 2-3. The vertical profile of the tangential component is provided in the same figure for comparison. The following observations can be drawn from this figure:

- The peak value of the radial component occurs very close to ground.
- At a height z < 30 (m), the radial component has a negative value, i.e. acts in an inward direction. Beyond this height (i.e. for z > 30 (m)), the radial component acts along the outward direction.

- The axial component acts in an upward direction.

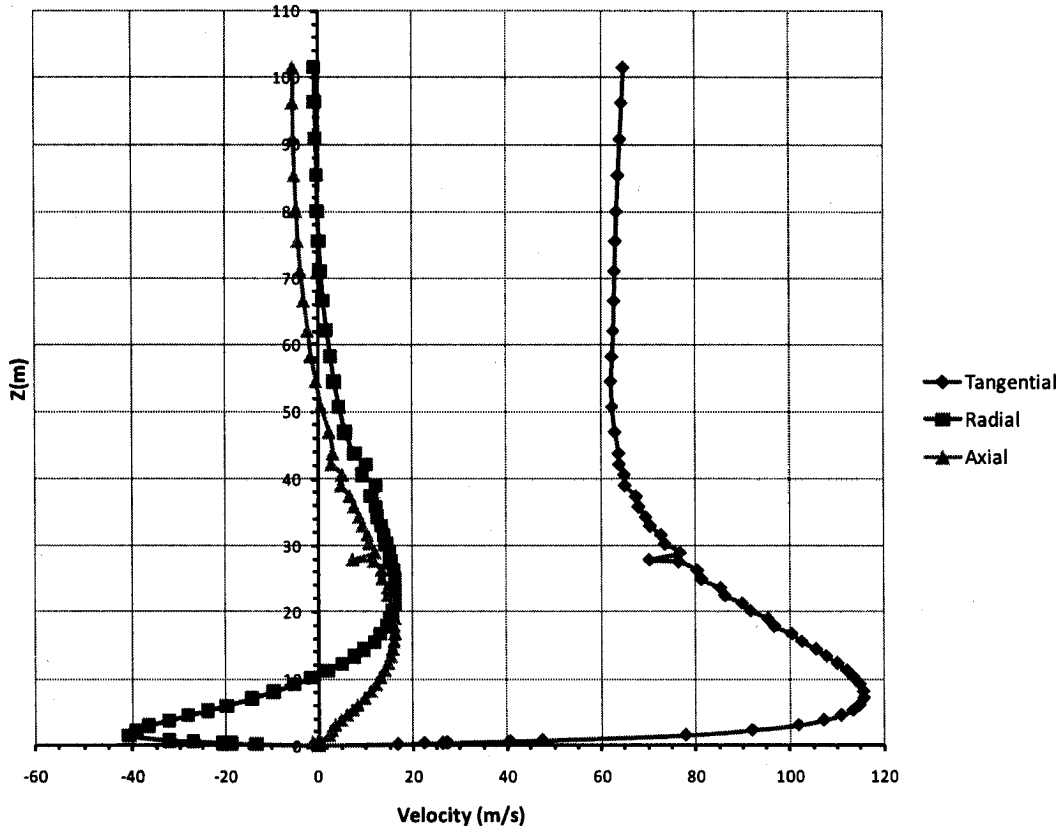

Fig. 2-4 Variation of the Three Velocity Components of F4 Tornado along the Height at r = 100 (m)

The near-to-centre velocity profile indicates the occurrence of vortex instability in this region. As a demonstration, the vertical profile of the three velocity components for r = 100 (m) is provided in Fig. 2-4. The peak radial velocity is located near the ground and has a negative value (inward). The direction of the radial component changes along the height from inward to outward. This component almost vanishes for heights greater than 70 (m). Also, the direction of the axial component varies along the height. It acts in an upward direction near the ground and switches to a downward direction at an elevation of 50 (m).

An assessment of the difference between the axisymmetric and the 3-D CFD data is conducted. This is done by plotting the variation of the velocity components along the circumference direction for selected values of r and z. This variation is compared to the corresponding value obtained from the axisymmetric data, which is an average value along the circumference. It is noticed that the variation of the 3-D data within the circumference is relatively small. No significant difference is shown between the peak points and the axisymmetric value along the circumference.

As a demonstration, the variations of the tangential component along two circumferences are shown in Fig. 2-5. The two circumferences are located at a radial distance r = 158 (m) and correspond to elevations z = 28 (m), and 10 (m), respectively. The plot shows the relatively small variation of the velocity values compared to the mean (axisymmetric) value. For z = 28 (m), the 3-D data varies between 139 (m/sec) and 145 (m/sec), while the corresponding axisymmetric value is 142 (m/sec).

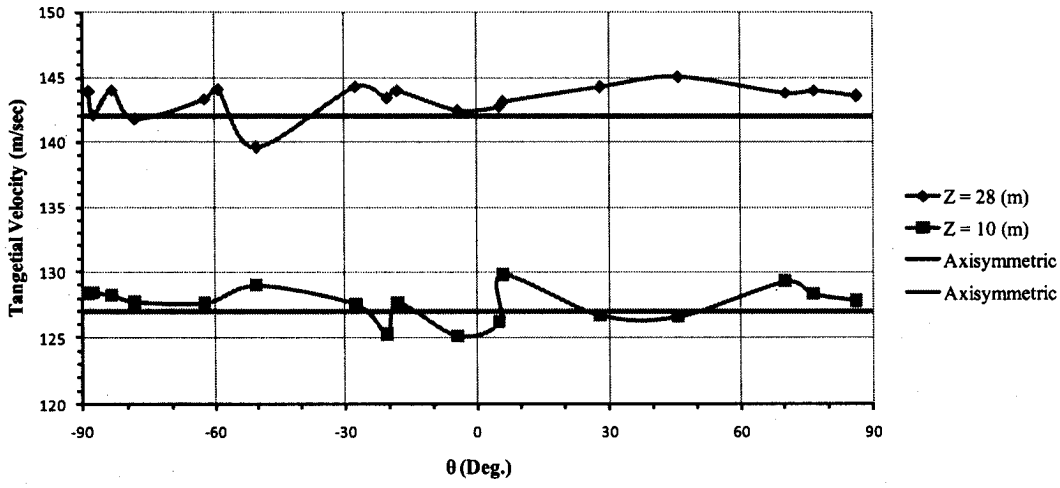

Fig. 2-5 Variation of the Tangential Velocity Component along Two Circumferences at r = 158 (m)

Similarly, the variation of the radial component along the circumference is shown in Fig. 2-6 for radial distance r = 158 (m) and z = 5 (m). The difference between the 3-D values along the circumference to the mean (axisymmetric) value, shown in Fig. 2-6, is relatively small.

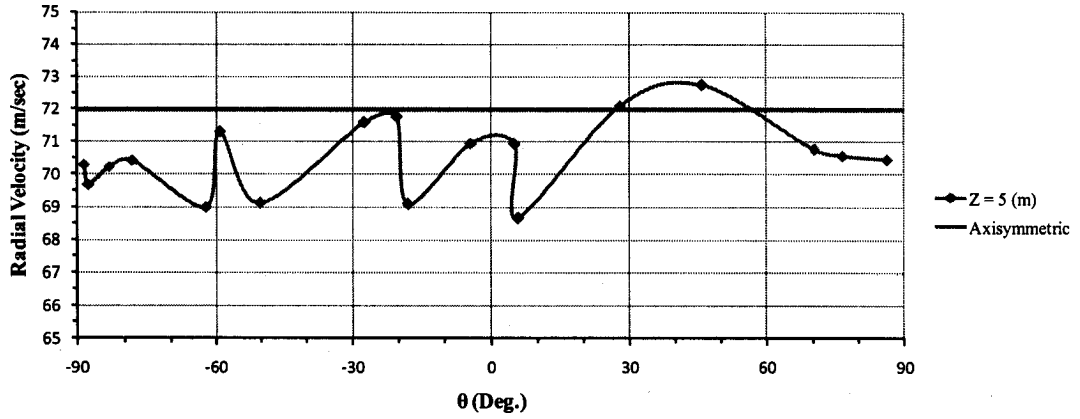

Fig. 2-6 Variation of the Radial Velocity Component along Two Circumferences at r = 158 (m)

2.4 F2 – Tornado Wind Field

Unfortunately, no field data measurements are available in literature for F2 tornadoes. This is despite the fact that 86% of categorized tornadoes are associated with F2 tornadoes or less as stated by the ASCE No. 74 guidelines (1991). With the lack of field data, the following procedure is employed to estimate a velocity field for F2 tornadoes from the CFD data:

1- Based on the ASCE No. 74 guidelines (1991), the gust wind speeds of F4 and F2 tornadoes are 116 (m/sec) and 70.2 (m/sec), respectively. Accordingly, the ratio between the F4 and the F2 gust wind speed is $\frac{116}{70.2} = 1.65$.

2- The field measurements of F4 tornado predicted a maximum tangential velocity of 142 (m/sec). Accordingly, an estimate of the maximum tangential velocity for the F2 tornado is $\frac{142}{1.65} = 86$ (m/sec).

3- As reported in Section (3), a velocity scale ratio $V_s = 13$ is established between the CFD data and the field measurements. This scale factor is applied to the set of data corresponding to various swirl ratios of 0.1, 0.4, 0.7, 0.8, 1, and 2. The maximum tangential velocity associated with the scaled values of different swirl ratio data is compared to the value of 86 (m/sec) estimated for the F2 tornadoes.

4- The comparison indicates that a swirl ratio S = 1 gives the best agreement with the maximum tangential velocity 86 (m/sec) estimated for the F2 tornadoes.

5- Accordingly, the set of data associated with S = 1 is used to simulate F2 tornadoes, together with the previously established scale factors $V_s = 13$ and $L_s = 4000$.

The peak values of the three components of the resulting wind field and their locations are provided in Table 2-1. Similar to the F4 wind field, the peak value of the three components occur at different locations.

The F2 tornado velocity profile has the same characteristics as the F4 profile described earlier with different values. Also, the locations at which the peak values occur are different between the F2 and F4 tornado fields. As a demonstration, the vertical profiles of the three velocity components for r = 100 (m) and r = 50 (m) are provided in Fig. 2-7 and Fig. 2-8, respectively.

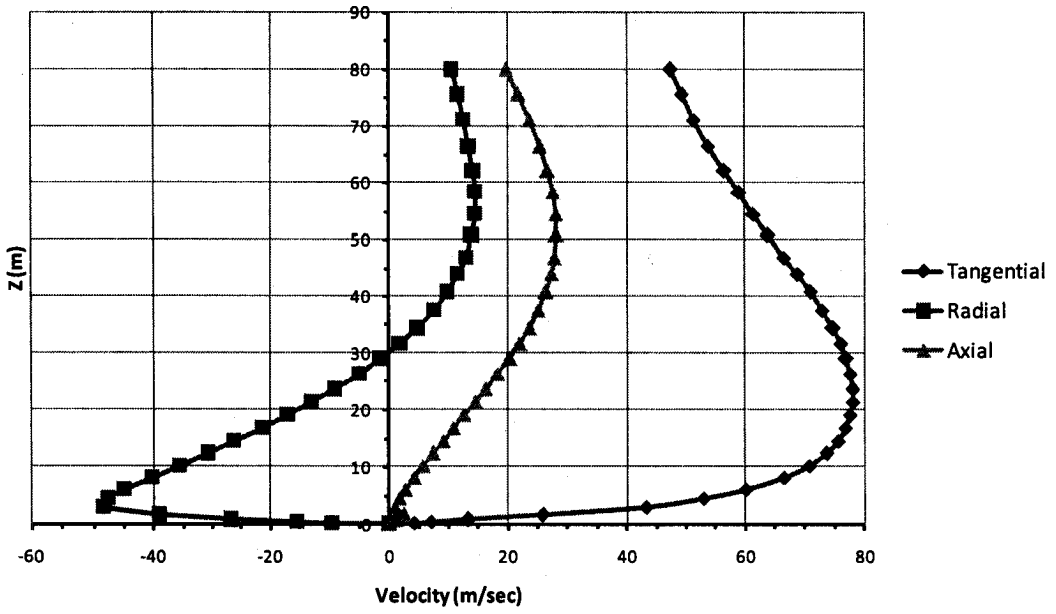

Fig. 2-7 Variation of the Three Velocity Components of F2 Tornado along the Height at r = 100 (m)

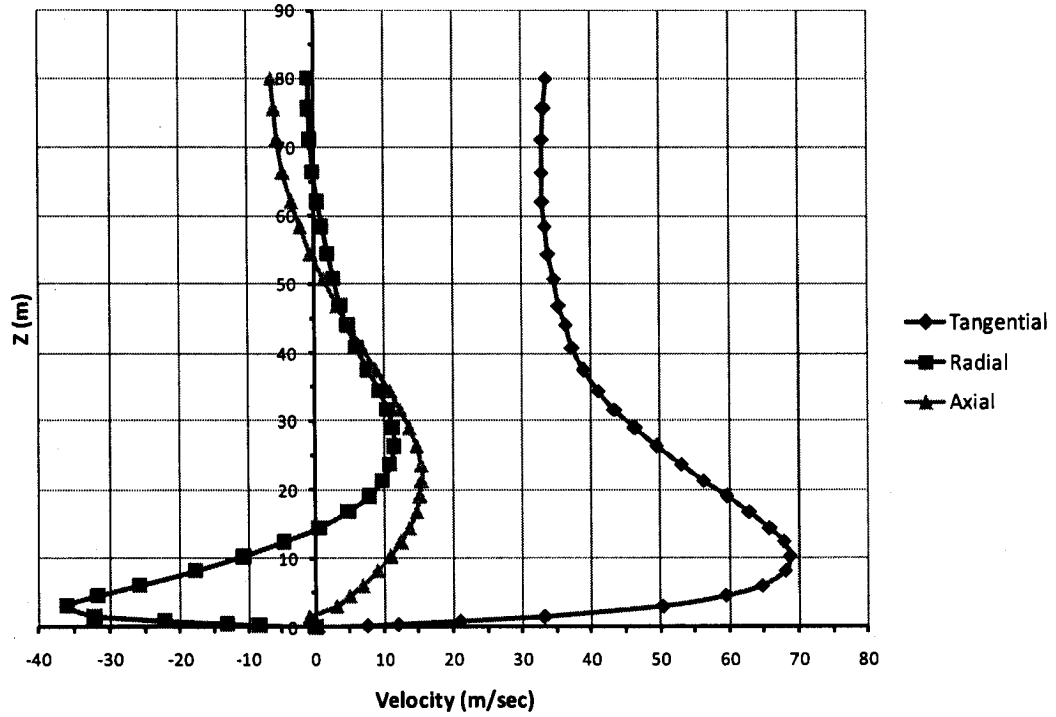

Fig. 2-8 Variation of the Three Velocity Components of F2 Tornado along the Height at r = 50 (m)

2.5 Evaluation of the Tornado Velocity Components at Arbitrary Location in the Tower and Conductors

The plan view of a transmission tower is shown in Fig. 2-9. The following steps are conducted to evaluate the tornado velocity components at the arbitrary point "a" shown in the figure:

1- The centre of the tower (point 0) is considered the origin of the set of axes used in the analysis. The location of the centre of the tornado relative to the centre of the tower is defined by the polar coordinates R and θ. An assumption is made regarding the location of the tornado and, consequently, the values of R and θ. Knowing R and θ and the coordinates of point "a", the coordinates R_{fa} and θ_{fa}, shown in Fig. 2-9, can be evaluated. They present the polar coordinates of point "a" relative to the centre of the tornado. In the view of the geometry of the tower, the vertical coordinate of point "a" is known and is identified by the variable Z_{fa}.

2- Based on the established value for the length scale $L_s = 4000$, the following equations can be used to obtain the model coordinates R_{ma} and Z_{ma} corresponding to R_{fa} and Z_{fa}, respectively.

$R_{ma} = R_{fa} / 4000$

$Z_{ma} = Z_{fa} / 4000$

Meanwhile, the model coordinate θ_{ma} remains the same as the full scale value θ_{fa}.

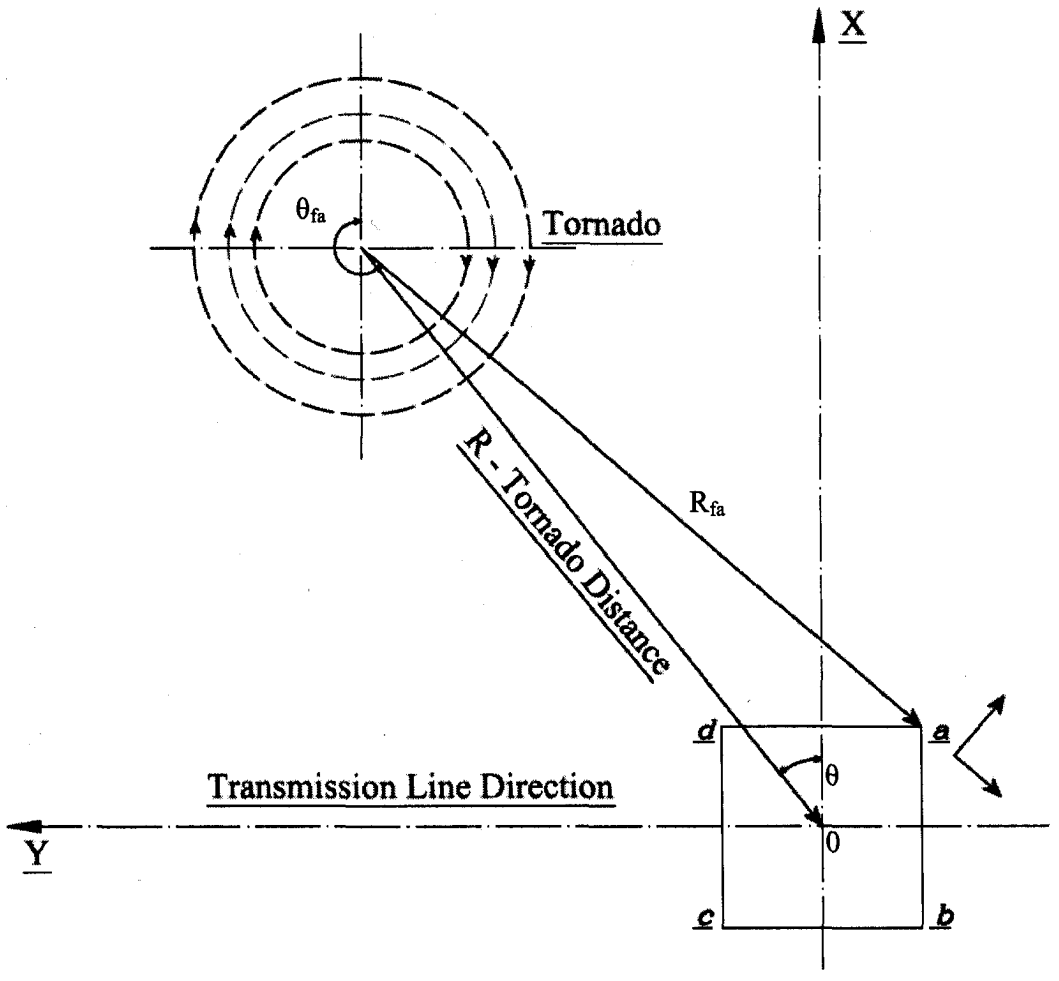

Fig. 2-9 Plan View of Transmission Tower and Tornado

3- Knowing R_{ma}, Z_{ma} and θ_{ma}, the 3-D set of data can be used to obtain the model radial velocity V_{rma}, tangential velocity V_{tma}, and axial velocity V_{ama} components. However, the values of R_{ma}, Z_{ma} and θ_{ma} might not coincide with any of the coordinate values at which the CFD data is provided. Accordingly, a three-dimensional linear interpolation scheme is conducted between the CFD data points to obtain the values of V_{rma}, V_{tma} and V_{ama}.

4- Based on the established velocity scale $V_s = 13$, the corresponding full scale velocity V_{AX}, V_{RD} and V_{TN} are given by :

$$V_{AX} = V_{ama} \times 13$$

$$V_{RD} = V_{rma} \times 13$$

$$V_{TN} = V_{tma} \times 13$$

The evaluation of the velocity components is conducted in a similar way for the axisymmetric data, with less computational effort since the variation with "θ" is eliminated.

2.6 Description of the Transmission Line System

Manitoba Hydro transmission tower type A-402-0 is chosen as a generic guyed tower to study the behaviour of transmission towers under F4 and F2 tornado loads. A photograph of the considered line system is provided in Fig. 2-10.

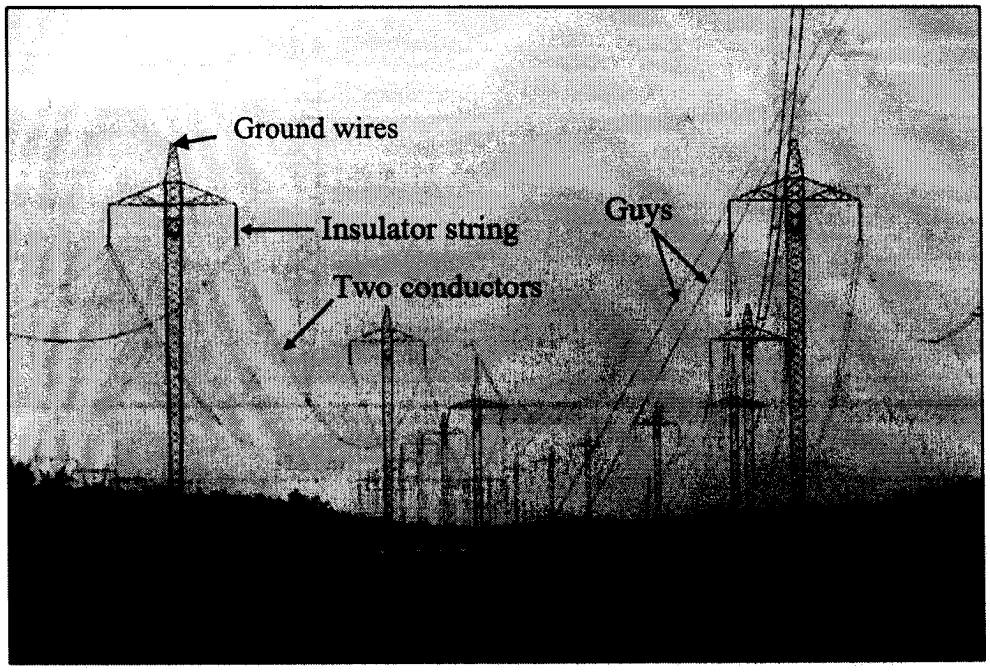

Fig. 2-10 Transmission Line System (Source: Manitoba Hydro Company, Canada)

The tower is supported using four guys, which are connected to the tower using two cross arms orthogonal to the conductors cross arms, located at an elevation of 35.18 (m). Four conductors hang between every two consecutive towers, two from each side, with an average span of 480 (m). The conductors are connected to the tower using insulators that are allowed to swing in two perpendicular planes.

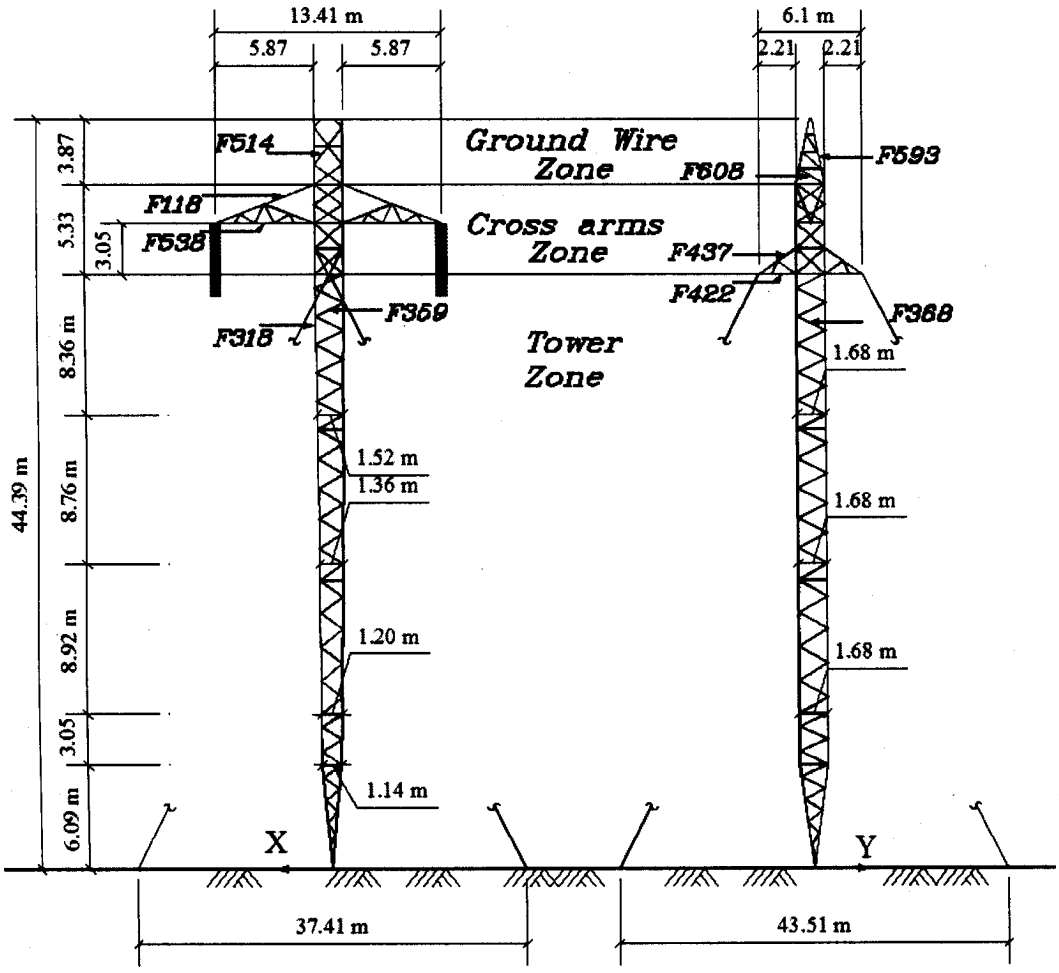

Fig. 2-11 Geometry of the Modelled Guyed Tower Type A-402-0.

One ground wire is attached to the top of the towers for lightning protection. The geometry of the towers is shown in Fig. 2-11. The total height of the tower is 44.39 (m),

with conductors attached at an elevation 38.23 (m). The material and geometric properties of the conductors, ground wire, guys, and insulators are provided in Shehata, *et al.* (2005).

2.7 Finite Element Modelling of Transmission Line/Tower

The tower, conductors, ground wire, guys, and insulators are modelled using the finite element commercial program SAP2000 (CSI 2008). Details of the model are discussed below.

2.7.1 Tower Modelling

A two-nodded non-linear three dimensional frame element with three translation and three rotational degrees of freedom per node is used to model the tower members. Each tower member is modelled using one element. Rigid connections are assumed between the tower members. This assumption is used to simulate the multi-bolted connections that are capable of transferring moments. The global coordinate system used in the simulation is shown in Fig. 2-12. The Y axis is along the direction of the conductors, the X axis is perpendicular to the conductors, and the Z axis is the vertical direction. Five towers and the in-between conductors and ground wire are included in the model. The middle one is the tower of interest and the other 4 towers are considered to simulate the exact stiffness of the entire system. The model includes three cable spans from each side of the tower of interest. It was shown by Shehata, *et al.* (2005) that such a number of cable spans provides an accurate prediction for the cable reactions transferred to the middle tower.

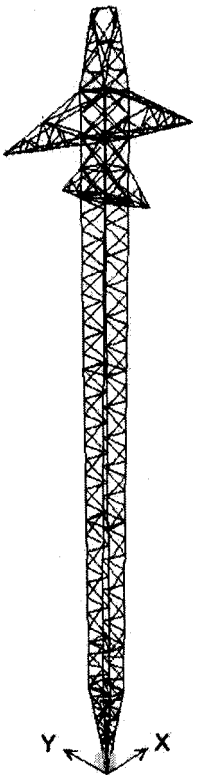

Fig. 2-12 Three Dimensional Tower Model with Global Coordinate System

2.7.2 Conductors, Ground Wire and Guys Modelling

The conductors, the ground wire and the guys exhibit a highly nonlinear behaviour. A non-linear three dimensional cable element is used to model these components. This element uses an elastic cable formulation to simulate the behaviour of slender cables under the effects of self-weight, pretension force, and external wind loading. Tension stiffness, sagging, and the geometric nonlinearities, resulting from large deformations and the P-delta effect, are included in the element formulation. The cable element has two nodes with three translation degrees of freedom at each node. The target pretension force of the cable is defined, and then nonlinear iterations are conducted to achieve this target pretension force. The stiffness matrix of the cable is calculated at the end of this load

increment. This stiffness matrix takes into account the tension stiffening resulting from the pretension force. The subsequent load increment involves the application of the tornado wind loads. Each cable span is divided into thirty cable elements.

2.7.3 Insulator strings modelling

Each insulator acts as a three dimensional pendulum. The insulators are modelled using two-nodded three dimensional truss elements with three translation degrees of freedom at each node. One element is used to model one insulator. An intermediate hinge is assumed at the connection between the insulators and the tower cross arms, allowing the insulators to rotate freely in two perpendicular planes.

2.8 Evaluation of Forces on Transmission Tower and Cables

The steps conducted to evaluate the tornado forces acting on the tower and the conductors associated with the tornado wind field are discussed below.

2.8.1 Forces Acting in Horizontal Plane

The wind force acting on a nodal point of the tower in a certain direction " i " is calculated using the following equation provided in the ASCE No. 74 guidelines (1991).

$$F_{wi} = \frac{1}{2} \rho_a (Z_v V_i)^2 G C_f A_i \quad (3)$$

Where F_{wi} is the wind force in " i " direction (N), ρ_a is the air density = 1.225 (kg/m^3); Z_v is the terrain factor; V_i is the tornado velocity component in " i " direction (m/sec); A_i is the projected area of all the elements connected to the considered node and perpendicular to the " i " direction; G is the gust response factor and C_f is the drag force coefficient . The value of G, and Z_v, are taken equal to 1 as recommended by the ASCE No. 74 guidelines (1991). A value of C_f equal to 1 is assumed for the conductor as

specified in the ASCE No. 74 guidelines (1991) and ANSI (1993). For the tower, the values of C_f are obtained from Table 2.6-1 of the ASCE No.74 guidelines (1991).

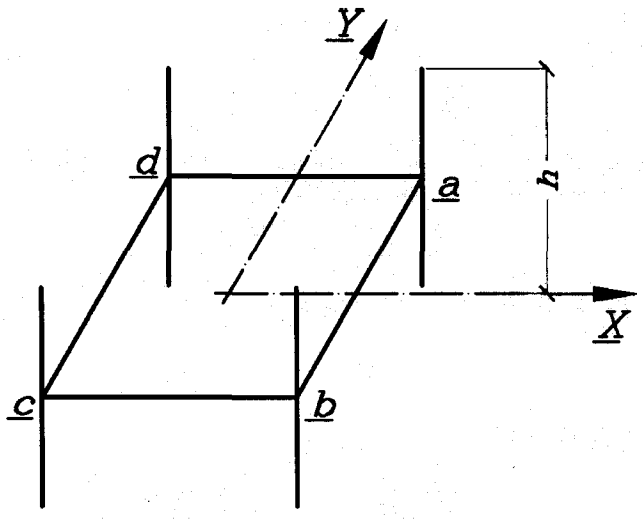

Fig. 2-13 Typical Horizontal Diaphragm of Transmission Tower

Fig. 2-13 shows a typical horizontal diaphragm of a transmission tower. The steps conducted to calculate the tornado forces acting on the nodal points a, b, c, and d are presented below:

1. The tangential V_{TN} and Radial V_{RD} components of the wind load are evaluated at points a, b, c, and d as illustrated before.
2. The velocity components V_{RD} and V_{TN} are resolved to evaluate the velocity components V_x and V_y acting along the cartesian coordinates for the four points a, b, c, and d.
3. Average velocities V_x' and V_y' are calculated for the four points along the X and Y directions, respectively.

4. In view of Eq. (3), the force F_x and F_y acting along X and Y directions are given by:

$$F_x = \frac{1}{2} \rho_a (V_x')^2 \ C_{fx} \ A_x \quad (4)$$

$$F_y = \frac{1}{2} \rho_a (V_y')^2 \ C_{fy} \ A_y \quad (5)$$

Where A_x and A_y are the projected area of all the elements connected to the considered node and perpendicular to the X and Y directions, respectively. The force coefficients C_{fx} in the X direction is calculated using the average of the force coefficients at the windward nodes of each direction. A similar step is done for the Y direction to calculate C_{fy}.

5. The forces F_x and F_y are distributed between the windward and leeward faces using the shielding factor K, given in NBCC (1990).
6. The force components on the windward and leeward faces are distributed between the nodes on each face based on the projected area served by each node.

A similar procedure is used to obtain the nodal forces acting on the conductors, ground wire and guys.

2.8.2 Forces Acting in Vertical Plane

The tower is divided into a number of segments; each segment is bound by two consecutive horizontal diaphragms of the tower. The sequence of distribution of loading depends on whether the vertical velocity is acting upward or downward.

For the downward case, the upper face of the segment is considered the windward face, while the lower face is considered the leeward face. The calculations start by evaluating the force acting on the top segment. First, the vertical forces acting on the top of the

tower are calculated using the same procedures employed for the evaluation of the horizontal forces, with the exception of using the axial velocity instead of the radial and tangential velocities. These top forces are distributed between the upper and lower face of this top segment using the shielding factor "K". The calculations proceed by considering the second top segment. The forces acting on the lower face of the top segment are now considered as the total force acting on the second top segment. Distribution takes place, once again, between the upper and lower face, as conducted for the top segment. The same steps are conducted progressively for various segments until the ground level is reached. For the upward case, the same steps are conducted, starting from the ground level until the top of the tower is reached. In this case, the lower face of the segment is considered as the windward face, while the upper face is considered as the leeward face.

The nodal vertical forces F_z for the conductors, the ground wire and the guys are calculated by applying Eq. (4).The value C_{fx} is replaced by $C_{fz} = 1.0$ and A_x by A_z, which is the projected area of the lines in the plane perpendicular to the Z-direction.

2.9 Steps of Analysis

The following steps are conducted to evaluate the response of a tower due to a specific tornado configuration:

1. The tower, the conductors, the ground wire, and the guys are modelled as described in Section (2.7). In addition to the tower of interest, two towers from each side of this specific tower are considered in the numerical model. The model includes five towers and six bays for each conductor, spanning between the five towers and the end hinged supports (see Fig. 2-14 for illustration). Each tower

member is modelled using a frame element, while thirty cable elements are used to model each conductor and ground wire span.

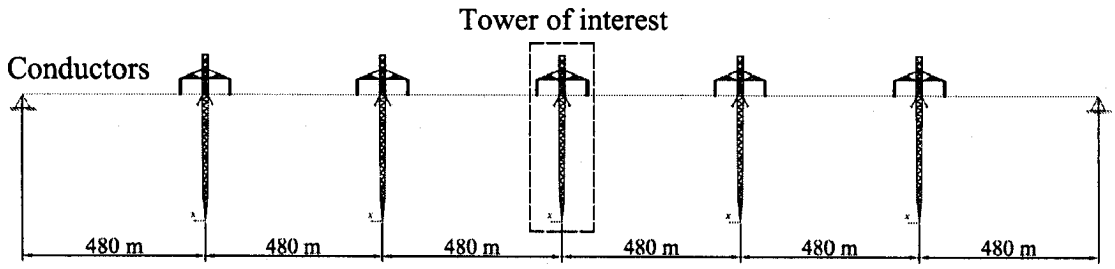

Fig. 2-14 Transmission Line System

2. The CFD data of the tornado model (either F4 or F2) is retrieved and stored.
3. A tornado configuration, i.e. its location relative to the centre of the tower of interest, is assumed based on selected values for the parameters R and θ shown in Fig. 2-9.
4. The procedure described in Section (2.5) is adopted to evaluate the tangential, radial, and axial velocity components at the nodal point of the tower of interest, and of the nodal points of the conductors, the ground wire and the guys as well.
5. The horizontal and vertical forces acting on the nodal points are evaluated using the procedures outlined in Section (2.8).
6. A set of nonlinear analysis is conducted for the transmission line as described below. The internal forces that develop in various members of the tower of interest due to the considered tornado configuration are evaluated.

2.10 Case Study

The transmission line system described in Section (2.6) is analyzed under tornado loading following the procedure outlined in the previous section. Two sets of analysis are

conducted using both the axisymmetric and the 3-D F4 tornado data. A comparison is carried out between the internal forces developing in selected members of the tower using these two sets of data. Another set of analysis is conducted using the 3-D F2 tornado data. A comparison is conducted between the internal forces associated with the F4, F2 tornadoes and those resulting from normal wind loads evaluated based on the ASCE No. 74 guidelines (1991).

For the two tornado scales (F2 and F4), three analyses are conducted using a fixed value for the distance R and three different values for the angle θ of 0°, 45°, and 90°, respectively. The values of R are taken equal to 158 (m) and 96 (m) for the F4 and F2 tornado, respectively. These values correspond to the location leading to the peak tangential velocity value at the tower of interest.

2.11 Results of the Analysis

The results of the nine conducted nonlinear analysis are presented for some selected members of the tower of interest. As shown in Fig. 2-11, the tower is divided into three zones. The tower zone is located below the supporting guys. The cross arms zone and the ground wire zone are located at the upper part of the tower. For the tower and the ground wire, the results are presented for one chord and two diagonal members, labelled as diagonal (1) and diagonal (2), respectively. Diagonal (1) and diagonal (2) are members located in plans parallel and perpendicular to the transmission line, respectively. The results of the analyses are provided in Table 2-2. For each set of analysis, the absolute maximum (tension) or minimum (compression) values resulting from the three "θ" configuration are provided for each member. The values of "θ" corresponding to these critical values are given in Table 2-2.

Table 2-2 Axial Forces in Selected Tower Members

Member				F4 Tornado (Axisymmetric CFD)		F4 Tornado (3-D CFD)		F2 - Tornado (3-D CFD)	ASCE*
		No.	Type	Axial Force (kN)	θ°	Axial Force (kN)	θ°	Axial Force (kN)	Axial Force (kN)
Tower Zone		*F318*	Chord	-657	*0*	-638	*0*	-75	34
		F368	Diagonal (1)	-61	*0*	-59	*0*	-3	3
		F359	Diagonal (2)	-106	*90*	-95	*90*	-6	1
Cross arms Zone	Guy	*F437*	Upper Chord	516	*90*	468	*90*	59	17
		F422	Lower Chord	-400	*90*	-362	*90*	-44	31
	Conductor	*F118*	Upper Chord	46	*45*	52	*45*	30	25
		F538	Lower Chord	-67	*45*	-72	*45*	-40	39
Ground Wire Zone		*F593*	Chord	-70	*0*	-72	*0*	-18	2
		F608	Diagonal (1)	8	*0*	5	*0*	1	1
		F514	Diagonal (2)	17	*0*	17	*0*	5	1

ASCE* : The reported values represent the absolute peak forces

The internal forces reported in the table, associated with normal wind loads, are calculated using 10 (m) reference wind velocity of 32.6 (m/sec), which is believed to be the wind speed used in designing this transmission line according to Manitoba Hydro, Canada. The following observations can be drawn from the results reported in the table:

- The difference between the results obtained using the 3-D and the axisymmetric data is small. It does not exceed 15% for all the reported cases.
- The F4 tornado leads to internal forces that are significantly higher than those resulting from the F2 tornado. This indicates that it might not be practical to design the tower members to resist an F4 tornado. It is known that F2 accounts for 86% of categorized tornadoes.

- The F2 tornado produces internal forces that are higher than those calculated under normal wind loads.
- For chord members located in the main body of the tower (tower zone and ground wire zone), the peak forces occur at $\theta = 0^{\circ}$, i.e. when the tangential components of the tornado wind field are parallel to the line direction.
- For diagonal members located in the main body of the tower (tower zone and ground wire zone), the peak values for diagonal (1) and diagonal (2) occur when the tangential components of the tornado wind field are parallel to the member vertical plane.
- For some members in the cross arm zone, the peak forces occur at $\theta = 45^{\circ}$. This configuration produces unbalanced forces on the conductor spans adjacent to the tower, leading to a resultant longitudinal force in the conductors. Such a force leads to an out-of-plane bending effect in the cross arms, which creates large force in the chord members in this region. Similar behaviour was reported by Shehata and El Damatty (2007) when they studied the tower behaviour under downbursts.

2.12 Conclusions

A numerical scheme for evaluating the response of transmission line structures to tornado loading is developed in this study. The tornado wind field is based on a Computational Fluid Dynamic (CFD) model that was developed and validated experimentally in a previous study. The CFD data, together with the tornado field measurements and the information provided in the design codes, are used to establish the wind field associated with F4 and F2 scale tornadoes. The procedure used to obtain the wind loads due to the tangential, radial, and axial velocity components of the wind field is described. A three-

dimensional finite element model for a transmission line system is developed. The model focuses on evaluating the response of one of the guyed towers of the system to tornado loads. The model includes a simulation for the tower of interest, in addition to two towers and three spans for the conductors, and the ground wire from each side of the tower of interest. The analysis is carried out in a nonlinear manner by including the effects of conductors' pretension, sagging, secondary moment, and large deformations.

A set of analysis is conducted under F4 scale tornado assuming that the tornado is located at the position leading to maximum tangential velocity at the tower of interest. The analysis is carried out using both axisymmetric and three-dimensional sets of tornado fields. The analysis is also repeated using a three-dimensional F2 tornado field, where the tornado is also assumed to be located at the position leading to maximum tangential velocity at the tower of interest. The following conclusions can be stated from the analyses conducted in the study:

- The vertical profiles of the F4 and F2 tornado wind fields have patterns that are different than the conventional boundary wind profile.
- The internal forces obtained from the analysis conducted using three-dimensional CFD data do not significantly differ than those obtained using the axisymmetric CFD data. The maximum difference is less than 15%.
- The peak values of the axial forces in the tower of interest are sensitive to the relative location between the centre of the tornado and the tower.
- The internal axial forces under F4 tornado are significantly higher than those resulting from the F2 tornado.

- The peak values of the axial forces resulting from the F2 tornado wind field are higher than the values resulting from normal wind load with reference velocity 32.6 (m/sec).

In light of these findings, it can be concluded that it is important to consider the tornado loading acting on towers and lines when designing a transmission line system.

2.13 References

American National Standards Institute (ANSI) (1993)," National Electrical Safety Code (NESC)", *Accredited Standards Committee C2,* USA.

American Society of Civil Engineers (ASCE) (1991), "Guidelines for electrical transmission line structural loading", *ASCE Manuals and Reports on Engineering Practice,* No. 74, NY.

Baker, D. E. (1981). "Boundary layers in laminar vortex flows." Ph.D. thesis, Purdue University.

Dempsey, D., and White, H., (1996) "Winds wreak havoc on lines.", *Transmission and Distribution World*, vol. **48**(6), pp. 32–37.

Fluent 6.2 User's Guide (2005), Fluent Inc.,Lebanon

Hangan, H., and Kim, J. (2008). "Swirl ratio effects on tornado vortices in relation to the Fujita scale." *Wind and Structures,* 11(4), 291-302.

Lee, Wen-Chau., and Wurman, J. (2005). "Diagnosed three-dimensional axisymmetric structure of the Mulhall tornado on 3 May 1999." *J.Atmos.Sci.,* **62**(7), 2373-93.

National Research Council of Canada (NRCC) (1990)," Supplement to the National Building Code of Canada 1990". *Associate Committee on the National Building Code*, Canada.

SAP2000 V.12 (2008), CSI Analysis Reference Manual, Computer and Structures, Inc. Berkeley, California, USA

Sarkar, P., Haan, F., Gallus, Jr., W., Le, K. and Wurman, J. (2005). "Velocity measurements in a laboratory tornado simulator and their comparison with numerical and full-scale data." *37th Joint Meeting Panel on Wind and Seismic Effects*. Tsukuba, Japan, May.

Savory, E., Parke, G. A. R., Zeinoddini, M., Toy, N., and Disney, P. (2001). "Modelling of tornado and microburst-induced wind loading and failure of a lattice transmission tower." *Eng.Struct.*, **23**(4), 365-375.

Shehata, A. Y., and El Damatty, A. A. (2008). "Failure analysis of a transmission tower during a microburst." *Wind and Structures, an International Journal,* **11**(3), 193-208.

Shehata, A. Y., and El Damatty, A. A. (2007). "Behaviour of guyed transmission line structures under downburst wind loading." *Wind and Structures, an International Journal,* **10**(3), 249-268.

Shehata, A. Y., El Damatty, A. A., and Savory, E. (2005). "Finite element modelling of transmission line under downburst wind loading." *Finite Elements Anal.Des.*, **42**, 71-89.

Wurman, J. (1998). "Preliminary results from the ROTATE-98 tornado study", *Preprints, 19th conf. On severe local storms,* Minneapolis, MN, 14-18 September, 120-123.

CHAPTER 3

BEHAVIOUR OF TRANSMISSION LINE STRUCTURES UNDER TORANDO WIND LOADING[2]

3.1 Introduction

Localized severe wind events, in the form of downbursts and tornadoes, are referred to as "High Intensity Winds (HIW)". Such events are responsible for more than 80% of all weather-related transmission line failures worldwide (Dempsey and White 1996). Despite this fact, the wind loads specified in the design codes for transmission line structures are based on large-scale wind storms. The wind fields associated with HIW have different profiles and unique characteristics compared to the boundary layer wind fields of large-scale events. Accordingly, wind loads due to HIW are different than those associated with the large-scale events. The research presented in this study is part of an extensive research program conducted at the University of Western Ontario, Canada, developed to understand the behaviour of transmission line structures under HIW. The current study focuses on assessing the behaviour of guyed transmission towers under tornado wind loading.

The development process of HIW, which usually occur during thunderstorms, was described by McCarthy and Melsness (1996). A tornado was defined by, Fujita (1981), as a rotating wind vortex moving at high speeds, affecting a relatively narrow path. Despite the many failures of transmission towers resulting HIW events, research studies related to this subject have been limited. Previous studies can be classified into two categories: a) Studies conducted to identify the wind field associated with HIW, and b)

[2] A version of this chapter is being prepared for publication in the *Journal of Wind and Structures*

Studies conducted to assess the structural response of transmission lines during HIW. Fujita and Pearson (1973) classified tornadoes based on their intensity and size. The intensities are defined by the gust wind speed, and the sizes are defined by the path length and width. The rating ranges from the smallest size, "F0", to the largest, "F5". Field measurements for tornadoes were conducted by Sarkar, *et al.* (2005) and Lee and Wurman (2005) for two different F4 tornadoes. Due to the difficulty of obtaining full-scale data, especially for the near ground region, laboratory simulations are used. These include Tornado Vortex Chambers (TVC), in which tornadoes are represented as vortices. The TVC's provide a good simulation of the characteristics inside a tornado, but the results are found to be sensitive and to be affected by the applied boundary conditions. For the near ground region, numerical simulations can provide a good assessment for the flow field. A Computational Fluid Dynamics (CFD) simulation for a small-scale tornado model was conducted by Hangan and Kim (2008) using the commercial program FLUENT (2001). The obtained wind field was validated in view of the experimental program conducted by Baker (1981) using a Ward-type vortex chamber. The failure of a self supported lattice tower under tornadoes and downburst wind profiles was investigated by Savory, *et al.* (2001). The tornado wind profile used in this study is based on the model developed by Wen (1975). The chosen tornado corresponded to F3 Fujita scale. The dynamic analysis was conducted for the tower alone, without modelling the transmission lines, and without considering the vertical velocity component of the tornado field. Hamada, *et al.* (2009) developed a numerical model for the analysis of transmission lines under tornadoes. The model included a simulation for the towers and the conductors. The wind field resulting from the Hangan and Kim (2008) simulation was

included in this numerical model. Due to the localized nature of HIW, the corresponding wind loads acting on the tower and the conductors vary significantly with the location of the HIW event relative to the tower. Various tower members can have different critical HIW locations that lead to maximum forces in these members. This was also shown in the studies conducted by Shehata and El Damatty (2007) and Shehata, *et al.* (2005) to assess the behaviour of guyed transmission lines under downburst loading.

In the current study, the numerical model developed by Hamada, *et al.* (2009) is used to conduct an extensive parametric study to assess the behaviour of a guyed transmission tower under tornado loading. The model includes a simulation for the tower of interest in addition to a number of adjacent towers and the in-between conductors. The parametric study is conducted by varying the location of the tornado relative to the tower of interest. A nonlinear finite element analysis is conducted under the tornado loads associated with each tornado location. The maximum and minimum internal forces obtained from the entire analyses are determined for all the tower members. The parametric study is conducted using both the F2 and F4 tornado fields. The Chapter begins by briefly describing the applied tornado wind fields. This is followed by a brief description of the finite element model. Results of the parametric study are presented, and then used to describe the structural behaviour of the tower under tornado loading. The results of the parametric study are then used to assess the sensitivity of the members' peak forces with the parameters defining the location of the tornado. Finally, the main conclusions obtained from the study are summarized.

3.2 F4 and F2 Tornado Wind Field

A Computational Fluid Dynamics (CFD) simulation for a small-scale tornado model was conducted by Hangan and Kim (2008) using the commercial program FLUENT (2001). The simulation was first conducted using swirl ratio S with a value of 0.28, which is the same swirl ratio applied in the experimental program conducted by Baker (1981) using a Ward-type vortex chamber. The experimental results were used to validate the CFD model. The numerical analysis was then extended by Hangan and Kim (2008) by considering values for S = 0.10, 0.4, 0.7, 0.8, 1.0 and 2.0, respectively.

By comparing the numerical results to the field measurements, Hangan and Kim (2008) estimated that the F4 tornado corresponds to a swirl ratio S=2. The proper length "L_s = 4000" and velocity scale "V_s = 13" factors between the numerical and the full-scale data were also established in the same study. In the study conducted by Hamada, *et al.* (2009), it was established that a swirl ratio S = 1 provides a good simulation for the F2 scale tornadoes. As such, the wind fields of fully developed F4 and F2 tornadoes can be estimated from the CFD data corresponding to S = 2 and S = 1, respectively, after scaling the data using the length "L_s = 4000" and velocity scale "V_s = 13" factors. The velocity profiles vary with space in a three dimensional manner, and are presented as functions of the cylindrical coordinates r, θ and z, measured relative to the tornado centers. The tornado wind fields have three velocity components; the axial component $V_{ma}(r, \theta, z)$, the radial component $V_{mr}(r, \theta, z)$, and the tangential component $V_{mt}(r, \theta, z)$. In addition to the three-dimensional wind field, an axisymmetric wind field for a F4 tornado is generated by averaging the three velocity components along the circumferential direction, and eliminating the variation of the velocities with θ.

3.3 Finite Element Modelling of Transmission Line System

The transmission line system simulated in the current study is a generic guyed tower used in Manitoba Hydro transmission line systems. The chosen guyed tower is labelled as Type A-402-0. The tower height is 44.39 (m) and is supported by four guys attached to the tower, with two cross arms at an elevation 35.18 (m) relative to the ground. Two conductors are connected to the towers cross arms using a 4.27 (m) insulator at a height of 38.23 (m). One ground wire is connected to the top of the tower. The conductors and ground wire span is 480 (m). The conductors and ground wire sag is 20 (m) and 13 (m), respectively. Fig. 3-1 shows a schematic of the transmission line system. The geometric and material properties of the conductors, ground wire and guys are provided by Shehata, *et al.* (2005).

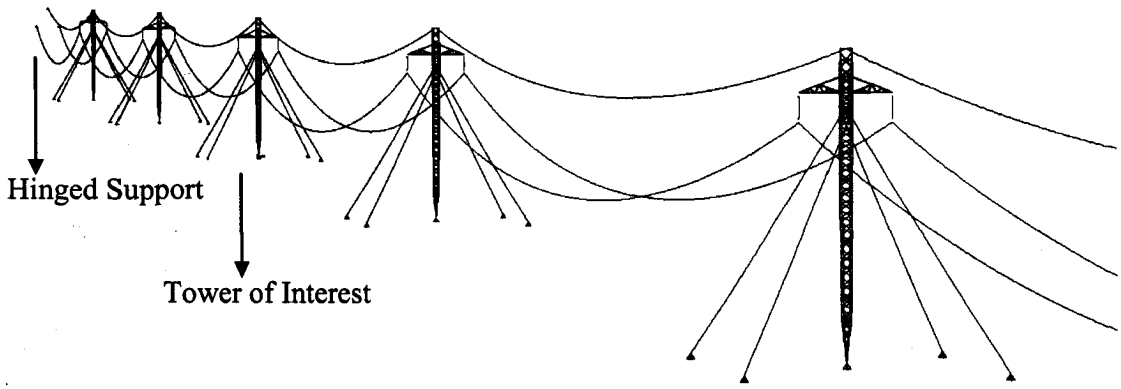

Fig. 3-1 Transmission Line System

The simulated transmission line system consists of the tower of interest and two towers from each side, which are included in order to properly simulate the rigidity of the system. As shown in Fig. 3-1, the model includes five towers with six bays for conductors and ground wire. Such a number of bays was recommended by Shehata, *et al.*

(2005), in order to accurately account for the forces transferred from the conductors to the tower of interest. The transmission line system is modelled using the numerical finite element commercial program SAP 2000 (CSI 2008).

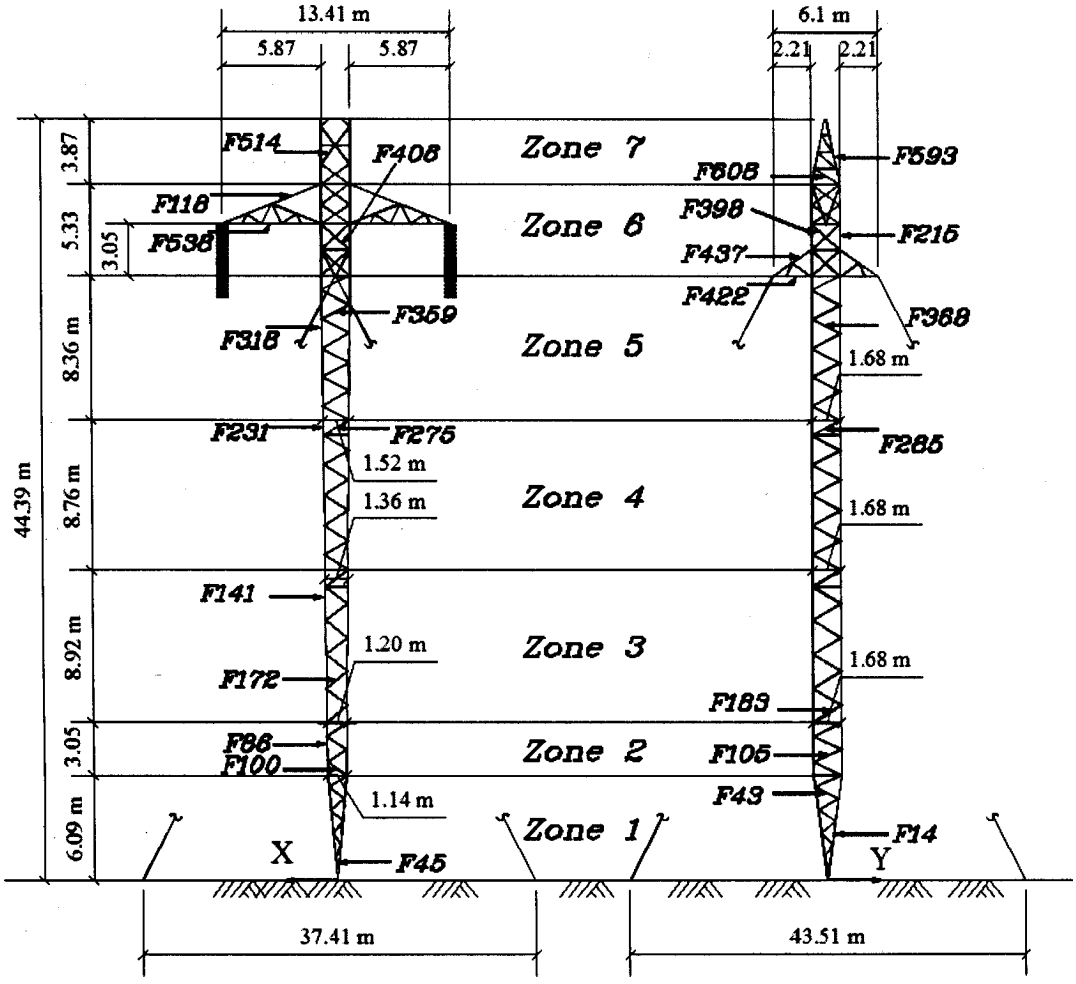

Fig. 3-2 Geometry of the Modelled Guyed Tower Type A-402-0

As shown in Fig. 3-2, the tower is divided into seven zones. Zones 1 to 5 are located below the supporting guys. Zone 6 represents the cross arm area of the conductors and the guys. Zone 7 is the upper part of the tower, which supports the ground wire.

The tower members are modelled using two nodded three-dimensional frame elements. Each member is modelled using one element, with three translation and three rotational degrees of freedom per node. Rigid connections are assumed between the tower members in order to simulate the multi bolted connections used in the construction of the tower. Three-dimensional nonlinear cable elements are used to model the conductors, the ground wire and the guys. Conductors and ground wires exhibit highly nonlinear behaviour, due to their large spans and slender cross sections. The cable element nonlinear formulation includes the effects of tension stiffness, sagging and geometric nonlinearity, resulting from large deformations and the P-delta effect. More details regarding the cable element formulation are provided by Hamada, *et al.* (2009). The insulators, connecting the conductors to the tower cross arms, are modelled using two-nodded three-dimensional truss elements, having three translation degrees of freedom at each node.

3.4 Evaluation of the Tornado Velocity Components and Forces on Transmission Tower and Cables

The set of axes used in the analysis are shown in Fig. 3-3. As shown in the figure, the origin of the axes is located at the centre of the tower of interest. The Y-axis is along the direction of the lines, the X-axis is perpendicular to the lines, and the Z-axis is parallel to the vertical direction. The polar coordinates R and θ are used to define the location of the centre of the tornado relative to the tower of interest. The procedure used to evaluate the tornado velocity components at an arbitrary location in the transmission line are described in details by Hamada, *et al.* (2009).

The following equation provided in the ASCE No. 74 guidelines (1991) is used to evaluate the wind forces acting on the tower and the conductors' nodes in a certain direction "i".

$$F_{wi} = \frac{1}{2} \rho_a (Z_v V_i)^2 G C_f A_i \quad (1)$$

Where F_{wi} is the wind force in " i " direction (N), ρ_a is the air density = 1.225 (kg/m^3); Z_v is the terrain factor; V_i is the tornado velocity component in the " i " direction (m/sec); A_i is the projected area of all the elements connected to the considered node and perpendicular to the " i " direction; G is the gust response factor; and C_f is the drag force coefficient . The value of G, and Z_v, are taken equal to 1 as recommended by the ASCE No. 74 guidelines (1991). A value of C_f equal to 1 is assumed for the conductor as specified in the ASCE No. 74 guidelines (1991) and ANSI (1993). For the tower, the values of C_f are obtained from Table 2.6-1 of the ASCE No.74 guidelines (1991). The evaluations of wind forces on the tower and the lines are described in details by Hamada, *et al.* (2009).

3.5 Parametric Study

The parametric study is conducted by carrying out a large number of static analyses. The self weight of the towers and the lines are considered in the analysis. Each analysis corresponds to a specific location for the tornado, defined by the polar coordinates R and θ, as shown in Fig. 3-3. The analyses are conducted in a quasi-static manner despite the convective velocity of the tornadoes. This is justified by the fact that, the applied tornado field is scaled such that the maximum tangential velocities for the F4 and the F2 tornadoes are equal to those observed in the field, which include both the local and convective velocity components. As such, the effect of the convective component is

accounted for implicitly in the tornado field. The conducted parametric study consists of three parts. Part one assesses the behaviour of the transmission line under both the axisymmetric and the 3-D F4 tornado wind field. In the second part, the behaviour is assessed under the F2 tornado wind field. In the third part, the analyses are conducted under both the F4 and the F2 tornadoes, while simulating the middle tower alone, i.e. without including the conductors. This is done in order to assess the importance of considering the conductors in the analysis and design of transmission lines.

3.5.1 Transmission Line System under F4 Tornado Wind Field

Two sets of analyses are conducted, using both the axisymmetric and the 3-D F4 tornado data, respectively. The tornado wind field has a maximum tangential velocity of 142 (m/sec), which occurs at a radius r = 158 (m) and a height z = 28 (m). The maximum radial velocity is 79 (m/sec) and occurs at a radius r = 273 (m) and a height z = 7 (m).

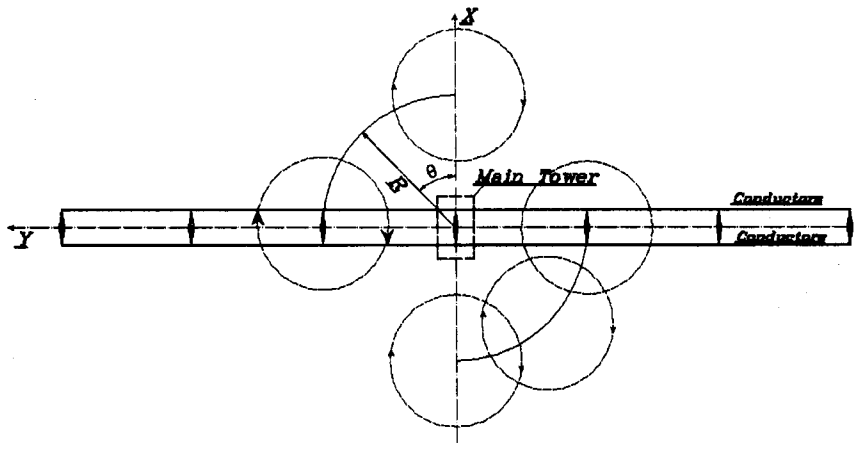

Fig. 3-3 Tornado Parameters Employed in the Parametric Study

The vertical velocity component fluctuates between upward and downward directions at different regions of the tornado wind field, with a maximum upward value of 62 (m/sec).

Table 3-1 Results of the Parametric Study Due To F4 Tornado Wind Fields

	Member		F4 Tornado (Axisymmetric)				F4 Tornado (3-D)			
	No.	Type	Maximum Axial Force		Minimum Axial Force		Maximum Axial Force		Minimum Axial Force	
			(kN)	Tornado	(kN)	Tornado	(kN)	Tornado	(kN)	Tornado
Zone 1	F14	Chord	127	R = 100 θ = 240	-453	R = 200 θ = 90	80	R = 100 θ = 210	-427	R = 200 θ = 90
	F43	Diagonal (1)	18	R = 200 θ = 135	-8	R = 200 θ = 330	9	R = 200 θ = 135	-4	R = 200 θ = 315
	F45	Diagonal (2)	11	R = 100 θ = 240	-45	R = 200 θ = 120	43	R = 200 θ = 315	-38	R = 200 θ = 90
Zone 2	F86	Chord	164	R = 100 θ = 210	-449	R = 200 θ = 90	140	R = 200 θ = 180	-440	R = 200 θ = 0.0
	F105	Diagonal (1)	85	R = 200 θ = 150	-66	R = 200 θ = 330	71	R = 200 θ = 150	-61	R = 200 θ = 330
	F100	Diagonal (2)	46	R = 200 θ = 300	-37	R = 200 θ = 120	35	R = 200 θ = 300	-33	R = 200 θ = 120
Zone 3	F141	Chord	363	R = 200 θ = 180	-652	R = 200 θ = 330	378	R = 200 θ = 180	-678	R = 200 θ = 0.0
	F183	Diagonal (1)	71	R = 200 θ = 150	-56	R = 200 θ = 330	74	R = 200 θ = 150	-59	R = 200 θ = 330
	F172	Diagonal (2)	14	R = 200 θ = 0.0	-12	R = 200 θ = 270	12	R = 200 θ = 330	-16	R = 400 θ = 120
Zone 4	F231	Chord	444	R = 200 θ = 180	-807	R = 200 θ = 330	453	R = 200 θ = 180	-763	R = 200 θ = 330
	F285	Diagonal (1)	48	R = 200 θ = 300	-35	R = 200 θ = 150	40	R = 200 θ = 330	-37	R = 300 θ = 135
	F275	Diagonal (2)	73	R = 200 θ = 300	-62	R = 200 θ = 120	75	R = 200 θ = 300	-68	R = 200 θ = 90
Zone 5	F318	Chord	324	R = 200 θ = 180	-726	R = 200 θ = 330	332	R = 200 θ = 180	-698	R = 200 θ = 330
	F368	Diagonal (1)	66	R = 200 θ = 150	-81	R = 200 θ = 330	60	R = 200 θ = 135	-71	R = 200 θ = 330
	F359	Diagonal (2)	97	R = 200 θ = 300	-107	R = 200 θ = 90	97	R = 200 θ = 300	-96	R = 200 θ = 90
Zone 6 Tower	F215	Chord	94	R = 200 θ = 135	-152	R = 200 θ = 270	105	R = 200 θ = 135	-153	R = 200 θ = 315
	F398	Diagonal (1)	115	R = 400 θ = 300	-15	R = 300 θ = 45	104	R = 300 θ = 300	-14	R = 500 θ = 30
	F406	Diagonal (2)	40	R = 300 θ = 120	-125	R = 300 θ = 300	44	R = 200 θ = 120	-118	R = 300 θ = 300
Zone 6 Guy	F437	Upper Chord	687	R = 300 θ = 120	8	R = 500 OW+P.S.*	659	R = 300 θ = 135	6	R = 300 θ = 225
	F422	Lower Chord	6	R = 200 θ = 300	-469	R = 300 θ = 120	6	R = 200 θ = 300	-443	R = 300 θ = 120
Zone 6 Conductor	F118	Upper Chord	81	R = 500 θ = 90	-45	R = 500 θ = 270	85	R = 500 θ = 90	-45	R = 400 θ = 270
	F538	Lower Chord	84	R = 400 θ = 270	-129	R = 400 θ = 90	82	R = 400 θ = 300	-128	R = 400 θ = 90
Zone 7	F593	Chord	86	R = 200 θ = 150	-84	R = 200 θ = 330	86	R = 200 θ = 150	-87	R = 200 θ = 330
	F608	Diagonal (1)	9	R = 200 θ = 0.0	-9	R = 200 θ = 180	9	R = 200 θ = 0.0	-8	R = 200 θ = 180
	F514	Diagonal (2)	27	R = 500 θ = 90	-27	R = 500 θ = 270	30	R = 500 θ = 90	-30	R = 400 θ = 270

OW+P.S. : Own weight + pretension force*

The location of the tornado varies by considering five values of R equal to 0.0, 100 (m), 200 (m), 300 (m), 400 (m), and 500 (m), respectively. For each value of R, 16 different values of θ are considered, ranging between 0.0° and 330°, with an increment of 15°. The results of the analyses are presented for several selected chord and diagonal members of

the tower. In this presentation, diagonal (1) and diagonal (2) represent members located in planes parallel and perpendicular to the transmission line, respectively.

For zone (6), the results are presented for upper and lower chord members of the conductors' cross-arms and the guys' cross-arms. For each selected member, the maximum and minimum force resulting from the entire parametric study analysis is reported in Table 3-1. In the same table, the tornado parameters R and θ corresponding to the maximum and minimum forces are provided.

The following observations can be drawn from the results provided in the table:

- The maximum and minimum axial forces of the tower members vary significantly with the location of the tornado relative to the tower.
- The difference between the internal forces, resulting from the axisymmetric and the 3-D data, is not large. For 65% of the selected members, the axisymmetric data leads to higher forces compared to the 3-D data.
- The difference between the results of the axisymmetric and 3-D analyses are more pronounced in zones 1, 2 and 3, in compression to the rest of the zones. This can be interpreted by the occurrence of large instability in the wind field in this region, which is detected only in the 3-D data, as reported by Hangan and Kim (2008).

3.5.2 Transmission Line System under F2 Tornado Wind Field

The maximum tangential velocity of the F2 tornado is 78 (m/sec) and occurs at a radius r = 96 (m) and a height z = 19 (m). The maximum radial velocity is 49 (m/sec) and corresponds to a radius r = 146 (m) and a height z = 6 (m). This parametric study is conducted using the same range for the parameters R and θ used in the previous section.

The results of this parametric, in terms of peak internal forces for various members of the tower and the associated critical tornado locations, are provided in Table 3-2.

Table 3-2 Results of the Parametric Study Due to F2 Tornado, Downburst and Conventional Wind Fields

Member			F2 Tornado (3-D CFD)				D.B. Loading	ASCE	M.H. Forces	
	No.	Type	Maximum Axial Force		Minimum Axial Force		Axial Force	Axial Force	Members Capacity	Compression Force
			(kN)	*Tornado*	(kN)	*Tornado*	(kN)	(kN)	(kN)	(kN)
Zone 1	*F14*	Chord	-21	*R = 50 / θ = 180*	-130	*R = 200 / θ = 180*	48	46	162	-154
	F43	Diagonal (1)	1	*R = 300 / θ = 135*	-0.3	*R = 300 / θ = 330*	1	1	14	-2
	F45	Diagonal (2)	-0.3	*R =100 / θ = 300*	-12	*R = 200 / θ = 180*	4	4	9	-1
Zone 2	*F86*	Chord	-14	*R =100 / θ = 180*	-122	*R = 200 / θ = 180*	50	48	179	-180
	F105	Diagonal (1)	7	*R =200 / θ = 135*	-7	*D 100 / θ = 330*	4	4	15	-6
	F100	Diagonal (2)	5	*R = 100 / θ = 300*	-5	*R = 200 / θ = 180*	2	1	11	-7
Zone 3	*F141*	Chord	7	*R = 200 / θ = 150*	-114	*R = 200 / θ = 300*	62	59	179	-180
	F183	Diagonal (1)	7	*R = 200 / θ = 150*	-6	*R = 100 / θ = 330*	4	3	15	-6
	F172	Diagonal (2)	3	*R = 400 / θ = 300*	-5	*R = 200 / θ = 120*	1	1	11	-7
Zone 4	*F231*	Chord	34	*R = 100 / θ = 150*	-145	*R = 200 / θ = 300*	62	58	209	-203
	F285	Diagonal (1)	4	*R = 100 / θ = 330*	-3	*R = 100 / θ = 135*	2	2	12	-4
	F275	Diagonal (2)	10	*R = 100 / θ = 315*	-16	*R = 200 / θ = 180*	5	6	21	-9
Zone 5	*F318*	Chord	37	*R = 200 / θ = 150*	-157	*R = 200 / θ = 315*	53	69	220	-219
	F368	Diagonal (1)	7	*R = 100 / θ = 150*	-7	*R = 100 / θ = 315*	4	4	12	-7
	F359	Diagonal (2)	13	*R = 100 / θ = 315*	-14	*R = 200 / θ = 180*	7	7	24	-11
Zone 6 Tower	*F215*	Chord	23	*R = 200 / θ = 135*	-58	*R = 200 / θ = 315*	25	37	302	-206
	F398	Diagonal (1)	25	*R = 400 / θ = 300*	-4	*R = 300 / θ = 45*	11	4	46	-21
	F406	Diagonal (2)	12	*R = 200 / θ = 120*	-36	*R = 200 / θ = 315*	19	21	46	-36
Zone 6 Guy	*F437*	Upper Chord	135	*R = 300 / θ = 120*	5	*R = 100 / θ = 30*	39	28	99	0
	F422	Lower Chord	0.1	*R = 400 / θ = 300*	-93	*R = 300 / θ = 120*	33	36	172	-156
Zone 6 Conductor	*F118*	Upper Chord	36	*R = 400 / θ = 90*	13	*R = 400 / θ = 300*	21	28	65	0
	F538	Lower Chord	-11	*R = 400 / θ = 300*	-54	*R = 400 / θ = 90*	28	45	149	-146
Zone 7	*F593*	Chord	24	*R = 100 / θ = 180*	-27	*R = 400 / θ = 90*	11	3	51	-28
	F608	Diagonal (1)	1	*R = 100 / θ = 330*	-1	*R = 100 / θ = 150*	1	1	12	-2
	F514	Diagonal (2)	9	*R = 400 / θ = 90*	-10	*R = 400 / θ = 270*	5	2	55	-29

In the same table, a comparison is carried out between the internal forces resulting from the F2 tornado and those resulting from normal wind loading and downburst loading. This particular tower was designed using a 10 (m) reference wind speed of 32.6 (m/sec). Therefore, the peak forces in the selected members are calculated under normal wind loads using ASCE No. 74 guidelines (1991) for exposed rural terrain, and reference wind speed of 32.6 (m/sec) . The members' internal forces under downburst, with reference velocity = 32.6 (m/sec) were provided by Shehata and El Damatty (2007). In these calculations, four values for the angle $\theta = 90^{\circ}, 45^{\circ}, 30^{\circ}$ and 0° are employed. In the last two columns of the table, the strength capacity of the members, as well as the design compression forces, as calculated by Manitoba Hydro Company, Canada, are provided.

The following observations can be drawn from the results shown in the table:

- The peak values of the axial forces in the tower members under the F2 tornado wind field are sensitive to the relative location between the centre of the tornado and the tower. The critical tornado locations that lead to these peak forces differ for various members of the tower. The critical tornado locations for the F2 tornado are almost the same as those for the F4 tornado.
- The members' axial forces, resulting from the F2 tornado, are significantly less than those due to the F4 tornado.
- The peak axial forces due to F2 tornado exceed the corresponding values resulting from normal wind and downburst loading. However, these peak forces are less than the members' capacities for all cases, with the exception of member F437, which is an upper chord member in the guy cross arm. It should be noted that the

strength design of the members might have been governed by other load cases, such as ice loading.

3.5.3 Transmission Tower Alone under F4 and F2 Tornado Wind Fields

The purpose of this part of the study is to assess the importance of considering the conductors and ground wires in the analysis and design of transmission line systems under tornado loading. In addition, the results of this study can serve to estimate the internal forces induced in the tower members in case of failure of the conductors during a tornado event.

The parametric study conducted in Sections 5.1 and 5.2 for the transmission line system, under F4 and F2 tornadoes, is repeated, while considering the intermediate tower alone, i.e. without considering the conductors and the ground wire. The analyses are conducted using the axisymmetric F4 and the 3-D F2 tornado wind fields, and employing the same range for the parameters R and θ applied in the previous two parametric studies. The results of this study are reported in Table 3-3. In the last column of the table, the members' internal forces, resulting from the combined effect of self-weight and conductors' pretension forces are reported.

By comparing the forces reported in Table 3-3 to those provided in Table 3-1 and Table 3-2, it can be concluded that the reduction in the members' forces, due to the exclusion of the conductors and the ground wire, is more significant at zones 6 and 7. Some members, in zones 1 to 5, experience higher internal forces when the conductors are excluded, e.g. Diagonal (2) members. This is due to the over-hanging beam behaviour, further explained in Section (3.6.1).

Table 3-3 Results of the Parametric Study Conducted for Tower Alone

Member				Tower Only under F4 Tornado		Tower Only under F2 Tornado		Tower and Conductors Self-weight
		No.	Type	Maximum Axial Force (kN)	Minimum Axial Force (kN)	Maximum Axial Force (kN)	Minimum Axial Force (kN)	Axial Force (kN)
Zone 1		*F14*	Chord	175	-366	-7	-110	-27.60
		F43	Diagonal (1)	25	-6	1	-1	0.04
		F45	Diagonal (2)	15	-63	1	-12	-1.50
Zone 2		*F86*	Chord	191	-380	-5	-105	-26.40
		F105	Diagonal (1)	86	-61	6	-7	0.10
		F100	Diagonal (2)	60	-46	7	-6	-0.03
Zone 3		*F141*	Chord	258	-550	2	-99	-25.25
		F183	Diagonal (1)	73	-51	7	-6	-0.07
		F172	Diagonal (2)	20	-20	3	-6	0.03
Zone 4		*F231*	Chord	302	-595	16	-82	-23.75
		F285	Diagonal (1)	51	-36	4	-3	-0.10
		F275	Diagonal (2)	67	-56	9	-14	-0.07
Zone 5		*F318*	Chord	190	-513	10	-80	-23.00
		F368	Diagonal (1)	63	-79	7	-7	0.03
		F359	Diagonal (2)	96	-78	12	-12	0.02
Zone 6	Tower	*F215*	Chord	80	-116	15	-16	-13.30
		F398	Diagonal (1)	99	-12	20	-6	1.00
		F406	Diagonal (2)	7	-36	4	-8	-6.70
	Guy	*F437*	Upper Chord	622	4	95	5	8.35
		F422	Lower Chord	2	-361	-1	-55	-4.50
	Conductor	*F118*	Upper Chord	14	-12	4	-2	25.70
		F538	Lower Chord	21	-21	5	-7	-36.60
Zone 7		*F593*	Chord	11	-11	2	-2	-0.10
		F608	Diagonal (1)	9	-9	1	-1	-0.06
		F514	Diagonal (2)	5	-5	1	-2	-1.00

3.6 Behaviour of Transmission Line under F4 – Tornado

The purpose of this section is to understand the structural behaviour of the guyed tower under tornado loading in view of the results of the parametric study. An attempt will be made to interpret the values of the critical tornado locations obtained for members of various zones of the tower. The interpretation will be conducted using the results of the analysis under the F4 – axisymmetric tornado field. The behaviour under the F2 tornado follows the same trend with smaller amplitudes for the members' internal forces.

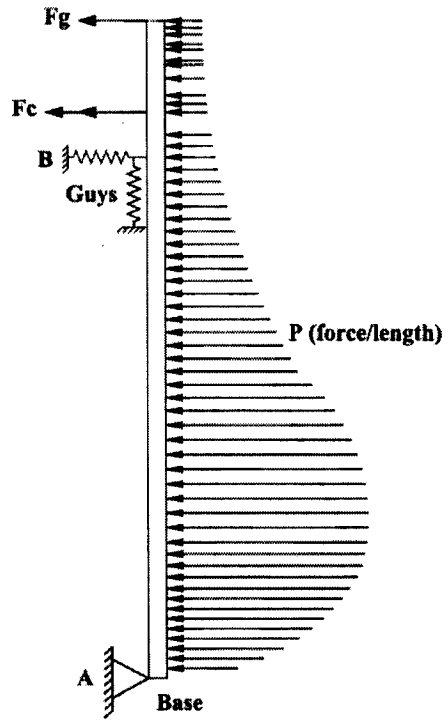

Fig. 3-4 Simulation of the Tower as an Overhanging Beam

A schematic of the structural system of the guyed tower is shown in Fig. 3-4. In this figure, the tower is represented as a beam simply hinged at its base and supported by a spring system, simulating the stiffness of the guys. The distributed load, P (force/length) as shown in Fig. 3-4, results from the tornado loads acting on the body of the tower.

Meanwhile, the two concentrated forces, Fc and Fg, result from the tornado loads acting on the conductors and ground wire, respectively.

3.6.1 Zones (1) to (5)

These zones are located between points A and B, shown in Fig. 3-4. The distributed load P and the concentrated loads, Fc and Fg, tend to have opposite effects on the straining actions that develop in these zones. As such, the straining actions are expected to increase with an increase in "P" and a decrease in both "Fg" and "Fc". The results shown in Table 3-1 indicate that the peak force in these zones are associated with values of R = 200 (m) and R = 100 (m). The vertical profile of the tornado wind field has maximum tangential and radial velocities at r = 158 (m) and 273 (m), respectively. Such profiles for the two velocity components at these two locations are provided in Fig. 3-5.

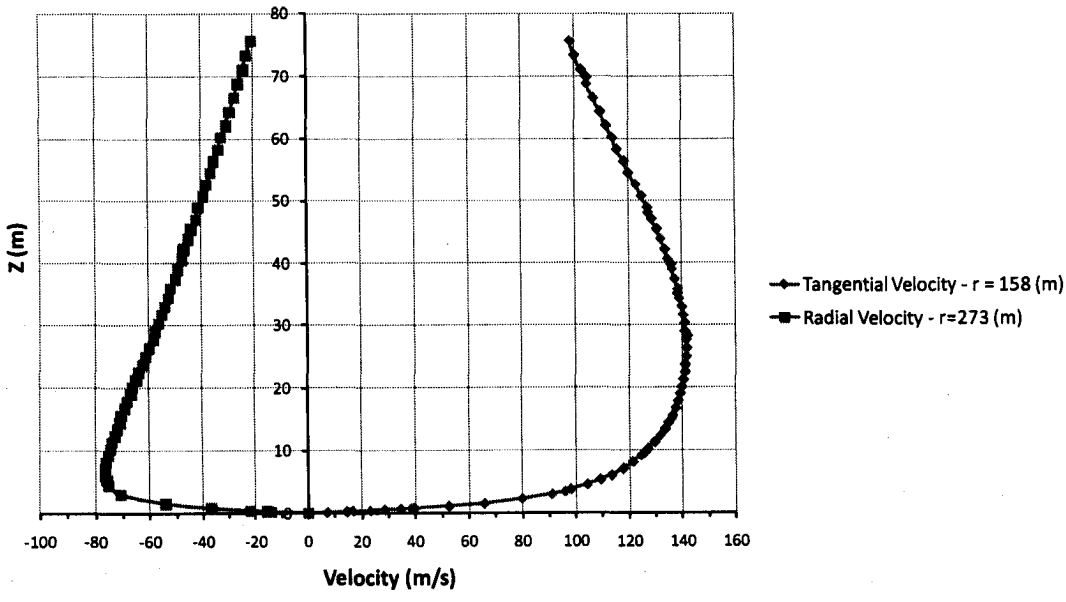

Fig. 3-5 Variation of Tangential and Radial Velocity Components along the Height at r = 158 and 273 (m), respectively

The resultant horizontal velocity is the vectorial summation of the radial and tangential components. It appears that this resultant velocity has a maximum profile at R = 200 (m), which is an intermediate value between R = 158 (m) and R = 273 (m). Accordingly, R = 200 (m) is expected to lead to both maximum values for the distributed load P, and relatively small values for Fg and Fc. Therefore, it leads to peak forces in a number of members of zones, (1) to (5). The interpretation for the value of R = 100 (m) associated with some of the peak forces, mainly for members in zones (1) and (2), can be conducted in view of the schematic shown in Fig. 3-6, Fig. 3-7, Fig. 3-8, Fig. 3-9, Fig. 3-10, and Fig. 3-11. The vertical profiles of the tangential and radial velocities for different values of r are given in the first two figures.

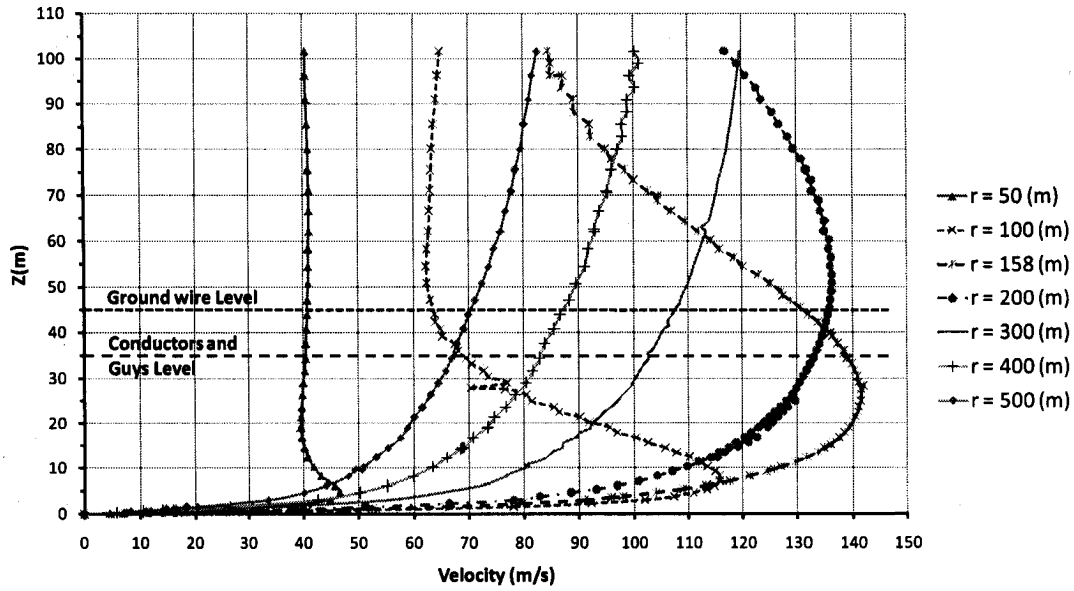

Fig. 3-6 Vertical Profile of Tangential Component for Different Radial Distances from Tornado Centre (F4 Tornado)

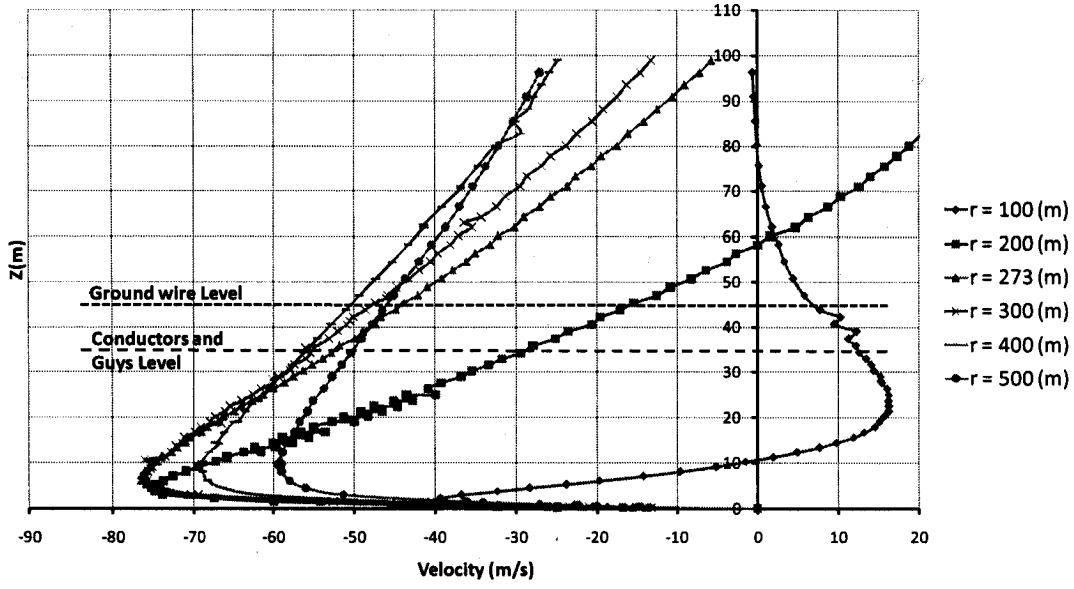

Fig. 3-7 Vertical Profile of Radial Component for Different Radial Distances from Tornado Centre (F4 Tornado)

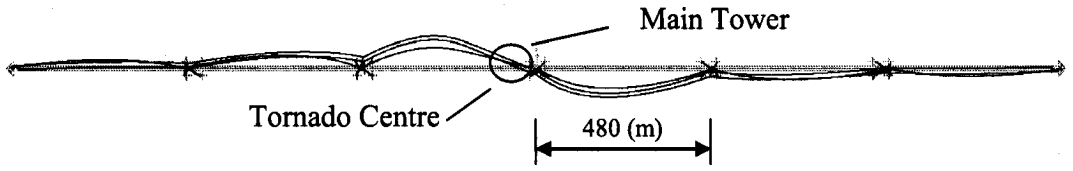

Fig. 3-8 Behaviour of Transmission line Due to Relative Tornado Distance R = 100 (m) and $\theta = 90^{o}$

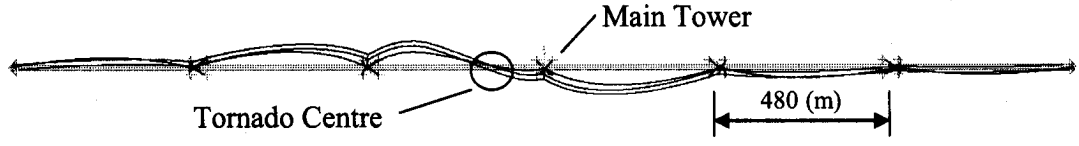

Fig. 3-9 Behaviour of Transmission line Due to Relative Tornado Distance R = 200 (m) and $\theta = 90^{o}$

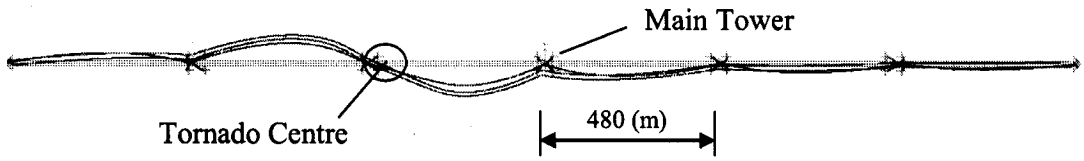

Fig. 3-10 Behaviour of Transmission line Due to Relative Tornado Distance R = 400 (m) and $\theta = 90^{o}$

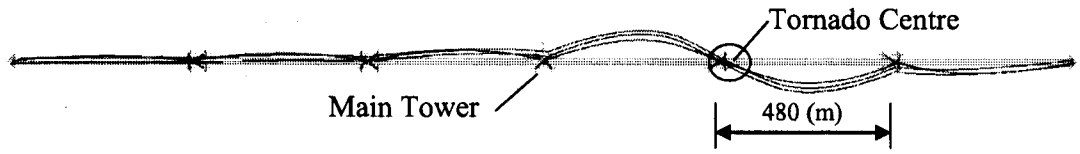

Fig. 3-11 Behaviour of Transmission line Due to Relative Tornado Distance R = 500 (m) and $\theta = 270^{o}$

The other three figures show schematics of the forces resulting from the tangential velocity component acting on the conductors adjacent to the tower associated with R = 100 (m), R = 200 (m), R = 400 (m), and R = 500 (m), respectively. The distribution of forces show that for R = 500 (m), which is almost equivalent to the conductors' span, the two conductors adjacent to the tower are subjected to forces acting along the same direction. This is opposite for the case of R = 100 (m), where the adjacent spans are subjected to opposite forces. As such, one would expect that the transverse reactions at the tower location increases gradually when R increases from 100 (m) to 500 (m).

The peak force in members of zone (1) and (2), associated with R = 100 (m), can be interpreted in view of the discussed above. This value of R = 100 (m) leads to small values of the forces "Fc" and "Fg", with moderate values for the distributed load "P". The minimization of "Fc" and "Fg" increases the straining actions in zones (1) and (2), and leads to peak force in zones (1) and (2).

3.6.2 Zone (6) Conductors Cross Arms

Fig. 3-2 shows the location of the members F118 and F538, selected to present the results of the parametric study. The internal forces in these two members will be mainly affected by the reaction provided by the conductors to the cross arms. As discussed previously, the maximum value of this reaction occurs for large values of R, which makes the adjacent spans loaded along the same direction. As such, the peak forces in these two members are associated with R = 400 (m) and 500 (m), both with $\theta = 90^{\circ}$. The conductor loading resulting from this configuration is shown in Fig. 3-12. The unbalanced loads acting on the two spans adjacent to the tower, along with the nonlinear behaviour of the conductors lead to a resultant force acting on the conductor cross arms along the longitudinal direction of the conductors. This leads to an out-of-plane bending moment, leading to a compression force on member F118. This compression force exceeds the tension resulting from the conductors' own weight. As a result, the member is subjected to a net of compression force of 45 (kN).

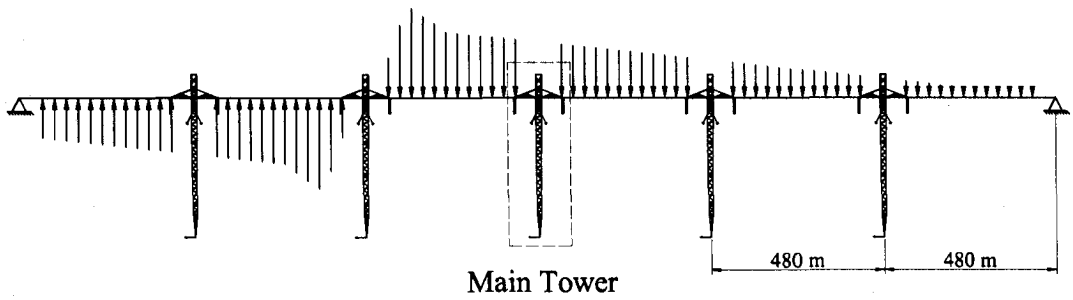

Fig. 3-12 Representation of Unbalance Transverse Forces on the Conductors Spans Adjacent to the Tower of Interest

Various load cases considered in the design of this tower, which considers normal wind loads, do not predict any compression force in this member. This emphasises the importance of considering HIW loads in this area of the tower.

3.6.3 Zone (6) Guys Cross Arms

Fig. 3-2 and Fig. 3-13 show the location of the two members selected in presenting the results of the parametric study. F437 and F422 are upper and lower chord members, respectively. The peak forces in F437 and F422 are in tension and compression, respectively.

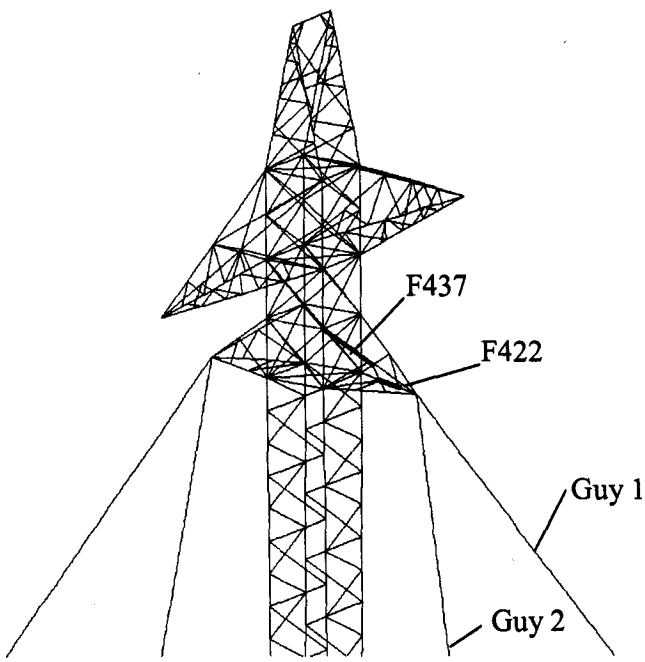

Fig. 3-13 Guys' Cross Arms Orientation

A plan view of the conductors, guys and tornado configuration (R = 300 (m), $\theta = 120^{o}$) leading to peak forces in member F437 and F422 is shown in Fig. 3-14. The two members are connected to guys 1 and 2 and, therefore, the forces in these members are

affected mainly by the magnitude of the forces in guys 1 and 2. Under this loading configuration, guys 2 and 4 are under compression. Since the guys cannot resist compression forces, this tornado configuration will lead only to forces in guys 1 and 3, which will resist the radial and tangential components, respectively.

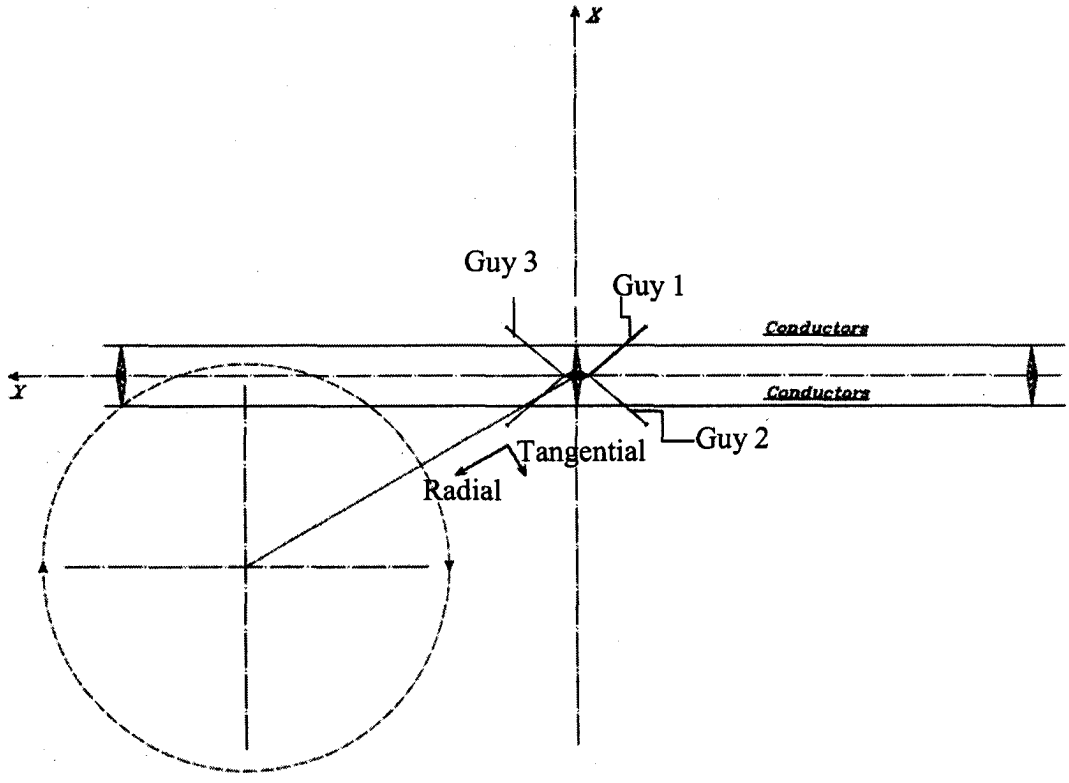

Fig. 3-14 Horizontal Projection of F4 Tornado Located at Relative Distance R = 300(m) with Angle $\theta = 120^{\circ}$

The maximum force in guy 1 and, consequently the peak force in F437 and F422, occur when guy 1 is almost parallel to the radial component. This provides an interpretation for the critical value of $\theta = 120^{\circ}$. The reaction of the guys increases with the increase of both the distributed load "P" and the concentrated loads "Fc" and "Fg". As mentioned before, P has large values for R ranging between 158 (m) and 273 (m), while "Fc" and "Fg" have large values for $R \geq 300$ (m), due to the effect of the span loads. It turns out that a value

of R = 300 (m) achieves the maximum effect for the combination of P, and Fc and Fg, which leads to a maximum force in guy 1 and, consequently, maximum forces in the two considered members.

3.7 Cable Forces Under Axisymmetric F4 Tornado Wind Field

Table 3-4 show the peak forces that develop in the conductors, ground wires and guys as a result of the F4-tornado. The "Initial" value represents the initial pretension values assumed in the analysis. The "Maximum" And 'Minimum" values represent the magnitude of maximum and minimum tension forces. Since cables do not resist compression, no negative values are reported in the table.

Table 3-4 Variation of the Pretension Forces in Conductors, Ground wire and Guys

Structural Element	Pretension Force		
	Initial (kN)	Maximum (kN)	Minimum (kN)
Guys	5	709	1
Conductors	82	222	82
Ground Wire	8	72	8

The results show a significant increase in the cable forces, which should be considered in the design of the transmission line system in order to assure a satisfactory performance during tornadoes.

3.8 Sensitivity Study

A study is conducted to assess the sensitivity of the peak member forces to the variation of the two parameters R and θ, which define the relative location of the tornado. The

sensitivity study is conducted using the F4 axisymmetric tornado field. Results are presented for chord and diagonal members located at different zones of the tower. For each member, the variation of the peak forces with θ is first provided for a fixed value of R that corresponds to the critical tornado location of the member. The variation of the peak forces with R is then presented using the critical value of θ corresponding to the critical tornado location of the member. Fig. 3-15 to Fig. 3-20 show the results for three members belonging to the tower zone, i.e. located within zones 1 to 5. These are labelled as F141, F183 and F172, which are chord, diagonal (1) and diagonal (2) members, respectively. In Fig. 3-21 to Fig. 3-24, the results of the sensitivity analysis for members F422 and F118 are presented. They are chord members in the guy and conductor cross arms, respectively. The following observations can be drawn from the figures:

1) All members' internal forces exhibit significant fluctuations with the two tornado location parameters R and θ.
2) With the exception of member F422, the sign of the members' forces changes with θ.
3) With the exception of a small range for R for member F183, the variation of R does not change the sign of the internal forces.
4) For chord members, the variations of the forces with R, in the post peak regions, are relatively small. This is applicable for the chord members located either in the tower or the conductors zone.
5) The peak values of the members' forces and the associated critical values for R and θ, leading to those peak forces, coincide with the values reported in Table 3-1.

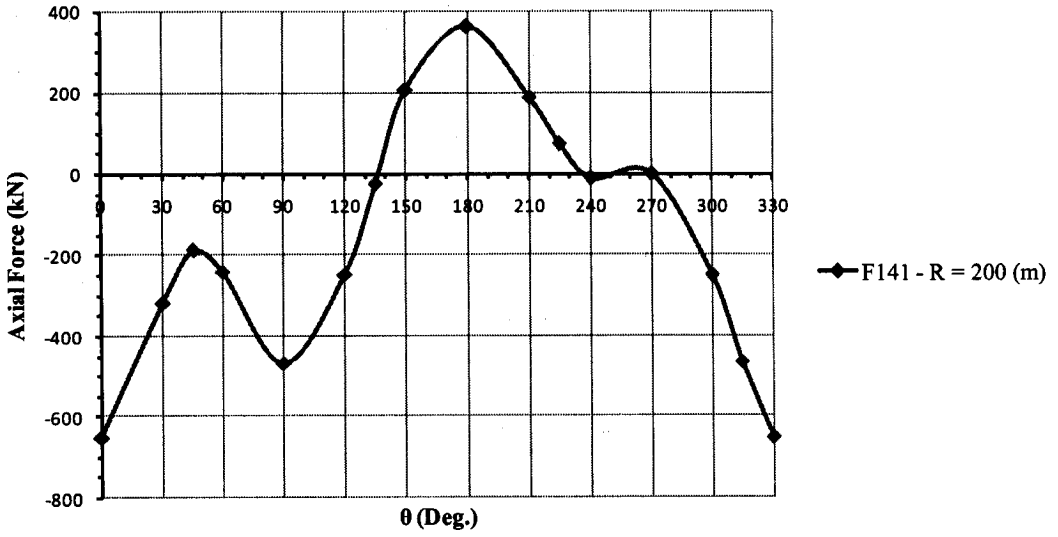

Fig. 3-15 Variation of the Axial Force in Member F141 for Different Values of θ with R = 200(m)

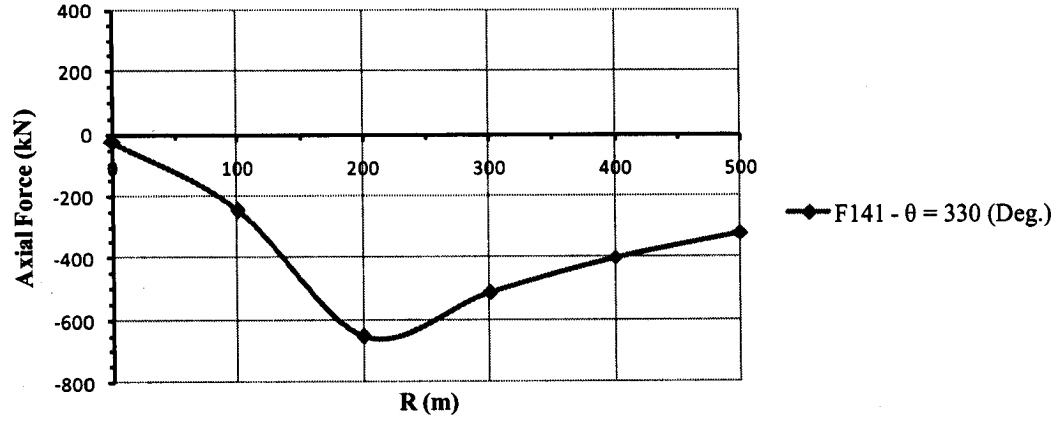

Fig. 3-16 Variation of the Axial Force in Member F141 for Different Values of R with $\theta = 330^{\circ}$

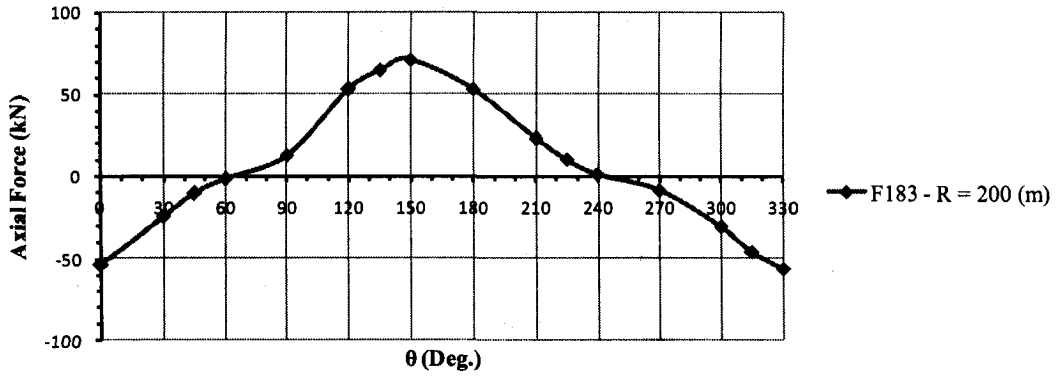

Fig. 3-17 Variation of the Axial Force in Member F183 for Different Values of θ with R = 200(m)

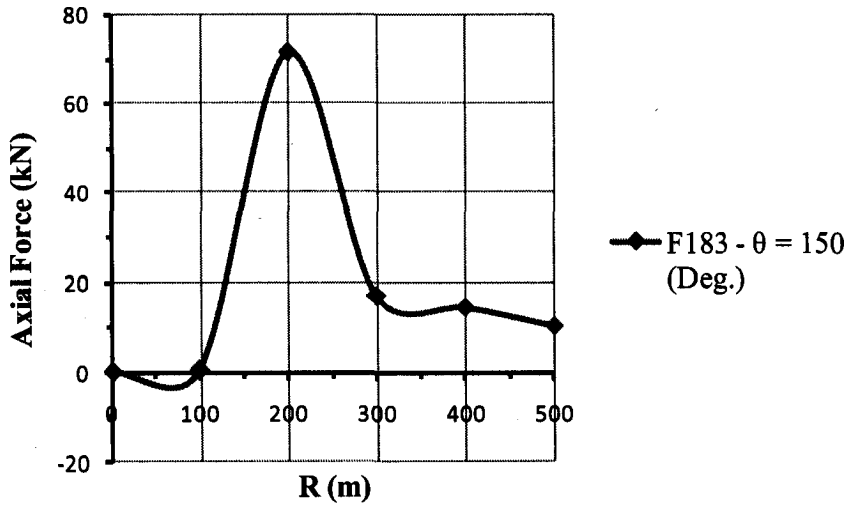

Fig. 3-18 Variation of the Axial Force in Member F183 for Different Values of R with θ = 150°

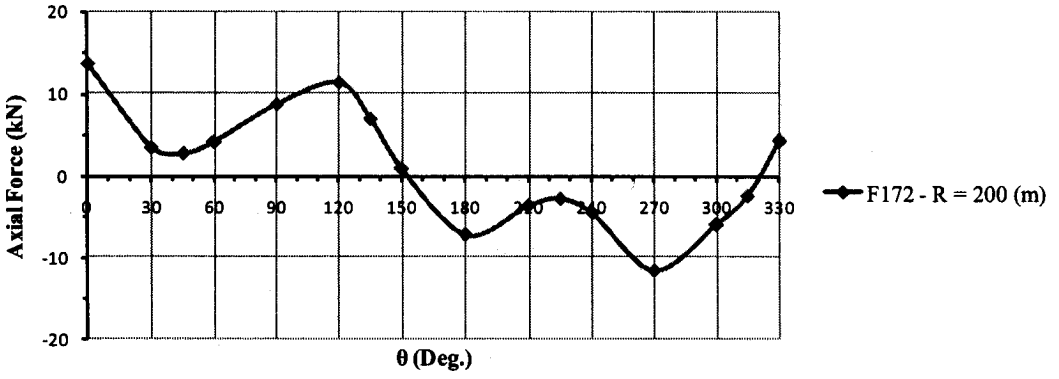

Fig. 3-19 Variation of the Axial Force in Member F172 for Different Values of θ with R = 200(m)

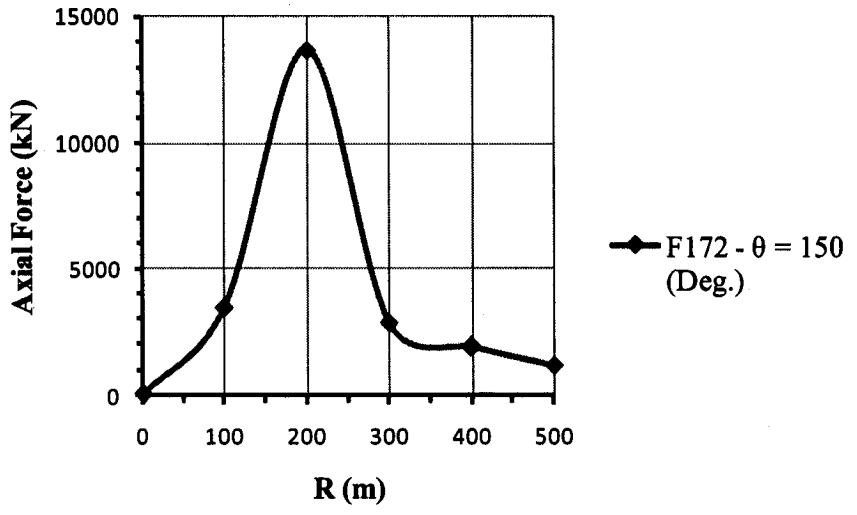

Fig. 3-20 Variation of the Axial Force in Member F172 for Different Values of R with θ = 0°

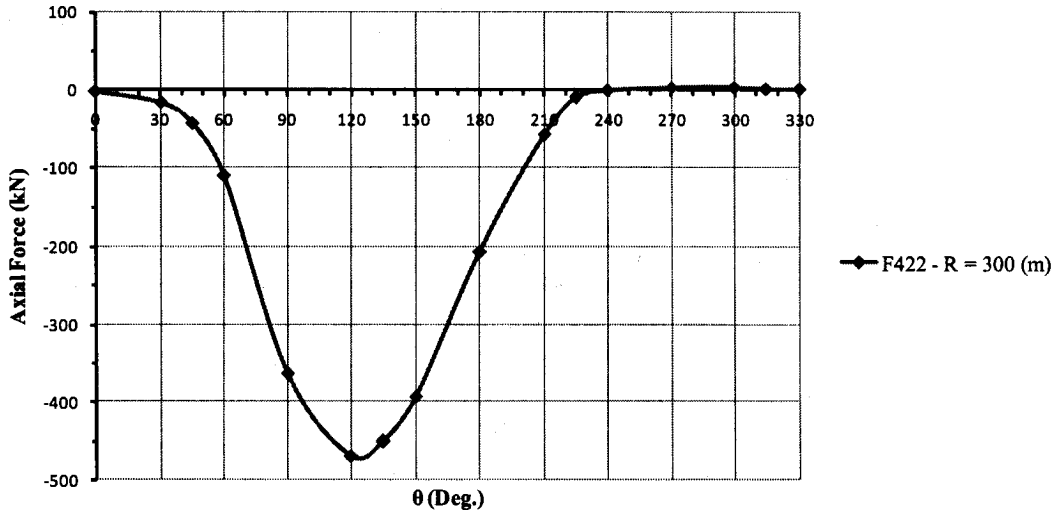

Fig. 3-21 Variation of the Axial Force in Member F422 for Different Values of θ with R = 300 (m)

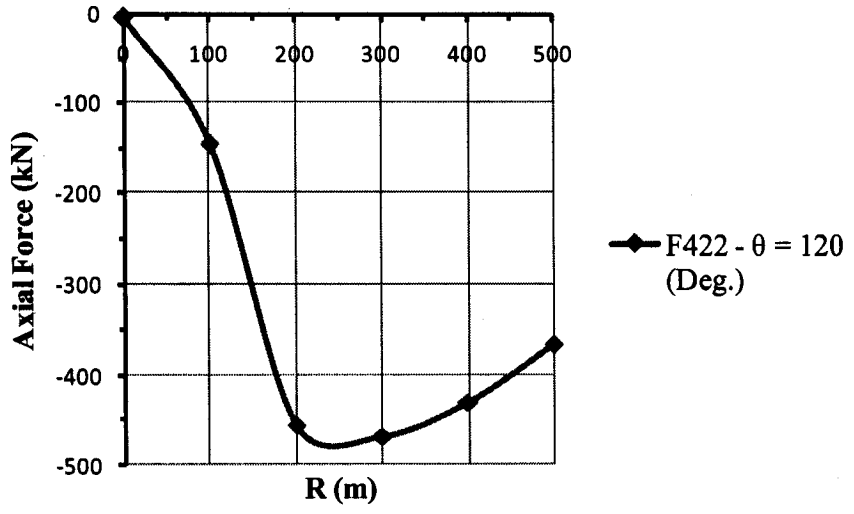

Fig. 3-22 Variation of the Axial Force in Member F422 for Different Values of R with θ = 120°

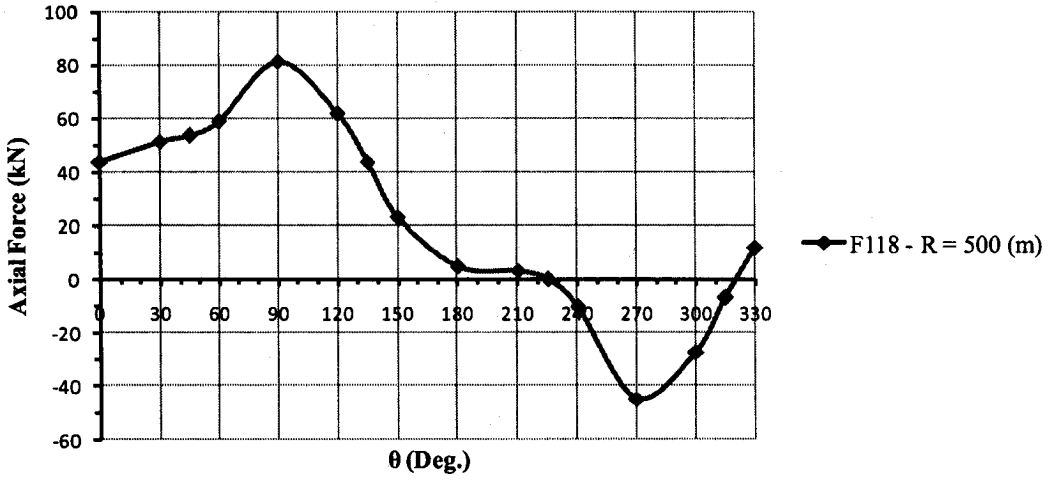

Fig. 3-23 Variation of the Axial Force in Member F118 for Different Values of θ with R = 500 (m)

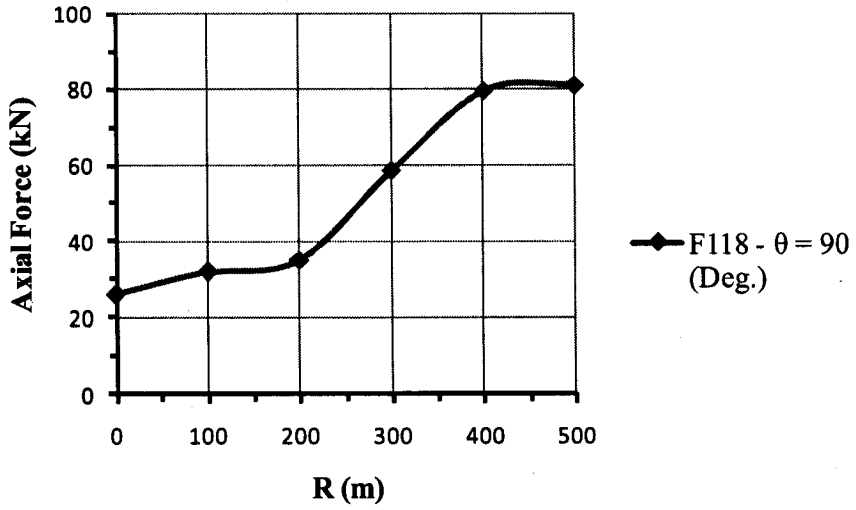

Fig. 3-24 Variation of the Axial Force in Member F118 for Different Values of R with θ = 90°

3.9 Conclusions

The following conclusions can be drawn from the parametric study conducted in this Chapter:

- The forces in all tower members change significantly with the variation of the parameters R and θ, which define the location of the tornado relative to the tower.
- Different type of members, either chord or diagonal, as well as members located in different zones of the tower, have independent critical values of R and θ that lead to peak forces in these members. This emphasizes the need for conducting an extensive parametric study, by varying the location of the tornado, in order to predict the peak forces in all members of the tower.
- Analyses conducted using the 3-D and the axisymmetric sets of data reveal no significant variation in the members' internal forces. The difference is more pronounced in the tower zones near the ground, because of the instability of the wind in this region, which can be only observed in the 3-D fluid dynamic analysis.
- The F2 tornado leads to peak member forces that are significantly less than those resulting from the F4 tornado.
- A comparison is carried out between the peak forces due to F2 tornado to those resulting from normal wind and downbursts loading. In this comparison, the wind speed used in the design of the tower was employed to evaluate the normal wind forces. Such a comparison shows that the member forces due to F2 tornado exceed the downburst and normal wind forces. However, for the majority of the members, the F2 tornado forces are found to be less than the capacity of the members.
- Some tornado locations result in unbalanced forces acting on adjacent spans of the conductors. This leads to a resultant force that acts on the tower cross arms along

the longitudinal direction of the conductors. This force leads to an out-of-plane bending effect on the cross arms and, consequently, compression forces in some of the upper chord members. These compression forces exceed the tension forces that develop in these members due to the self weight of the conductors. As a result, these members become subjected to compression forces, which are not typically accounted for under normal wind load cases.

3.10 Acknowledgements

The author would like to acknowledge Manitoba Hydro Company, Canada, Natural Sciences and Engineering Research Council of Canada (NSERC), and Centre for Energy Advancement through Technological Innovation (CEATI) for their kind support for this research work. The author acknowledges Prof. H. Hangan and Dr. J-D. Kim at the Boundary Layer Wind Tunnel Laboratory, The University of Western Ontario, Canada, for their efforts in providing the tornado wind data.

3.11 References

American National Standards Institute (ANSI) (1993)," National Electrical Safety Code (NESC)", *Accredited Standards Committee C2,* USA.

American Society of Civil Engineers (ASCE) (1991), "Guidelines for electrical transmission line structural loading", *ASCE Manuals and Reports on Engineering Practice,* No. 74, NY.

Baker, D. E. (1981). "Boundary layers in laminar vortex flows." Ph.D. thesis, Purdue University.

Dempsey, D., and White, H., (1996) "Winds wreak havoc on lines.", *Transmission and Distribution World*, vol. **48**(6), pp. 32–37.

Fluent 6.2 User's Guide (2005), Fluent Inc.,Lebanon

Fujita, T. T. (1981), "Tornadoes and downbursts in the context of generalized planetary scales", *J. Atmos. Sci.*, **38**, 1511-1534.

Fujita, T.T., and Pearson, A.D. (1973). " Results of FPP Classification of 1971 and 1972 Tornadoes," *Preprints, Eighth Conference on Severe Local Storm, American Meteorological Societ,* Boston, Mass., USA, pp. 142-145.

Hamada, A., El Damatty, A. A., Hangan, H., Shehata, A. Y. (2009), " Finite element modelling of transmission line structures under tornado wind loading", *Wind and Structures, an International Journal*

Hangan, H., and Kim, J. (2008). "Swirl ratio effects on tornado vortices in relation to the Fujita scale." *Wind and Structures,* 11(4), 291-302.

Lee, Wen-Chau., and Wurman, J. (2005). "Diagnosed three-dimensional axisymmetric structure of the Mulhall tornado on 3 May 1999." *J.Atmos.Sci.,* **62**(7), 2373-93.

McCarthy, P.,Melsness, M. (1996) "Severe weather elements associated with September 5, 1996 hydro tower failures near Grosse Isle, Manitoba, Canada." Manitoba Environmental Service Centre, Environment Canada,, 21pp.

SAP2000 V.12 (2008), CSI Analysis Reference Manual, Computer and Structures, Inc. Berkeley, California, USA

Sarkar, P., Haan, F., Gallus, Jr., W., Le, K. and Wurman, J. (2005). "Velocity measurements in a laboratory tornado simulator and their comparison with numerical and full-scale data." *37th Joint Meeting Panel on Wind and Seismic Effects.*

Savory, E., Parke, G. A. R., Zeinoddini, M., Toy, N., and Disney, P. (2001). "Modelling of tornado and microburst-induced wind loading and failure of a lattice transmission tower." *Eng.Struct.,* **23**(4), 365-375.

Shehata, A. Y., and El Damatty, A. A. (2007). "Behaviour of guyed transmission line structures under downburst wind loading." *Wind and Structures, an International Journal,* **10**(3), 249-268.

Shehata, A. Y., El Damatty, A. A., and Savory, E. (2005). "Finite element modelling of transmission line under downburst wind loading." *Finite Elements Anal.Des.,* **42**, 71-89.

Wen, Y. (1975). "Dynamic tornadic wind loads on tall buildings", *ASCE Journal of the Structural Division*, **101**(1), 169-185.

CHAPTER 4

DYNAMIC BEHAVIOUR OF TRANSMISSION LINE STRUCTURES UNDER TORNADO WIND LOADING[3]

4.1 Introduction

Electricity plays a vital and essential role in the function of modern society. This dependence is problematic in the case of power outages, often which result from the failure of electrical transmission lines. More than 80% of these line failures have been attributed to High Intensity Wind (HIW) events, such as tornadoes and downbursts. Despite this fact, the subject of analysis and design of transmission lines under HIW events has not yet matured, and the amount of research studies conducted regarding this topic has been limited. The design codes do not consider the wind loads resulting from HIW, as they are specific only to loads associated with large-scale normal wind events. The vertical profile of normal wind events is characterized by a monotonic increase in wind velocity with height. This profile is different from the wind profile associated with tornadoes, in which the maximum wind speed occurs near the ground. The tornado wind field has a significant vertical component, which does not exist for normal wind events. In addition, due to the localized nature of HIW events, the structural behaviour of transmission line systems exhibits unique features when subjected to HIW. One of these features is the significant variation of the forces acting on the towers and the conductors with the location of the tornado relative to the line system. Consequently, the internal forces in the members will vary with the location of the tornado. As a result, a tower can have various critical tornado locations, each one leading to peak forces in a group of

[3] A version of this chapter is being prepared for publication in the *Journal of Wind and Structures*

members. Studies regarding to the characterization of the tornado wind field can be divided into three categories: field measurements, laboratory tests, and numerical simulations. Field measurements have been conducted by Sarkar, *et al.* (2005) for the 1998 Spencer South Dakota F4 tornado, and by Lee and Wurman (2005) for the 1999 Mulhall F4 tornado. The full-scale measurements are typically inaccurate at the near ground region. Baker (1981) has developed a Tornado Vortex Chamber (TVC), in which tornadoes can be simulated experimentally as vortices. These simulations provide a good estimation of the characteristics inside a tornado, however, the results are found to be affected by the applied boundary conditions. In an early study, Fujita and Pearson (1973) classified tornadoes based on their intensity and size. The intensities were defined by the gust wind speed, and the sizes were defined by the path length and width. The rating ranges from the smallest damage, "F0", to the largest damage, "F5". A numerical simulation for the tornado wind field has been conducted by Hangan and Kim (2008) using the Computational Fluid Dynamics (CFD) software FLUENT (2001). They have validated their numerical model using the results of the laboratory tests conducted by Baker (1981). Very few attempts have been made to assess the structural response of transmission lines to tornadoes. The failure of a self supported lattice tower under modelled tornado and microburst wind profiles has been investigated by Savory, *et al.* (2001). The mathematical dynamic tornado wind model used in this study is based on the numerical model developed by Wen (1975) in which the tornado force, relative to the velocity component in the direction being considered, can be obtained per unit height of the obstacle at any given time. Only the horizontal wind profile corresponding to F3 tornado on the Fujita scale was used in the analysis without considering the vertical

component of the tornado. The turbulence component associated with the tornado and the downburst wind loading was neglected. The tower members were modelled as three-dimensional truss elements. The dynamic analysis was done for the tower alone including the self weight of the towers and the conductors, without modelling the transmission lines. The structural response showed initial quasi-static response before failure under the excessive tornado wind loads. Hamada, *et al.* (2009) developed a numerical model for the analysis of transmission lines subjected to tornado loading. The wind field data obtained from the Hangan and Kim (2008) numerical simulation was incorporated into this numerical model, after applying the proper scaling factors to account for F2 and F4 tornado fields. This numerical model involves a simulation for a main tower, along a number of adjacent towers and conductors, and ground wires spanning in between. Both the horizontal and vertical components of the tornado wind fields are accounted for in this numerical model. In Chapter 3 of this Thesis, Hamada, *et al.* (2009) numerical model was used to conduct an extensive parametric study, which was used to identify the critical locations for F4 and F2 tornadoes, leading to peak forces in various members of a guyed transmission line system. The results were also used to describe the structural behaviour of the guyed tower under various tornado locations. In the same study, the sensitivity of the members' internal forces to the variation of the parameters describing the location of the tornado was also assessed. In the above study, the parametric study was carried out by conducting a large number of quasi-static analyses by varying the location of the tornado relative to the studied tower. Loredo-Souza and Davenport (1998) investigated experimentally in wind tunnel the transmission line failures in strong wind events. The experimental work successfully agreed with the theoretical predictions obtained from the

statistical method, using influence lines. The study shows how the dynamic behaviour of the lines is mainly affected by the value of the aerodynamic damping, which can reach 60% of the critical damping. The aerodynamic damping is directly proportional to the wind velocity and inversely proportional to the lines mass. The study concluded that the background response is indeed the main contributor for the total fluctuating response. However, the resonant component can also be influential, depending on the line characteristics and wind velocities, which may lead to smaller values of the aerodynamic damping. Therefore, the study proves the importance of turbulence in the dynamic response of the lines, and shows the important role of the aerodynamic damping. Darwish, *et al.* (2009) modified the two-dimensional nonlinear finite element model of the transmission lines developed by Shehata, *et al.* (2005) to study the dynamic characteristics of the conductors under turbulent downburst loading. The modified model accounted for the large deformations and the pretension loading, and was used to predict the natural frequencies and mode shapes. In this study, the turbulence component was extracted from full scale data and added to the mean component of the downburst wind field developed by Kim and Hangan (2007). The study concluded the resonant component of the turbulence is negligible due to the large aerodynamic damping. In addition, the study discussed the effect of the pretension force on the natural period and mode shapes of the conductors. Loredo-Souza and Davenport (2003) reviewed the influence of the design procedure in the establishment of wind loading on transmission tower response. Davenport's gust response and statistical method using influence lines procedures for wind loading on transmission structures were compared. The second approach accounts for the effect of the higher mode. Based on the tower response

conducted in this research, Loredo-Souza and Davenport (2003) concluded that the dynamic response of transmission towers is strongly dependent on the turbulence intensity, and both the structural and aerodynamic damping of the towers. Also, the results showed that the second mode resonant response in some members, in which there was a reversal in forces based on the load position, was larger than the resonant response of the first mode.

In this chapter, the method of analysis is modified by carrying out a limited number of time-history dynamic analyses, instead of multiple quasi-static analyses. In each dynamic analysis, the tornado is assumed to have a convective velocity along a certain direction relative to the line. During various time intervals of the time-history analysis, the tornado has different locations relative to the tower. Consequently, the wind forces acting on various parts of the tower and the conductors will vary with time, as a result of this variation in tornado location. The time-history variations of the wind forces acting on different parts will have different profiles. The study is done to assess the effect of dynamic response on the behaviour of transmission lines subjected to tornado loading. Compared to the tower, it is expected that the behaviour of the conductors is more affected by a dynamic response. This is because the conductors typically have, in comparison to the tower, long periods of vibration, which match the dominant long period components of the wind loads.

The current study begins by providing a brief background of the tornado field used in the analysis, which is based on Hangan and Kim (2008) numerical simulation, along with the finite element model developed by Hamada, *et al.* (2009). The natural periods and mode shapes of the considered transmission line system are then determined by conducting free

vibration analyses. The time-history variation of the tornado forces, resulting from the translation of the tornado events, is presented at various locations in the tower and conductors. Time-history dynamic analyses are conducted and the results are compared to the findings obtained in the extensive quasi-static parametric study reported in the previous Chapter. Major conclusions obtained in view of this comparison are discussed.

4.2 F4 Tornado Wind Field

As mentioned above, the tornado wind field used in the current study is based on a three dimensional numerical simulation conducted and validated by Hangan and Kim (2008). This simulation was conducted on a reduced-scale tornado model, using various values for the swirl ratio "S". This parameter is related to the ratio between the tangential and radial velocities of the tornado. In the same study, Hangan and Kim (2008) compared the model results, after applying velocity and length scale factors, to full-scale measurements of an F4 tornado, which occurred in Spencer, South Dakota, USA, in May 30, 1998. This tornado was tracked by Wurman (1998) and the recorded data were then summarized by Sarkar, *et al.* (2005). Through this comparison Hangan and Kim (2008) concluded that the numerical data corresponding to a swirl ratio "S = 2" agrees well with the measured F4 tornado data. The appropriate length and velocity scale factors that should be applied to the numerical data, in order to simulate fully developed tornadoes were also obtained in this study. The resulting wind field for F4 tornadoes has three velocity components: the radial $V_{mr}(r, \theta, z)$, the tangential $V_{mt}(r, \theta, z)$ and the axial $V_{ma}(r, \theta, z)$ components. Those components vary with space as functions of the cylindrical coordinates r, θ, and z. They do not vary with time, since the CFD analysis predicted a steady-state condition of the tornado. An axisymmetric wind profile $V_m(r,z)$ of the three components is then calculated

by averaging the data along the circumferential direction, i.e. by eliminating the variation with θ. This set of axisymmetric data, simulating F4-scale tornadoes, is used in the current study.

4.3 Finite Element Modelling of Transmission Line System

A transmission line belonging to Manitoba Hydro, consisting of a number of identical guyed towers, labelled as type A-402-0 towers, is numerically simulated in this study. Each tower is supported by four guys at an elevation of 35.18 (m) relative to the ground. The towers, which have a height of 44.39 (m), are supported by hinges at the ground level. Two conductors are connected to the towers' cross arms from each side using 4.27 (m) length insulators. One ground wire is connected to the top of the towers for lighting protection. The conductors and ground wire have both a 480 (m) span and their mid-spans have a sag of 20 (m) and 13 (m), respectively. The geometry of a typical tower is shown in Fig. 4-1. The geometric and material properties of the conductors, ground wire and guys are provided in Shehata, *et al.* (2005).

A schematic of the developed numerical model is provided in Fig. 4-2. As shown in the figure, the numerical simulation includes the tower of interest, identified as the main tower, along with three conductor spans along each side of the main tower. The effect of the adjacent towers is simulated by replacing each tower with a spring system supporting the conductors at the tower locations. Each spring system consists of three linear springs, representing the stiffness of the tower and the connected insulator along three perpendicular directions. Simply supported conditions are assumed at the end of the conductors.

The number of conductors used was recommended by Shehata, *et al.* (2005), in order to accurately predict the forces transferred from the conductors to the main tower.

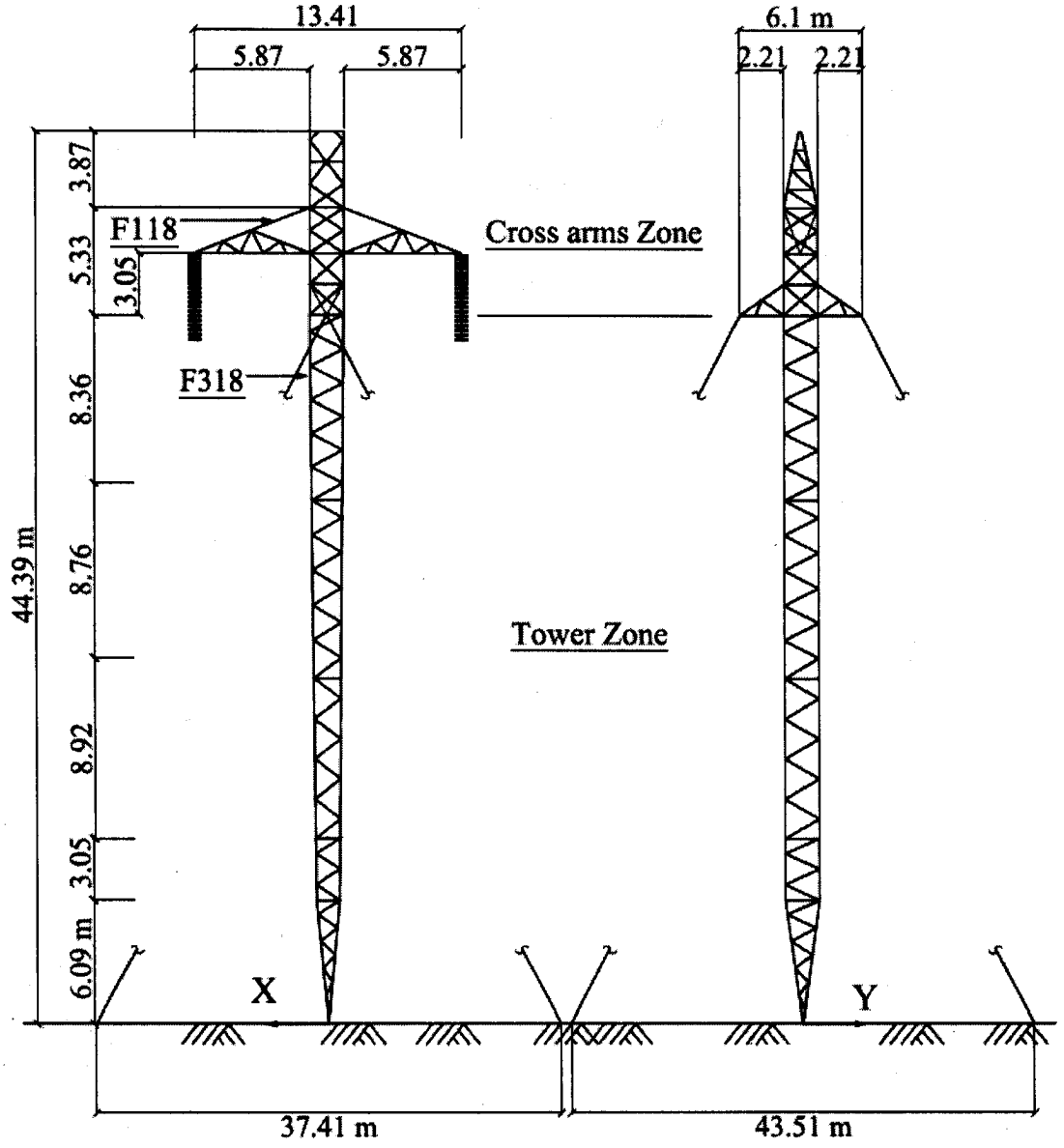

Fig. 4-1 Geometry of the Modelled Guyed Tower Type A-402-0

The numerical model for the transmission line system is developed using the finite element program SAP 2000 (CSI 2008).

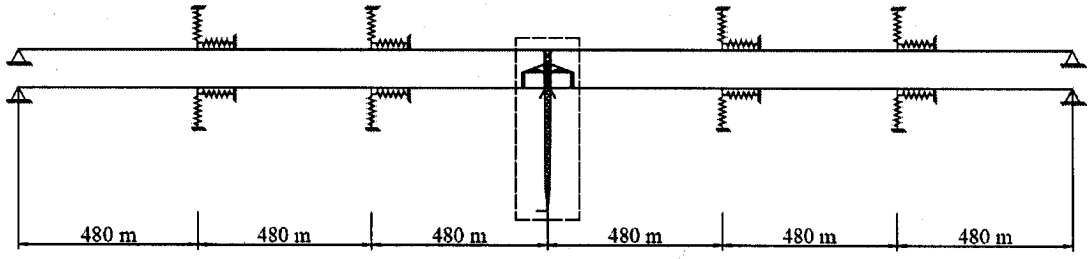

Fig. 4-2 Transmission Line System

Each member of the tower is modelled using one two-nodded, three-dimensional nonlinear frame element, having three displacement and three rotational degrees of freedom per node. A three dimensional nonlinear cable element is used to model the highly nonlinear behaviour of the conductors, the ground wire and the guys. The element accounts for the effects of tension stiffening, sagging and geometric nonlinearities. More details regarding the finite element model can be found in Hamada, *et al.* (2009).

4.4 Free Vibration Analysis of the Tower and the Lines

A free vibration analysis is conducted to estimate the natural period and mode shapes of the tower, the conductors and the ground wire.

4.4.1 The Tower

The natural periods of the tower are expected to be affected by the value of the initial pretension force applied to the guys. The evaluation of the natural periods of the tower involves conducting two sequential analyses. The first analysis is carried out to update the stiffness matrix of the tower, to account for the pretension force in the four guys. The second is a free vibration modal analysis to determine the natural periods and mode shapes. The analysis is repeated by applying two different values for the guys' pretension

forces. In addition, one analysis is conducted while replacing the guys with hinge supports, preventing the lateral movement of the tower at the guys' locations. The periods of the first five modes obtained from the analyses are provided in Table 4-1.

Table 4-1 Tower Natural Periods

Pretension	Mode	1	2	3	4	5
5 kN	T (sec)	0.98	0.88	0.69	0.39	0.29
10 kN	T (sec)	0.52	0.51	0.39	0.37	0.26
Hinge	T (sec)	0.38	0.30	0.15	0.12	0.12

The following observations can be drawn from of the results reported in the table:

- The periods of the first two modes have close values. This is true for the three considered cases.
- The guys' pretension forces have a significant effect on the natural periods of the tower. As the pretension force increases, the stiffness of the tower increases as well, and the natural periods of the structure approach the hinge case.

4.4.2 The Conductors

The conductors exhibit complex behaviour due to the effect of tension stiffening, and their highly nonlinear behaviour. The natural periods of the conductors are first evaluated by conducting a free vibration analysis, after updating the stiffness matrix to consider the effect of tension stiffening. The pretension force in the conductors is taken 82.344 (kN), which is the value applied to the real lines. This pretension force leads to a 20 (m) sag for the 480 (m) conductor span. The natural periods and the associated mode shapes along the transverse direction that result from this set of analysis, are given in Table 4-2 and

Fig. 4-3. As shown in the table, there is a small difference between the periods of the first three modes.

Table 4-2 Natural Periods of the Conductors in the Transverse Direction.

Pretension	Mode	1	2	3
82.344 (kN)	T (sec)	9.01	8.78	8.57

The analysis is repeated to evaluate the natural periods of the conductor in the vertical direction. The fundamental period in the vertical direction is found to have a value of 3.20 (sec). As expected, the conductors are more flexible in the transverse direction, compared to the vertical direction, due to the flexibility of the insulators in the transverse direction.

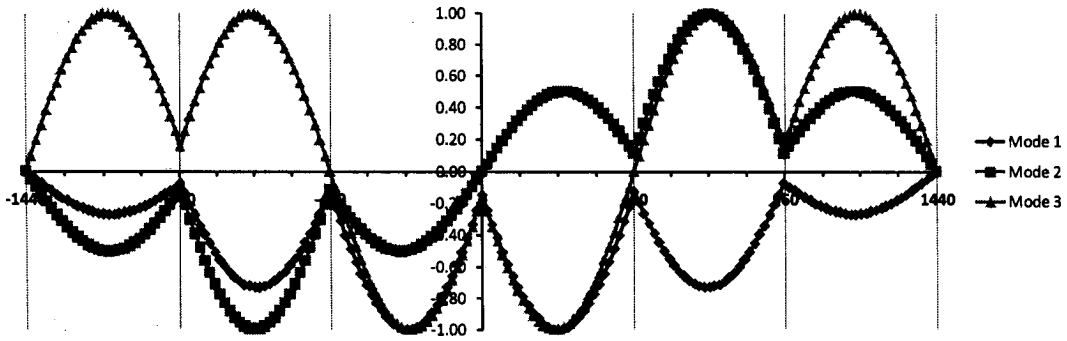

Fig. 4-3 First Three Mode Shapes of the Conductors

The fundamental periods of the conductors in both the transverse and the vertical directions are also evaluated by conducted sweep tests. This is done by applying a distributed harmonic load that leads to a deflection profile matching the fundamental mode shapes. A number of time-history analyses are conducted while varying the period of the applied load. The loading period, leading to absolute maximum response, represents the fundamental period of the conductors. The sweep tests are repeated while

varying the amplitude of the applied harmonic load. This is done to assess the variation of the fundamental periods with the excitation level. The results of the sweep test indicate that the variation of the fundamental periods with the excitation level is minor. The largest value for the transverse fundamental period is found to be 10 (sec), which is not significantly different from the value obtained from the free vibration analysis.

4.4.3 The Ground Wire

Similar to the conductors, free vibration analyses are conducted to evaluate the natural periods of the ground wire. The natural period values of the transverse modes are reported in Table 4-3. The analysis also predicts a fundamental period in the vertical direction of 3.4 (sec).

Table 4-3 Natural Periods of Ground Wire in Transverse Direction

Pretension	**Mode**	1	2	3
8 (kN)	**T (sec)**	6.70	6.69	6.68

4.5 Tornado Time-history Loading

The time-history analysis is conducted by assuming an initial location for the tornado relative to the main tower. An assumption is made regarding the direction of the translation motion of the center of the tornado. Two cases are considered in this study; parallel and perpendicular to the conductors, respectively. The tornado is assumed to have a transitional velocity of 20 (m/sec), a value recommended by Savory, *et al.* (2001). The translation motion of the tornado leads to a variation of its position, relative to the main tower and the conductors, with time. As a consequence, the tornado forces acting at various locations of the tower and the conductors will vary with time. At each time

interval, the steady-state wind field data are used to evaluate the instantaneous forces acting on the main tower and conductors. For each direction of motion of the tornado, one time-history analysis is conducted using a time step of 0.1 (sec). The time-history variations for the tornado forces acting at selected locations of the tower and the conductors, are provided below.

4.5.1 First Case – Tornado Path Parallel to the Transmission Line

Fig. 4-4 shows the initial location of the tornado, which is assumed to be 300 (m) left of the main tower. The tornado path, which is parallel to the transmission lines, is also shown in the figure. The time-history analysis is carried out until the tornado passes the main tower at a distance of 300 (m). With a translation velocity of 20 (m/sec), the total duration of the time-history analysis is 30 (sec).

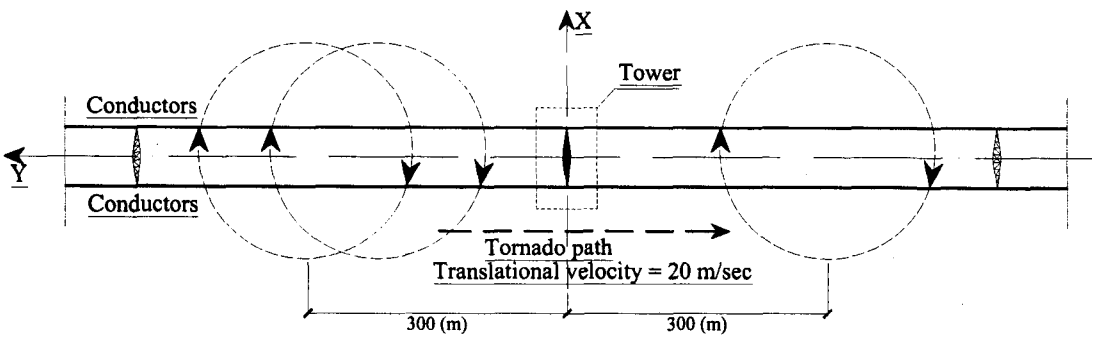

Fig. 4-4 Tornado Path for First Time-history Analysis.

To further analyze the spatial and time-history variations of the wind field, the time-history variations for the components of the tornado forces are plotted at the following locations:

a) Mid-span of the conductor connected to the main tower.

b) Connection between the conductor and main tower.

c) Mid-span of the ground wire connected to the main tower.

d) A nodal point located in the middle of the Tower zone at height = 20 (m).

These plots are provided in figures Fig. 4-5, Fig. 4-6, Fig. 4-7, Fig. 4-8, Fig. 4-9, Fig. 4-10, Fig. 4-11, Fig. 4-12, and Fig. 4-13.

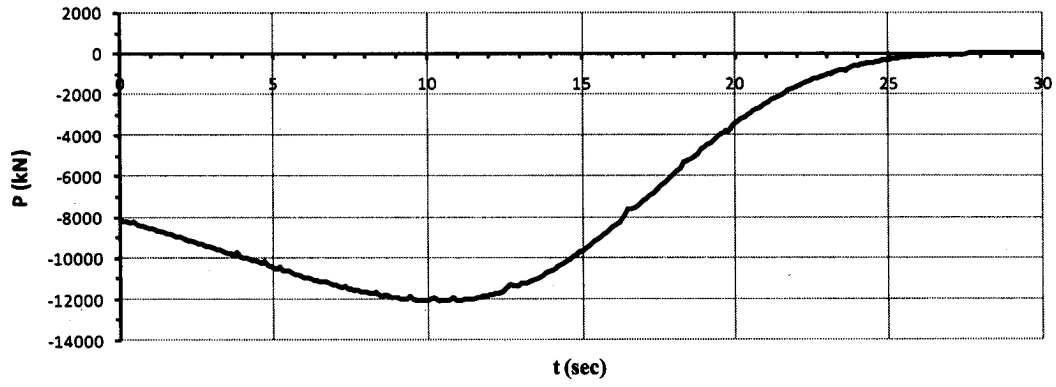

Fig. 4-5 Time-history of the Transverse Force Acting at the Conductor's Mid-span

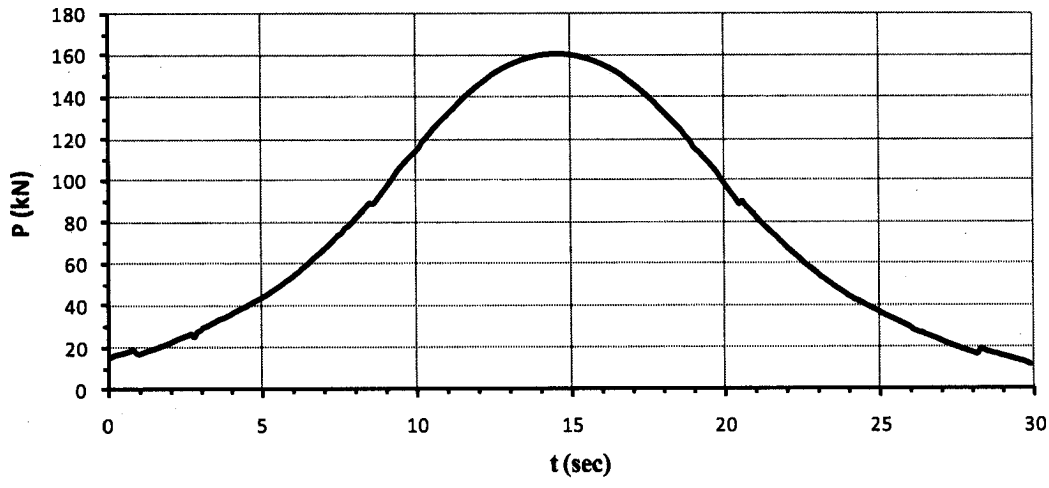

Fig. 4-6 Time-history of the Vertical Force Acting at the Conductor's Mid-span

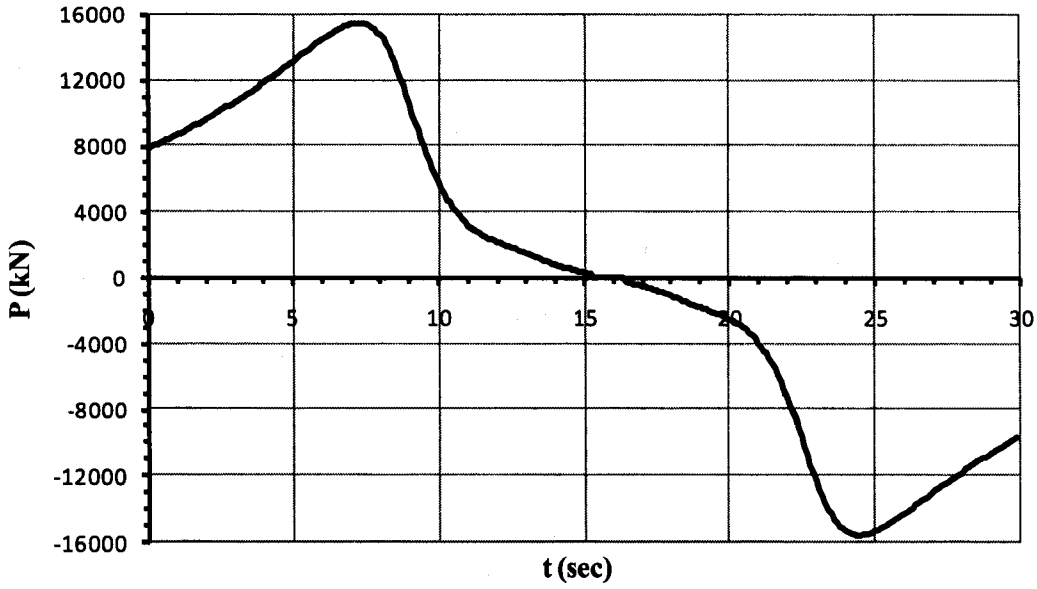

Fig. 4-7 Time-history of the Transverse Force Acting at the Conductor-Tower Connection

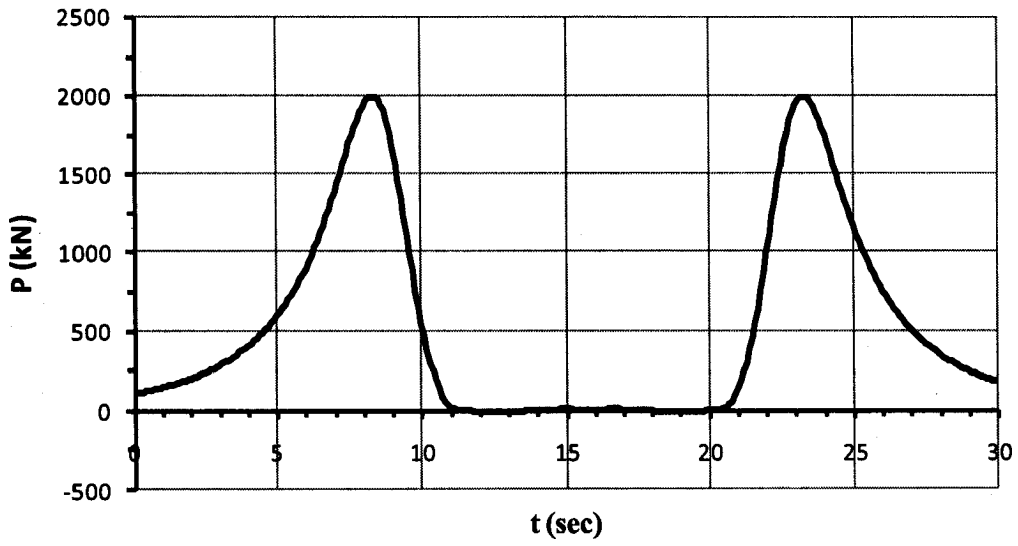

Fig. 4-8 Time-history of the Vertical Force Acting at the Conductor-Tower Connection

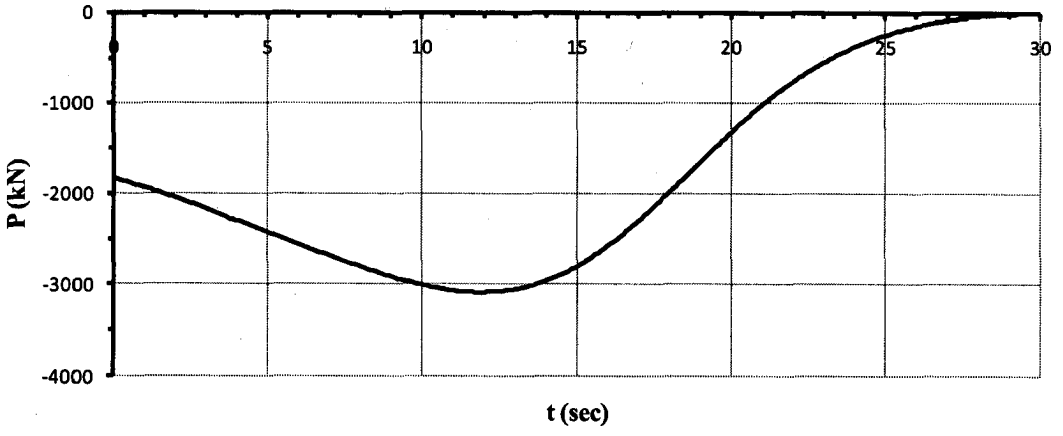

Fig. 4-9 Time-history of the Transverse Force Acting at the Ground Wire's Mid-span

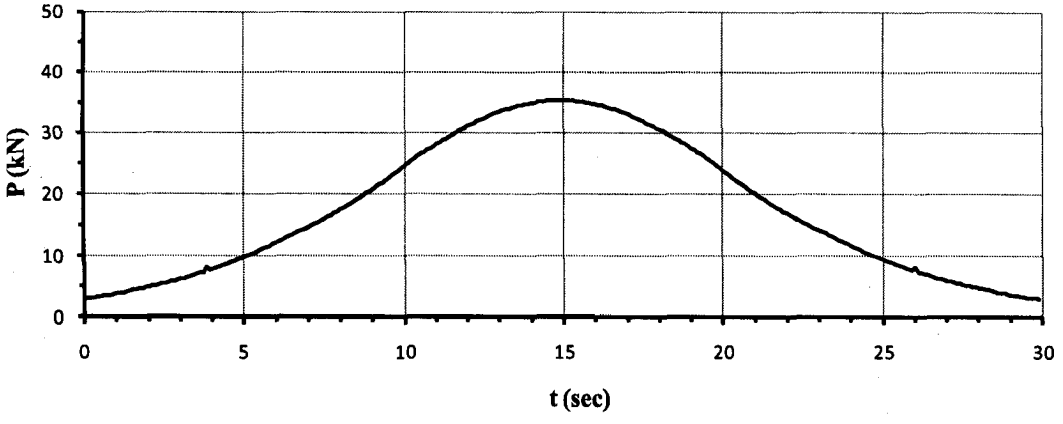

Fig. 4-10 Time-history of the Vertical Force Acting at the Ground Wire's Mid-span

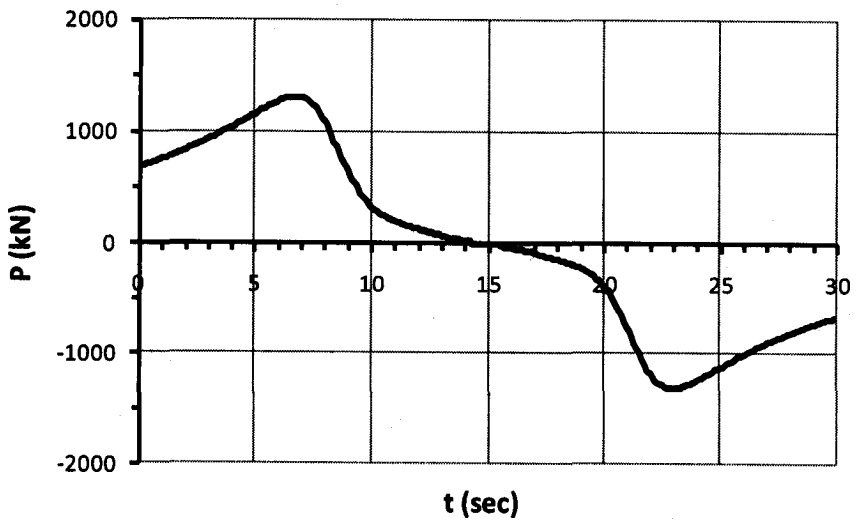

Fig. 4-11 Time-history of Force along the X-Direction at a Nodal Point of the Tower

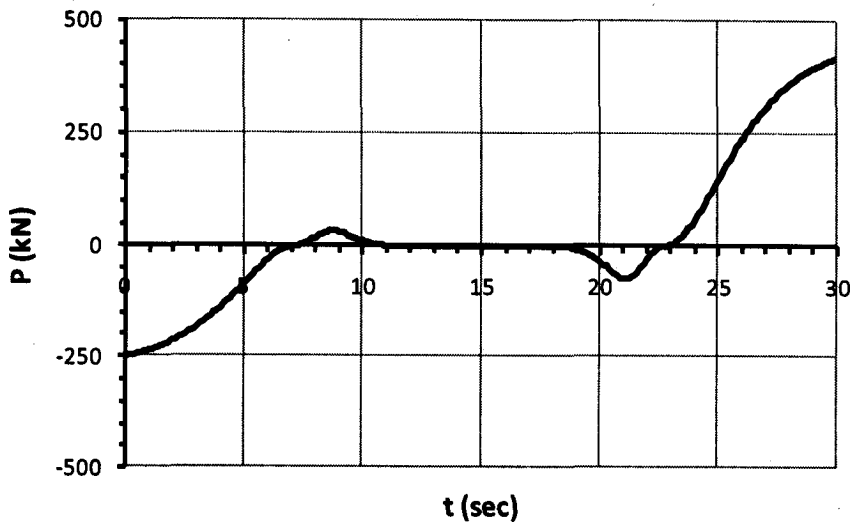

Fig. 4-12 Time-history of Force along the Y-Direction at a Nodal Point of the Tower

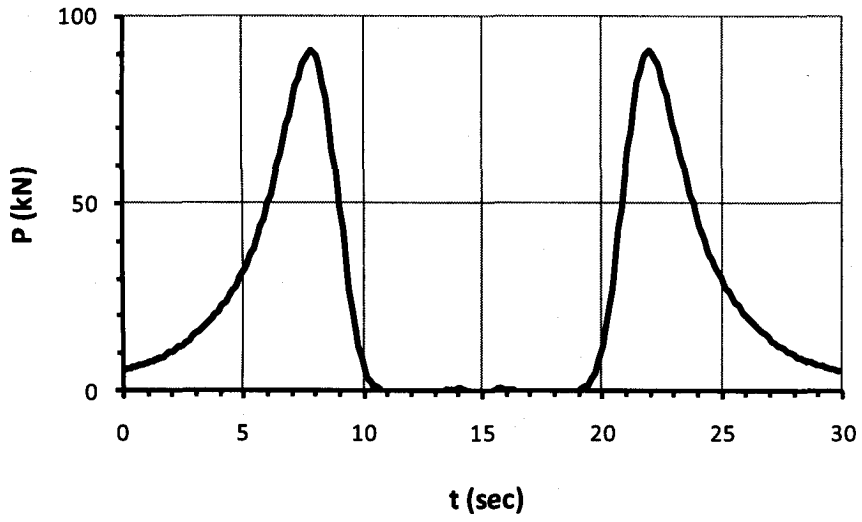

Fig. 4-13 Time-history of Force along the Z-Direction at a Nodal Point of the Tower

The figures indicate that the time-history profiles of the forces vary significantly from one point to another within the transmission line system. Also, at the same node, the time-history of the force components has different profiles. In general, the acting tornado forces have relatively long periods of oscillation. Among the plotted profiles, the minimum loading period is about 13 (sec), which is close to the conductors' fundamental period.

4.5.2 Second Case –Tornado Path Perpendicular to the Transmission Line

This case considers a tornado path that is perpendicular to the transmission line. The tornado range and its path are shown in the schematic given in Fig. 4-14.

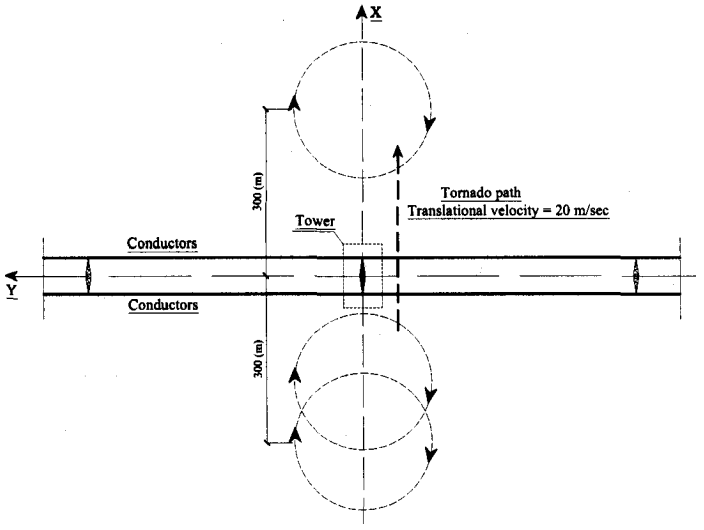

Fig. 4-14 Tornado Path for Second Time-history Analysis

4.6 Nonlinear Time-history Analysis

The analysis begins by solving the nonlinear load case "*Target*", which involves the evaluation of the stiffness matrix of the tower and the cables, while taking into consideration the effects of geometric nonlinearity, tension stiffening and sagging. This is followed by time steps nonlinear analyses conducted using the Newmark direct integration method. The nonlinear analysis takes into consideration the geometric nonlinearities resulting from the P-Delta, and large displacements effects. The output time step is taken equal to the input time step, to accurately capture the full effect of the loading.

Damping is simulated using the full damping matrix approach, which accounts for coupling between the modes. A proportional damping matrix is calculated as a linear combination of the stiffness and mass matrices. Details about the proportional damping matrix approach are provided by Bathe (1996).

A 4% structural damping ratio is assumed for the tower, as recommended by Loredo-Souza and Davenport (2003) and the ASCE No. 74 guidelines (1991). Regarding the line, the structural damping has a small value of about 0.05%, as reported by Loredo-Souza and Davenport (1998), which is neglected. The aerodynamic damping of the conductors plays a very important role in defining their responses under dynamic loading. It can be evaluated using Eq. (1), as shown by Loredo-Souza and Davenport (1998).

$$\zeta_{\text{aero}} = \left(\frac{C_D}{4\pi}\right)\left(\frac{\rho\, d^2}{m}\right)\left(\frac{V}{f\, d}\right) \tag{1}$$

Where ρ is the fluid density, d the cable diameter, m the mass of the lines per unit length, C_D the drag coefficient, f the natural frequency, and V is the magnitude of the wind velocity. The F4 tornado field has an average velocity outside the tornado core of 35 (m/sec). Inside the core, the wind velocity exceeds this value. A conservative estimate of the aerodynamic damping is calculated using V= 35 (m/sec), leading to an aerodynamic damping ratio equal to 33%.

4.7 Results of the Time-history Analysis

In order to assess the effect of dynamic behaviour, a comparison is carried in this section between the results of the time-history analyses and the results of extensive quasi-static parametric study, conducted along the two considered tornado paths. For the static analysis, time is a virtual quantity, reflecting a specific location of the tornado. Comparisons are presented here for some selected members of the tower and at specific locations of the conductor. As shown in Fig. 4-1, the tower is divided into two main zones. The tower zone is located below the supporting guys, while the cross arms zone is located at the upper part of the tower.

The transverse lateral and vertical displacements at mid-span of the conductor connected to the main tower under the first case of loading are plotted in Fig. 4-15 and Fig. 4-16, respectively.

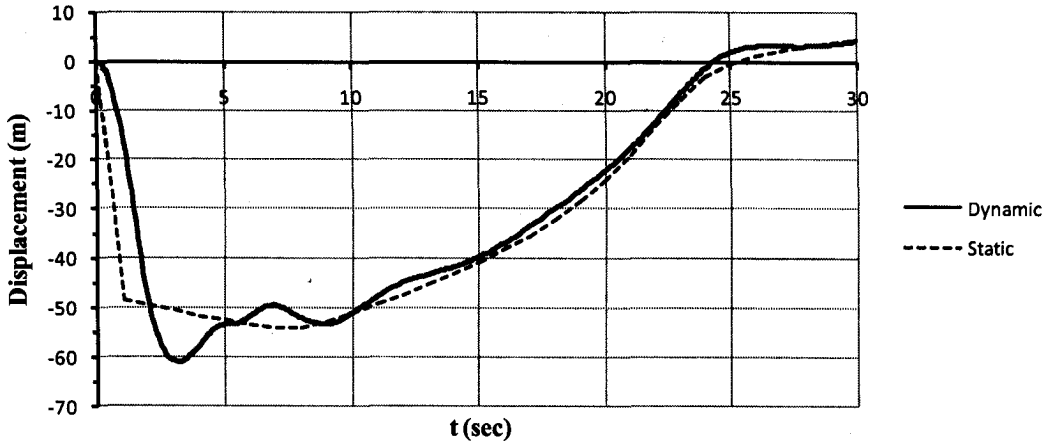

Fig. 4-15 Transverse Displacement at the Conductor's Mid-Span Due to Dynamic and Static Tornado Loading (First Loading Case)

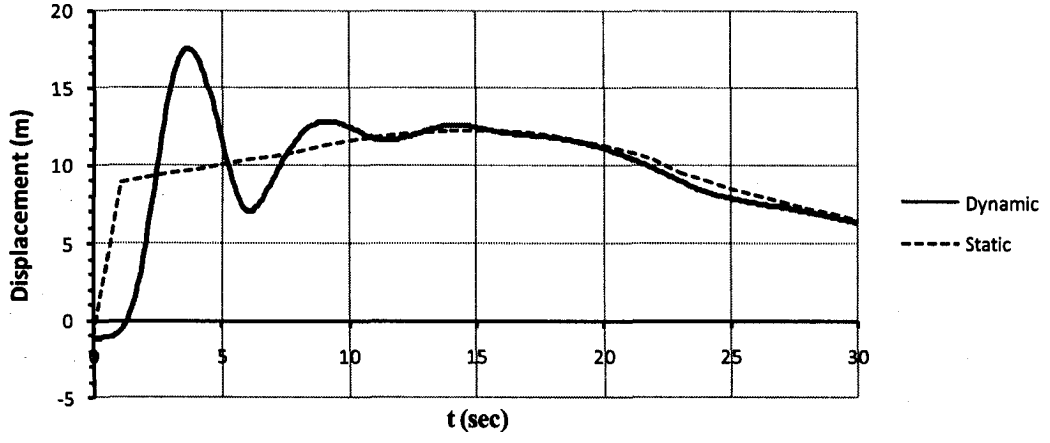

Fig. 4-16 Vertical of the Conductor's Mid-Span Due to Dynamic and Static Tornado Loading (First Loading Case)

The figures show that the dynamic response exceeds the static response, predominantly during the first ten seconds of loading. It should be noted that the wave superimposed on the static response has a period that almost matches the transverse and vertical periods of

the conductor. This indicates that a resonant component has contributed to the dynamic response.

Results for an upper chord member of the conductor' cross arm, member F118, are presented in Fig. 4-17 and Fig. 4-18 for load cases one and two, respectively. Both figures show a comparison between the member axial forces obtained from the dynamic and static analyses.

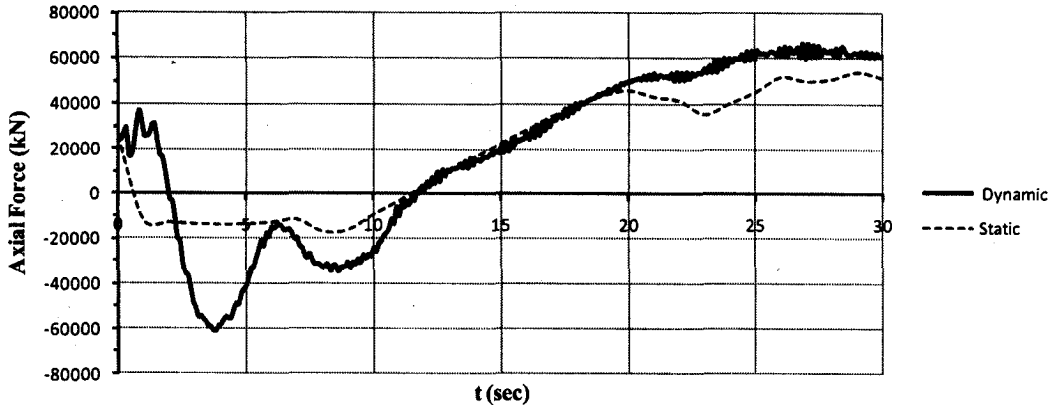

Fig. 4-17 Variation of Axial Force in Member F118 with Time Due to Dynamic and Static Analyses under First Load Case

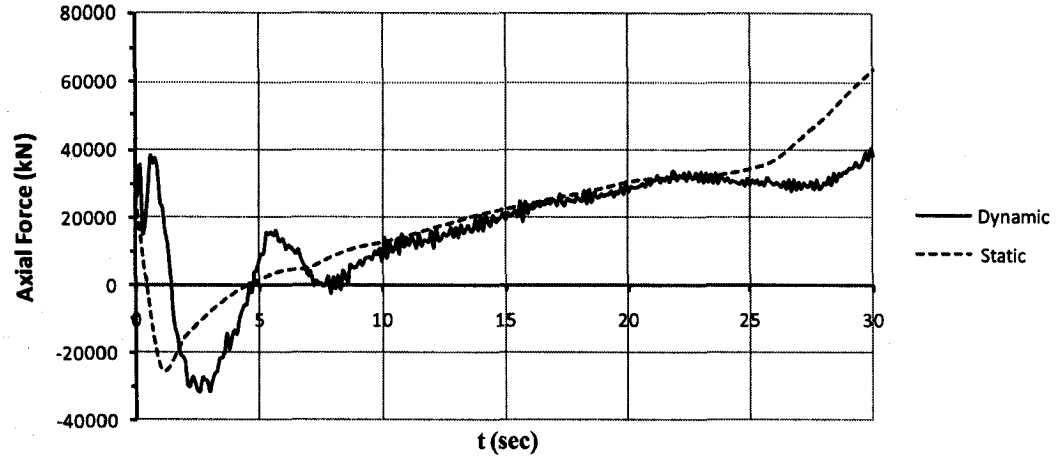

Fig. 4-18 Variation of Axial Force in Member F118 with Time Due to Dynamic and Static Analyses under Second Load Case

Similar to the conductor displacements, the dynamic analysis amplifies the forces in the cross arm member during the first ten seconds of loading. This effect is expected to result from the resonant component of the conductors, which lead to an amplification in the force transferred from the conductors to the cross arm.

To confirm this interpretation, the static and dynamic analyses are repeated, without including conductors and ground wire in the numerical model. The results corresponding to the first load case are plotted in Fig. 4-19.

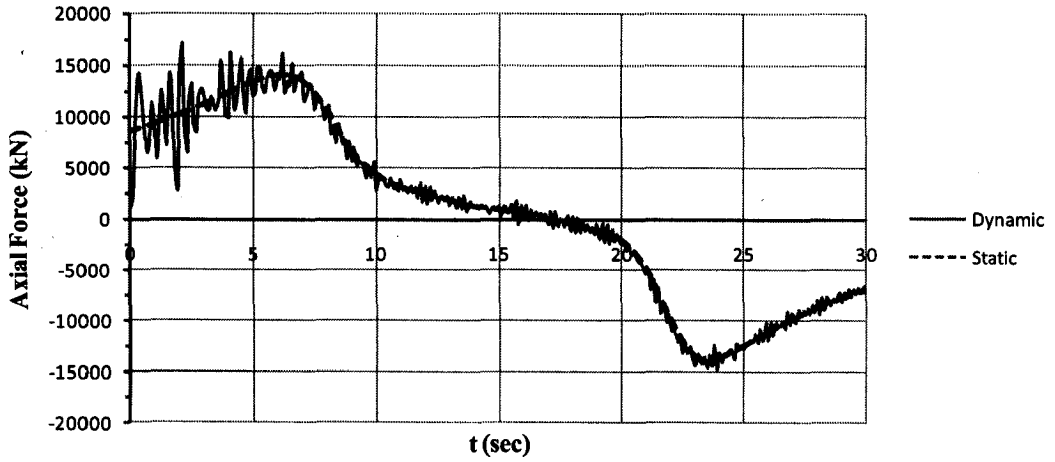

Fig. 4-19 Variation of Axial Force in Member F118 with Time Due to Dynamic and Static Analyses of the Tower Only

The long period component associated with the resonant response of the conductors does not appear when the tower is considered alone. However, a transient component, with an oscillation matching the period of the tower, appears in the dynamic analysis. This transient component is almost completely damped within five seconds of loading.

Fig. 4-20 shows the time-history variation of the axial load in the chord member F318, located in the tower zone due to first load case. The long-period wave resulting from the resonant response of the conductor does not appear for this member. The response of this

member is not significantly affected by the conductors' forces. A transient component appears in the dynamic response.

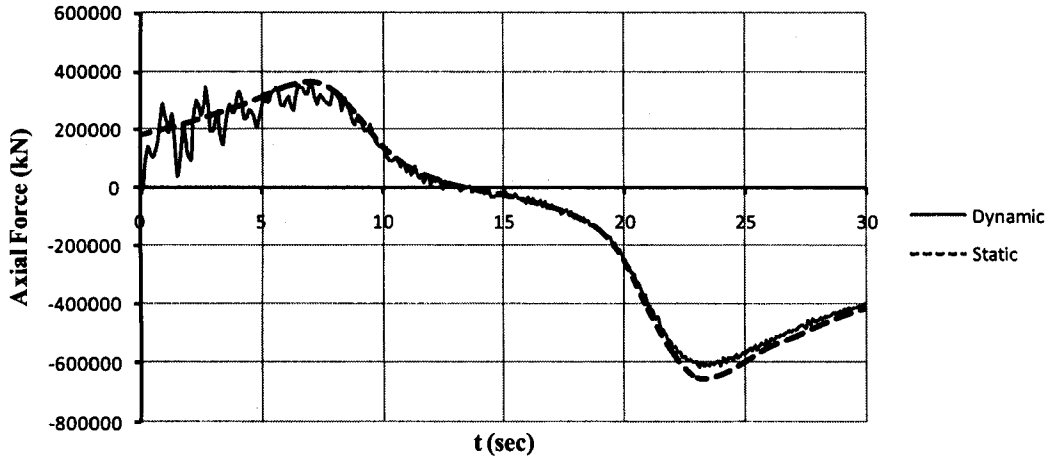

Fig. 4-20 Variation of Axial Force in Chord Member F318 with Time Due to Dynamic and Static Analyses under First Load Case

4.8 Conclusions

The current study investigates the dynamic response of transmission line structures under a moving tornado event. The steady-state tornado wind field is based on a model-scale Computational Fluid Dynamics (CFD) analysis that was conducted in a previous study. Numerical schemes are developed to evaluate the natural frequencies and mode shapes of the different components of the transmission line system. Time-history dynamic analyses are then conducted, by considering a velocity convective component of 20 m/sec for the tornado. At each time instant, the relative distance between the tornado and the structure changes. This leads to a time-history variation of the tornado forces. This time-history variation differs from one point to another. The analysis is conducted under an F4-tornado. Two sets of time-history analyses are conducted by considering tornado paths

that are parallel and perpendicular to the line. The following conclusions can be drawn from this study:

- The value of the pretension force in the guys has a significant effect on the natural frequencies of the tower. Increasing the pretension force in the guys increases the tower stiffness, and consequently, decreases the fundamental period.
- The natural periods of the conductors and ground wire are longer than the natural periods of the tower, especially in the transverse direction. Therefore, the conductors and ground wire are more susceptible to be excited by the dynamic component of the tornado load, which is dominated by a long-period component.
- The time-history analyses show that the dynamic response of the conductors exceeds the static response, mainly during the first ten seconds of loading. This indicates that a resonant component has contributed to the dynamic response. The resonant component also affects the internal forces in the tower cross arms, in which the dynamic response is also higher than the static. Due to the high aerodynamic damping of the conductors, this resonant component is damped out over time. The presence of the resonant component in the dynamic response of the conductors could be explained by the nature of the assumed loading. The instantaneous appearance of the tornado event does not allow for aerodynamic damping to be developed in the first period of response. This loading assumption does not consider the effect of the aerodynamic damping caused by conventional winds that would exist in a storm before a tornado event.
- The long period wave resulting from the resonant response of the conductor does not appear in the tower zone members' response.

In light of these findings, it can be concluded that it is important to consider the dynamic response of transmission lines when designing the upper part of transmission towers.

4.9 Acknowledgements

The author would like to acknowledge Manitoba Hydro Company, Canada, Natural Sciences and Engineering Research Council of Canada (NSERC), and Centre for Energy Advancement through Technological Innovation (CEATI) for their kind support for this research work. The author acknowledges Prof. H. Hangan and Dr. J-D. Kim at the Boundary Layer Wind Tunnel Laboratory, The University of Western Ontario, Canada, for their efforts in providing the tornado wind data.

4.10 References

American Society of Civil Engineers (ASCE) (1991), "Guidelines for electrical transmission line structural loading", *ASCE Manuals and Reports on Engineering Practice,* No. 74, NY.

Baker, D. E. (1981). "Boundary layers in laminar vortex flows." Ph.D. thesis, Purdue University.

Bathe, K-J. (1996), *Finite Element Procedures in Engineering Analysis*, Prentice-Hall, Englewood Cliffs, New Jersey.

Darwish, M. M., El Damatty, A. A., and Hangan, H. (2009), " Dynamic characteristics of transmission line conductors and behaviour under turbulent downburst loading", *Wind and Structures, an International Journal.*

Fluent 6.2 User's Guide (2005), Fluent Inc.,Lebanon

Fujita, T.T., and Pearson, A.D. (1973). " Results of FPP Classification of 1971 and 1972 Tornadoes," *Preprints, Eighth Conference on Severe Local Storm, American Meteorological Societ,* Boston, Mass., USA, pp. 142-145.

Hamada, A., El Damatty, A. A., Hangan, H., Shehata, A. Y. (2009), " Finite element modelling of transmission line structures under tornado wind loading", *Wind and Structures, an International Journal*

Hangan, H., and Kim, J. (2008). "Swirl ratio effects on tornado vortices in relation to the Fujita scale." *Wind and Structures,* 11(4), 291-302.

Kim, J., and Hangan, H. (2007). "Numerical simulations of impinging jets with application to downbursts." *J.Wind Eng.Ind.Aerodyn.,* **95**(4), 279-298.

Lee, Wen-Chau., and Wurman, J. (2005). "Diagnosed three-dimensional axisymmetric structure of the Mulhall tornado on 3 May 1999." *J.Atmos.Sci.,* **62**(7), 2373-93.

Loredo-Souza, A. M. and Davenport, A. G. (1998). "The effects of high winds on transmission lines." *Journal of Wind Engineering and Industrial Aerodynamics*, 74-76, 987-994.

Loredo-Souza, A., and Davenport, A. G. (2003). "The influence of the design methodology in the response of transmission towers to wind loading." *J.Wind Eng.Ind.Aerodyn.,* **91**(8), 995-1005.

National Research Council of Canada (NRCC) (1990)," Supplement to the National Building Code of Canada 1990". *Associate Committee on the National Building Code*, Canada.

SAP2000 V.12 (2008), CSI Analysis Reference Manual, Computer and Structures, Inc. Berkeley, California, USA

Sarkar, P., Haan, F., Gallus, Jr., W., Le, K. and Wurman, J. (2005). "Velocity measurements in a laboratory tornado simulator and their comparison with numerical and full-scale data." *37th Joint Meeting Panel on Wind and Seismic Effects*. Tsukuba, Japan, May.

Savory, E., Parke, G. A. R., Zeinoddini, M., Toy, N., and Disney, P. (2001). "Modelling of tornado and microburst-induced wind loading and failure of a lattice transmission tower." *Eng.Struct.,* **23**(4), 365-375.

Shehata, A. Y., and El Damatty, A. A. (2007). "Behaviour of guyed transmission line structures under downburst wind loading." *Wind and Structures, an International Journal,* **10**(3), 249-268.

Shehata, A. Y., El Damatty, A. A., and Savory, E. (2005). "Finite element modelling of transmission line under downburst wind loading." *Finite Elements Anal.Des.,* **42**, 71-89.

Wen, Y. (1975). "Dynamic tornadic wind loads on tall buildings", *ASCE Journal of the Structural Division*, **101**(1), 169-185.

Wurman, J. (1998). "Preliminary results from the ROTATE-98 tornado study", *Preprints, 19th conf. On severe local storms,* Minneapolis, MN, 14-18 September

CHAPTER 5

CONCLUSION

5.1 Summary

A procedure is developed to model and predict the structural performance of guyed transmission lines system subjected to tornado wind loads. The tornado wind field is based on a model scale Computational Fluid Dynamics (CFD) analysis developed and validated in a previous study. The CFD data, together with full scale wind measurements and design guideline recommendations are used to establish the wind fields associated with F4 and F2 tornadoes. The tornado wind field has a three dimensional steady-state spatial variation. The data along the circumference is averaged, leading to an axisymmetric set of F4 tornado data. The procedures used to obtain wind forces due to the radial, tangential, and axial velocity components of the wind field acting on the transmission line and towers node are described. A three-dimensional nonlinear finite element model for the transmission line system is developed. The model includes a simulation of the tower of interest, in addition to two towers and three spans of conductors and ground wires on each side of the tower of interest. The model accounts for the geometric nonlinearity resulting from both the large deformations of the lines and the P-delta effect. The cable element formulation, which is used to model the conductors, the ground wire, and the guys, includes the effect of tension stiffness and sagging.

The developed numerical model is used to conduct an extensive parametric study to assess the performance of guyed transmission towers under loads resulting from different tornado events. Both the F4 and F2 tornado wind fields are used. The parametric study is conducted in a quasi-static manner by carrying out a large number of analyses, each

analysis corresponds to a specific tornado location relative to the tower of interest. The conducted parametric study consists of three parts. Part one assesses the behaviour under F4 tornado wind field. In second part, the behaviour is assessed under F2 tornado wind field. In the third part, the analysis is conducted for the intermediate tower alone, i.e. without modelling the lines, under F4 and F2 tornadoes. The structural behaviour of the tower under various critical tornado locations is described. The results of the parametric study are used to assess the sensitivity of the member forces to the variation of the parameters describing the location of the tornado relative to the line.

The study proceeds by studying the dynamic response of transmission lines under tornado loads. The available CFD data are in the steady state manner with no variation with time. Thus, the loading time history used in the dynamic analysis is based on the translation of the tornado event. The natural periods and mode shapes of the considered transmission line system are first determined by conducting free vibration analyses. The developed finite element model is modified to account for the time-history variation of the tornado forces resulting from the translation of the tornado event. Time-history dynamic analyses are conducted and the results are compared with the quasi-static parametric study results.

5.2 Conclusions

The following conclusion can be drawn from this research:

1) The forces in all tower members change significantly with the variation of the parameters R and θ, which define the location of the tornado relative to the tower.
2) Different type of members, either chord or diagonal, as well members located in different zones of the tower, have independent critical values of R and θ that lead to peak forces in these members. This emphasizes the need of conducting an

extensive parametric study, by varying the location of the tornado, in order to predict the peak forces in all members of the tower.

3) Analyses conducted using the 3-D and the axisymmetric sets of data reveal no significant variation in the members' internal forces. The difference is more pronounced in the tower zones near the ground, because of the instability of the wind in this region, which can be only observed in the 3-D fluid dynamic analysis.

4) The F2 tornado leads to peak member forces that are significantly less than those resulting from the F4 tornado.

5) A comparison is carried out between the peak forces due to F2 tornado to those resulting from normal wind and downbursts loading. In this comparison, the wind speed used in the design of the tower was employed to evaluate the normal wind forces. Such a comparison shows that the member forces due to F2 tornado exceed the downburst and normal wind forces. However, for the majority of the members, the F2 tornado forces are found to be less than the capacity of the members.

6) Due to the unbalanced nature of tornadoes, some event locations result in unbalanced forces acting on adjacent spans of the conductors. This leads to a resultant force that acts on the tower cross arms along the longitudinal direction of the conductors. This force leads to an out-of-plane bending effect on the cross arms and, consequently, compression forces in some of the upper chord members. These compression forces exceed the tension forces that develop in these members due to the own weight of the conductors. As a result, these members

become subjected to compression forces, which are not typically accounted for under normal wind load cases.

7) The value of the pretension force in the guys has a significant effect on the natural frequencies of the tower. Increasing the pretension force in the guys increases the tower stiffness, and consequently decreases the fundamental period.

8) The natural periods of the conductors and ground wire are higher than the natural periods of the tower especially in the transverse direction. Therefore, the conductors and ground wire are more susceptible to be excited by the dynamic component of the tornado load, which is dominant by a long period component.

9) The time history analyses show that the dynamic response of the conductors exceed the static response, mainly during the first ten seconds of loading. This indicates that a resonant component has contributed to the dynamic response. The resonant component also affects the internal forces in the tower cross arms, where the dynamic response also is higher than the static. Due to the high aerodynamic damping of the conductors, this resonant component is damped out over time. The presence of the resonant component in the dynamic response of the conductors could be explained by the nature of the assumed loading. The instantaneous appearance of the tornado event does not allow for aerodynamic damping to be developed in the first period of response. This loading assumption does not consider the effect of the aerodynamic damping caused by conventional winds that would exist in a storm before a tornado event.

10) The long period wave resulting from the resonant response of the conductor does not appear in the tower zone members' response.

5.3 Recommendations for Future Research

This thesis investigates the structural behaviour of a guyed transmission line system. For future research, the following investigations are suggested:

- Extend the dynamic analysis of the transmission line to include the turbulence components of the tornado loading.
- Conduct similar studies by considering different terrain exposure and topography of the ground.
- Conduct similar studies by considering different configurations of transmission lines, such as self-supported towers.
- Conduct a progressive failure analysis of the transmission towers under different tornadoes.
- Develop a numerical model that accounts for the local buckling capacity of the tower members as well as the connection details between the tower members.